UNITED STATES

DEPARTMENT OF THE INTERIOR

GEOLOGICAL SURVEY

FOUR DEFINITIONS OF STRONG MOTION DURATION: THEIR PREDICTABILITY AND UTILITY FOR SEISMIC HAZARD ANALYSIS

by

Robin K. McGuire

and

Theodore P. Barnhard

OPEN-FILE REPORT 79-1515

1979

United States Department of the Interior

Geological Survey

FOUR DEFINITIONS OF STRONG MOTION DURATION: THEIR PREDICTABILITY AND UTILITY FOR SEISMIC HAZARD ANALYSIS

by

Robin K. McGuire

and

Theodore P. Barnhard

[Reports - Open-File] Report 79-1515

Denver, Colorado

I. INTRODUCTION

The duration of strong ground shaking has long been considered important in characterizing seismic shaking and in understanding the damage induced in engineering and natural structures (for example, Housner, 1970; Clough and Penzien, 1975). The reason for this view is that peak amplitudes of the motion do not fully describe all characteristics of seismic shaking that have been observed. In particular it is thought that, of two ground motions with the same peak acceleration, the motion with the longer duration will produce more damage in structures subjected to that motion.

Many quantitative definitions of strong motion duration have been proposed (Bolt, 1974; Trifunac and Brady, 1975; Trifunac and Westermo, 1977; Vanmarcke and Lai, 1977; Perez, 1974; McCann and Shah, 1979; Esteva and Rosenblueth, 1964; Housner, 1965, Aptikayev, 1975; Hays, 1975; Kameda and Ang, 1977). All of these definitions are based on the recorded accelerations (or derived velocities on displacements) at a site during an earthquake; none use properties of the source, such as the duration of rupture of the fault.

To date there have been no studies reported showing a quantitative relationship between strong motion duration and earthquake damage. Rather, the concept of the "duration of strong shaking" has been used in a qualitative way to explain damage (or lack of it) after an earthquake. An example is the ground motion in Anchorage, Alaska, during the 1964 Prince William Sound earthquake: the estimated peak acceleration was moderate (there were no accelerographs in the area) but the long duration of shaking induced soil failures and heavy damage in multi-story buildings. The 1966 Parkfield, California, earthquake produced recorded peak accelerations as great as 0.5 g, but the lack of damage is generally attributed to short duration of shaking.

The purpose of this report is to examine four proposed definitions of strong motion duration in order to determine their utility in the context of seismic hazard analysis. For a quantitative definition of duration to be useful for conventional seismic hazard studies, values of duration first must be predictable using only the earthquake magnitude, source-to-site distance, and a general description of soil conditions at the site. The reason is that these are the only available variables used in the current generation of seismic hazard maps. Second, the definition of duration must be useful, in addition to peak motion parameters, in determining the severity of seismic shaking. Peak motion hazard analyses and maps have been, and will continue to be, made as a first step in seismic hazard evaluation; the additional time, effort, and expense of conducting seismic hazard analyses for strong motion duration can only be justified if a measure of duration is used which provides significant additional information for estimating damage or designing structures.

Section II of this report describes the strong motion data used in this study, the definitions of duration examined, and the definitions used to quantitatively measure the severity of shaking. Section III indicates dependences of peak motion parameters on earthquake magnitude, distance, site conditions, and component direction. These relationships are included for completeness and to show that the data set is a "typical" one in the sense that typical peak motion parameter relations are obtained. Attempts to predict duration for given magnitudes, distances, and soil conditions are reported in Section IV. Section V shows the accuracy with which Modified Mercalli (MM) intensity, one measure of shaking severity, can be predicted using peak motion parameters and duration. In Section VI comparable results are reported using, as a measure of shaking severity, the hysteretic energy absorbed by a class of single-degree-of-freedom oscillators with bilinear force-defomation characteristics. Finally, discussion of and conclusions from these results are presented in Section VII.

II. DATA AND DEFINITIONS

Strong Motion Data

A set of 50 strong motion records, consisting of 3 components each, was selected to represent a range of magnitudes, distances, and geologic conditions. Fifteen records were classified as "rock" sites (including some sites underlain by a thin veneer of alluvium) and 35 as "alluvium" sites; several sources were used to determine these classifications (Boore and others, 1978; U.S. Geological Survey, 1977). It is recognized that classification of sites into these categories is quite subjective; other researchers might chose a different categorization scheme, particularly in light of new subsurface data which have become available since this work was initiated. For the present purpose of determining (1) magnitude and distance dependences of duration, and (2) usefulness of duration in estimating shaking severity, the soil classifications adopted here are considered adequate.

The records used, their soil classes, and the magnitudes and distances used in the regression analyses are described below and listed in table 1. Also shown is the MM intensity reported at the recording site for each record (McGuire and Barnhard, 1977). Local magnitudes were used insofar as possible. The distance from the recording site to the closest point of fault rupture was used if this was available (Boore and others, 1978); otherwise, epicentral distance was used. The volume II records published by the California Institute of Technology (1971) were used for processing. Figure 1 shows the magnitudes and distances of the records; the data represent as large a range of magnitudes and distances as is available for California strong motion records.

Definitions of duration

The first definition of duration examined in this study is the "bracketed duration" (herein designated D_B) proposed by Bolt (1974). This is defined as the time between the first and last excursion of the absolute value of acceleration above 0.05 g. Several other thresholds were also examined (0.1 g, 0.15 g, and 0.2 g) with results similar to those presented here.

The "fractional duration" (designated D_F) is defined as the time between the first and last excursions of the absolute value of acceleration above some fraction of the peak acceleration (Aptikayev, 1975). Results are reported here for the fraction 0.5; fractions of 0.67 and 0.75 were also examined with similar results.

The definition proposed by Trifunac and Brady (1975), based on work by Husid and others (1969), is designated D_{TB} herein. It is the time required for 90% of the Arias intensity (which is defined as the time integral of squared accelerations for the component of motion considered) to arrive; the duration of strong shaking is determined to begin when 5% of the Arias intensity has been recorded and to end when 95% has been recorded. Other percentages of the Arias intensity (50%, 60%, and 80%) were also considered, with results similar to those reported here for 90%.

The fourth definition of duration investigated is that proposed by Vanmarcke and Lai (1977), designated D_V herein. This definition requires that the strong motion duration satisfy two criteria: (a) the calculated mean square acceleration σ_a^2 during D_V, times D_V, equals the total energy observed for the entire accelerogram, and (b) the observed peak acceleration is the value that is calculated to occur once, on the average, for a stationary random Gaussian motion with mean-squared acceleration σ_a^2 and duration D_V.

Various other definitions of strong motion duration have also been proposed, as discussed in Section I. These generally require more complicated calculations and are often based on the duration of shaking at specified frequencies; they are all calculated from observed accelerations at a recording station (rather than, for instance, from the properties of the source). The purpose of this initial study is to investigate the utility of simple definitions of duration; hence more complicated definitions are not examined here.

Measure of Ground Motion Severity

The first measure of ground motion severity used is the Modified Mercalli intensity assigned to the locale in which each strong motion record was obtained. MM intensity is a subjectively interpreted measure which has the ability to distinguish at least gross differences in the overall severity of shaking.

Also investigated is a variety of single-degree-of-freedom (SDOF) dynamic structural models with bilinear force-deformation characteristics. Initial stiffnesses were selected to give initial frequencies of 10, 4, 2, 1, 0.5, and 0.25 hz, post-yield stiffnesses were 3% of initial stiffness, viscous damping was chosen to be 2% of critical, and yield displacements were set at 20% of the spectral displacements induced by the 1940 El Centro N-S accelerogram. Thus these models represent structures designed to remain in the elastic range for ground motions "one-fifth as strong" as the 1940 El Centro record, but to incur damage during more severe motions. Three measures of damage were used: (1) the maximum displacement induced in each system, (2) the hysteretic energy E absorbed by each system, and (3) the total (elastic and hysteretic) energy induced in each system. These three measures represent the range of ways in which damage to simple stuctures, as represented by these simple dynamic mathematical models, might be quantified. For maximum displacements it was found that elastic response spectra can be used to very accurately estimate the peak inelastic displacement, without the use of duration, confirming results reported earlier (McGuire, 1974). Damage measure (3) above leads to the same conclusions as damage measure (2), so only results for hysteretic energy are reported here.

III. PREDICTION OF PEAK MOTION PARAMETERS

To assure that the strong motion records in table 1 represent a data set "typical" of those used for seismic hazard studies, various parameters of the motions were regressed on earthquake magnitude, distance, soil conditions, and component direction. Parameters chosen for study were the peak acceleration a_g, peak velocity v_g, peak displacement d_g, and spectral displacement for six frequencies between 10 and 0.25 hz, with 2% damping (herein denoted SD_f, where f indicates frequency in hz). The form used for regression analysis was:

$$\ln y = c_1 + c_2 M + c_3 S + c_4 V + c_5 \ln R \qquad (1)$$

where y is one of the motion parameters described above, M is earthquake magnitude, S is a binary variable (zero or one) indicating rock or alluvium soil conditions, V is a binary variable (zero or one) indicating horizontal or vertical component, and R is distance in km. Coefficients c_1 through c_5, determined by least-square regression analysis, are listed in tables 2 and 3. Recorded values of a_g, v_g, d_g, and SD_1, normalized by M, S, and V, are plotted versus R in figures 2, 3, 4, and 5, respectively; values normalized by S, V, and R are plotted versus M in figures 6, 7, 8, and 9.

In regression analyses of this type reported in the literature, the term R + C is often used instead of variable R in equation (1) (for example, Esteva and Villaverde, 1974). For completeness, this term was also investigated, with values of C chosen to be 10, 25, and 40 km. Results of regression analyses using this form are reported in tables 2 and 3. Use of the term R + C reduces the residual uncertainty in observations only for peak motion parameters related to high frequencies (that is, peak acceleration and spectral displacement for high frequencies). This is consistent with the notion that, close to the source, high frequency properties of strong ground motion attenuate less rapidly with distance than at points farther from the source. Values of a_g reflect this behavior, as shown in figure 2. We feel that the attenuation of high frequency ground motion characteristics is much more complicated than can be modeled accurately for all magnitudes with a simple R + C term in a regression equation; the change in attenuation with distance is, at the very least, dependent on source size and hence on magnitude. Similarly, the magnitude dependence of ground motion characteristics likely depends on the source-to-site distance. Regressions incorporating these effects to predict a_g have been reported in the literature (Donovan and Bornstein, 1977). The data set used here, however, is not sufficient to allow quantitative conclusions to be drawn regarding the complicated dependence of ground motion characteristics on magnitude and distance. Thus, for simplicity and because equation (1) allows adequate first estimates of peak parameters, more complicated equation forms are not used in this study.

Tables 2 and 3 show that the ground motion characteristics of this data set exhibit the properties reported elsewhere. Specifically, high frequency characteristics attenuate faster with distance, and are less dependent on earthquake magnitude, than low frequency characteristics; vertical motions generally have lower amplitudes than horizontal motions; and alluvium soil conditions amplify low frequency characteristics but de-amplify high frequency characteristics, relative to rock sites. As a result of these regression analyses, this data set is considered adequate for representing peak ground motion parameters and for investigating the utility of ground motion duration in seismic hazard analysis.

Parameters a_g, v_g, d_g, and PSV_1 are taken here to be representative characteristics of strong shaking. The first three of these parameters are widely used both in seismic hazard analyses and in seismic-resistant design of structures; the last parameter, representative of intermediate-frequency spectral amplitudes, is included because these amplitudes often are not well estimated by v_g (see, for example, McGuire, 1978).

The peak accelerations from Volume II of the Caltech reports were used for regression analyses reported in this section, although some researchers in ground motion studies (for example, Boore and others, 1978) prefer the Volume I peak accelerations. There is not a significant difference between the Volume II values of a_g and the Volume I values (figure 10 shows a comparison of the two). Moreover, the Volume II data are more appropriate here because the Volume II digitized accelerograms were used to calculate responses in the nonlinear models. For some accelerograms (specifically the vertical components of records V314 and V315), the Volume II peak acceleration is larger.

IV. PREDICTION OF STRONG MOTION DURATION

Duration Predictions Using Peak Parameters

To determine if duration can be predicted from the peak parameters, we plotted values of duration according to each of the four definitions, versus each of the four peak parameters discussed in the previous section. Figures 11 through 14 show D_B plotted versus a_g, v_g, d_g, and PSV_1; figures 15 through 26 show similar plots for D_F, D_{TB}, and D_V.

From these comparisons come two observations. First, there is a large scatter in the data. Second, for D_F, D_{TB}, and D_V, large durations generally occur with low values of peak parameters, and large values of the peak parameters only occur with short durations. The implication for determining seismic design motions is important: we cannot do independent seismic hazard analyses for peak parameters and duration because these characteristics of motion are not statistically independent. It should be pointed out that the available California strong motion records are limited to earthquakes with local magnitudes $\leq$ 7.2; it is quite possible that larger earthquakes might produce motions with large peak amplitudes and long durations, although these events are relatively rare. At the least, any correlation between peak parameters and duration would have to be magnitude dependent. As a result of the comparisons shown in figures 11 through 26, no quantitative methods of estimating duration from peak parameters were investigated.

Duration Predictions Using Magnitude and Distance

To predict duration as a function of earthquake magnitude and distance, we first examined the behavior of duration as a function of magnitude, holding other variables fixed or to a small range. An example is shown in figure 27: D_B is plotted versus magnitude for records in the distance range $17 \le R \le 27$ km. Figure 28 is a similar plot for the distance range $40 \le R \le 65$ km. Similar comparisons are shown for the other duration definitions in figures 29 through 34. A comparable method was used to determine the behavior of duration with respect to distance: durations were plotted versus distance for the magnitude ranges $5.3 \le M \le 5.6$ and $6.3 \le M \le 6.6$. Figures 35 through 42 show these results.

From these plots it is evident there is large dispersion in observed values of duration for similar magnitudes, distances, soil conditions, and component direction. Given this dispersion, the simple form used previously is adequate to approximate the mean trends of duration with these variables:

$$\ln D = c_1 + c_2 M + c_3 S + c_4 V + c_5 \ln R \qquad (2)$$

where D is one of the duration definitions and c_1 through c_5, estimated by least-squares regresion analysis, are listed in table 4. All 150 components were used in regression analysis for D_F, D_{TB}, and D_V; only 82 components that indicated non-zero values for D_B were used in regression analysis for that duration definition.

The general trends indicated by the coefficients in table 4 are the same as those indicated by figures 27 through 42. For D_F, D_{TB}, and D_V, duration increases with M, R, S, and V; similar results for D_{TB} were reported by Dobry and others (1978). For D_B, duration increases with M and S but decreases with

V and R, confirming results reported by Bolt (1974). For all definitions except D_{TB}, the residual scatter is larger than is typical for peak parameter regressions (for instance table 2), meaning that duration is less accurately estimated for a given magnitude and distance than, for instance, peak acceleration. Residual uncertainty in D_{TB} is smaller than for the peak parameter regressions, in part because the marginal variance for $\ln D_{TB}$ is smaller than for the peak parameters or for the other duration definitions. The multiple correlation coefficient $\mathcal{R}$ for the regression analysis with D_{TB} is about the same (~0.75) as for peak parameters, meaning that about the same amount of scatter is explained by the regression.

Values of D_B normalized by R, S, and V are plotted versus M in figure 43; D_B values normalized by M, S, and V are plotted versus R in figure 44. The large residual uncertainty is evident, and is reflected in the standard deviation of 2.0 for $\ln D_B$ reported in table 4. This large uncertainty results from the definition of D_B: a single acceleration spike above 0.05 g gives a very short duration, as short as 0.02 sec, whereas several acceleration spikes may indicate a duration of 2 sec or more, an increase of a factor of 100. This behavior is evident in figures 27, 28, 35, and 36. Ignoring accelerograms with $D_B \leq 0.2$ seconds--that is, excluding them from the regression analysis--would reduce the residual uncertainty but not below that observed for the other duration definitions. This is apparent in figures 43 and 44, where a dashed line has been drawn above all observations of $D_B \leq 0.2$ sec.

Normalized values of D_F, D_{TB}, and D_V are plotted versus M and R in figures 45 through 50. The large scatter in the data indicate that the assumed functional variation of duration with M and R is adequate.

The figures discussed in this section, and table 4, show that there is a large uncertainty associated with predicting D_B, D_F, and D_V using earthquake magnitude and distance. The residual standard errors of estimate from the regression analyses are even larger than those calculated when peak acceleration is estimated from M and R. For D_B this would be the case even if very short duration records, caused by a single acceleration pulse, were eliminated from the analysis. Thus, we conclude that these three duration definitions cannot be estimated with accuracy. D_{TB} can be estimated with more accuracy only because its marginal variance is smaller than those of other duration definitions. Consistent with this, D_{TB} does not change greatly as a function of M or R, as is reflected in small regression coefficients c_2 and c_5 in table 2: changing M by 2 units, or doubling R, changes D_{TB} by only about 30%, in the mean. Therefore, a seismic hazard analysis for D_{TB} would indicate durations that change little as a function of the size of earthquakes expected on a fault and as a function of the distance from the fault to the site of interest.

A further complication is that durations D_F, D_{TB}, and D_V are not independent of peak parameter values. This means that hazard analyses for these duration definitions cannot be performed independently of analyses for a_g, v_g, and d_g. If such independent analyses were made, they might result in erroneously recommending that, for seismic design, a large acceleration (from a small magnitude earthquake on a nearby fault) be combined with a long duration (from a large earthquake on a distant fault), a combination which might not physically exist. While the dependence between duration and peak parameter values might not be critical in the sense suggested, this remains to be proven.

V. MM INTENSITY AS A MEASURE OF GROUND MOTION SEVERITY

Having examined the predictability of duration, we now investigate the utility of duration (if it could be predicted with accuracy) for indicating the severity of seismic shaking. The first measure of ground motion severity examined was MM intensity. This is a subjectively interpreted measure which allows at least gross differences in the severity of seismic shaking to be distinguished. The MM intensity associated with each accelerogram is plotted versus the peak parameters of the motion (a_g, v_g, d_g, and PSV_1) in figures 51 through 54. To estimate MM intensity from these peak parameters, the following equation was used:

$$MMI = c_1 + c_2 \, ln \, y + c_3 \, S + c_4 \, V \qquad (3)$$

where y is a_g, v_g, d_g, or PSV_1, and c_1 through c_4 are given in table 5. All of the peak parameters are about equally accurate for estimating MM intensity: the residual standard error is approximately 0.6 in all cases.

To determine which, if any, duration measure provides useful information for estimating MM intensity in addition to peak parameters, duration was added to the regression analysis using the form:

$$MMI = c_1 + c_2 \, ln \, y + c_3 \, S + c_4 \, V + c_5 \, D \qquad (4)$$

Values of coefficients c_1 through c_5 are given in table 5. In all cases c_5 is very close to zero, meaning that duration is not useful in addition to peak parameters for estimating MM intensity. To emphasize this visually, figures 55 through 58 show MM intensity normalized by v_g, S, and V (using equation (3)) plotted versus the four durations. For these data, which include only records with MMI$\leq$VIII, it is clear that the MM intensities, normalized by peak velocity, show no trend with duration. Also, use of a different functional form (for example, $\ln$ D) in place of D in equation (4) would lead to the same conclusion.

VI. HYSTERETIC ENERGY AS A MEASURE OF GROUND MOTION SEVERITY

As discussed in Section II of this report, the hysteretic energy absorbed by a class of oscillators with bilinear force-deformation characteristics was investigated as a measure of the severity of seismic shaking. Properties of these oscillators are described in Section II.

We first determined which of the peak motion parameters alone is most useful for estimating hysteretic energy for each oscillator. This was accomplished using the following form for regression analysis:

$$ln\ E = c_1 + c_2\ ln\ y \qquad (5)$$

where E is hysteretic energy in units of force times mm. The calculated coefficients are listed in table 6; in that table, E_{10} indicates hysteretic energy for the 10 hz oscillator, E_4 for the 4 hz oscillator, and so on. For each oscillator, only accelerograms that induced nonlinear behavior in that oscillator were included in the regression analysis; the number of accelerograms for each oscillator is indicated in table 6. The standard errors and multiple correlation coefficients indicate that a_g is most accurate for estimating high frequency energy, PSV_1 is most accurate for intermediate frequencies, and d_g is most accurate for low frequencies. These results are confirmed in figures 59 through 70, which show E_{10}, E_1, and E_4 plotted versus a_g, v_g, d_g, and PSV_1. Note in particular that PSV_1 very accurately estimates E_1 (figure 66), although the relationship is not linear in the logarithms as is assumed by equation (5).

To determine the usefulness of duration in estimating these hysteretic energies, the following equation was used:

$$ln\, E = c_1 + c_2\, ln\, y + c_3\, D \qquad (6)$$

Coefficients are listed in table 7 for E_{10} estimated by a_g and the four durations, for E_1 estimated by PSV_1 and the four durations, and for $E_{1/4}$ estimated by d_g and the four durations. In all cases the coefficients of the duration term are close to zero and the accuracy of the regressions is no better than the accuracy indicated by the corresponding regression without the duration term in table 6. These results are confirmed visually in figures 71 through 82 which show energy normalized by peak parameters plotted versus the four durations. These figures indicate that there is no functional dependence of energy, when normalized by peak parameters, on duration.

VII. CONCLUSIONS

We conclude from this study that none of the four definitions of duration, D_B, D_F, D_{TB}, or D_V, is useful for specification of seismic shaking hazard, when used in addition to peak motion parameters. This conclusion is made in the context of current probabilistic seismic hazard analyses in which estimates of peak motion parameters are available and in which only a magnitude-distance representation of the earthquake is used. Several aspects of this study lead to this conclusion.

First, three of the duration definitions cannot be estimated with accuracy using only earthquake magnitude and distance. The residual dispersion in duration estimated by M and R is even larger than that of peak acceleration, which is notorious for its uncertainty. The fourth duration definition, D_{TB}, can be more accurately estimated but only because, on average, it does not change greatly with M and R. There would be little point in mapping a ground motion characteristic that changes little as a function of the size and distance of earthquakes. A further complication, not examined in detail here but suggested by figures 11 through 26, is that some of the duration measures are not independent of peak parameter values. In particular, longer durations are generally associated with low amplitude motions for durations D_F, D_{TB}, and D_V. Specification of earthquake motion using these duration definitions requires careful scrutiny of the relationship between duration and amplitude to assure that realistic combinations of duration and peak parameters are used for design.

For the quantitative measures of ground motion severity examined here (MM intensity and hysteretic energy of nonlinear oscillators) an estimate of severity can be obtained using an appropriate peak parameter of the ground motion. For the systems examined, a_g is most appropriate for high frequencies, SD_1 for intermediate frequencies, and d_g for low frequencies. Knowledge of ground motion duration in addition to peak motion values does not allow more accurate estimation of the severity of shaking. Thus, even if duration values could be predicted with accuracy, they would not provide useful additional information for the simple methods of design (equivalent lateral force or response spectrum) typically used with seismic hazard maps.

Figure 83 illustrates these points well. It shows two accelerograms recorded in the N-S direction at El Centro during two earthquakes of about the same magnitude and distance. Next to each accelerogram in Figure 83 are shown the peak motion parameters, the calculated values of hysteretic energy for 10, 1, and 1/4 hz systems, and the durations according to the four definitions. Despite the similarity in earthquake size, distance, and site conditions, the records show widely different visual duration characteristics. One of the duration definitions (D_{TB}) calculates a longer duration for the "pulse-type" motion than for the "vibratory" motion. For frequencies of 1 hz and less, the "pulse-type" motion induces larger elastic spectral responses (by a factor of 2) and larger hysteretic energies than does the "vibratory" motion having a similar peak acceleration. Note, however, that the ground displacement correctly predicts the behavior for low frequencies. The response characteristics of these two records are not surprising, given their frequency contents; the point is that peak motion parameters provide a first-order estimate of the frequency content and that simple definitions of duration do not add any useful information.

These results should not be construed to mean that strong motion duration is not important in understanding seismically induced shaking and the resulting damage to structures: of course it is. Rather the point is that the simple definitions of duration examined here are not useful in conjunction with peak amplitudes, for estimating shaking severity using a magnitude-distance representation of the source. It is quite likely that values of duration using other definitions, based perhaps on source characteristics such as the duration of fault rupture, could be estimated with more accuracy than those examined here, which are based on recorded accelerograms.

In studies of duration the quantitative measure of seismic shaking severity should be adopted independently of the definitions of duration being studied, as has been done here. It would be easy to adopt a severity measure that is well correlated with a particular definition of duration, and to conclude that this duration estimates shaking severity accurately. (In an extreme case the two could be perfectly correlated.) Such an exercise would not justify the definition as a useful ground motion characteristic.

The emphasis in this study has been to identify a measure of the duration of shaking that can be used for better design of structures or for more accurately estimating seismically induced damage to existing structures. It is clear that the four definitions studied do not accomplish this. Frequency-based definitions incorporating geophysical characteristics (for example, source properties and potential surface wave generation) should be examined as the next step; doing so will be a major undertaking because of the complicated frequency-based definitions that are available and because data on source properties and geology between the source and the recording site must be assembled for each acceleration record investigated.

REFERENCES

Aptikayev, F. F., 1975, Uchet dlitel'nosti kolebaniy pri instrumental'noy otsenke seysmicheskoy intensivnosti [The bearing of the duration of seismic oscillations on instrumental evaluation of seismic intensity], in Nazarov, A. G., and Shebalin, N. V., eds., Seysmicheskaya shkala i metody izmereniya seismicheskoy intensivnosti [The seismic scale and seismic intensity measurement methods]: Moscow, Izdatel'stvo Nauka, p. 234-239.

Bolt, B. A., 1974, Duration of strong ground motion: World Conference on Earthquake Engineering, 5th, Rome, 1973, Proceedings, p. 1304-1313.

Boore, D. M., Joyner, W. B., Oliver, A. A. III, and Page, R. A., 1978, Estimation of ground motion parameters: U.S. Geological Survey Circular 795, 43 p.

California Institute of Technology, 1971, Strong motion earthquake accelerograms--digitized and plotted data: Earthquake Engineering Research Laboratories, Report. EERL 71-50, v. II, pt. A, and subsequent parts B through Y.

Clough, R. W., and Penzien, Joseph, 1975, Dynamics of structures: New York, McGraw-Hill, 634 p.

Dobry, R., Idriss, I. M., and Ng, E., 1978, Duration characteristics of horizontal components of strong motion earthquake records: Seismological Society of America Bulletin, v. 69, no. 5, p. 1487-1520.

Donovan, N. C., and Bornstein, A. E., 1978, Uncertainties in seismic risk procedures, Journal, Geotechnical Engineering Division, A.S.C.E., v. 104, no. GT7, p. 869-887.

Esteva, Luis, and Rosenblueth, Emilio, 1964, Espectros de temblores a distancias moderadas y grandes: Socieidad Mexicana de Ingenieria Sismica Boletin, v. 2, no. 1, p. 1-18.

Esteva, Luis, and Villaverde, R. 1974, Seismic risk, design spectra, and structural reliability: World Conference on Earthquake Engineering, 5th, Rome 1973, Proceedings, v. 2, p. 2586-2596.

Hays, W. W., 1975, A note on the duration of earthquake and nuclear-explosion ground motions: Seismological Society of America Bulletin, v. 65, no. 4, p. 875-883.

Housner, G.W., 1965, Intensity of earthquake ground shaking near the causative fault: World Conference on Earthquake Engineering, 3rd, Auckland, 1965, Proceedings, v. 1, p. III-94 to III-109.

Housner, G. W., 1970, Strong ground motion: Chapter 4 in Wiegel, R. L., ed., Earthquake engineering: Englewood Cliffs, N.J., Prentice-Hall, p. 75-92.

Husid, Raul, Medina, H., and Rios, J., 1969, Analisis de Terremotos Nortearmericanos y Japoneses: Universidad de Chile, Instituto de Investigaciones y Ensayes de Materiales, Revista, v. 8, p. 55-82.

Kameda, H., and Ang, A. H-S., 1977, Simulation of strong earthquake motions for inelastic structural response: World Conference on Earthquake Engineering, 6th, New Delhi, 1977, Proceedings, p. 2-149 to 2-154.

McCann, M. W. Jr., and Shah, H. C., 1979, Determining strong-motion duration of earthquakes: Seismological Society of America Bulletin, v. 69, no. 4. p. 1253-1265.

McGuire, R. K., 1974, Seismic structural response risk analysis, incorporating peak response regressions on earthquake magnitude and distance: Massachusetts Institute of Technology, Department of Civil Engineers, Report R74-51, 371 p.

McGuire, R. K., 1978, Seismic ground motion parameter relations: Journal, Geotechnical Engineering Division, A.S.C.E., v. 104, no. GT4, p. 481-490.

McGuire, R. K., and Barnhard, J. A., 1977, Magnitude, distance, and intensity data for C.I.T. strong motion records: U.S. Geological Survey, Journal of Research, v. 5, no. 4, p. 437-443.

Perez, V., Time dependent spectral analysis of thirty-one strong motion earthquake records: U.S. Geological Survey, Open-File Report, November 1974, 33 p.

Trifunac, M. D., and Brady, A. G., 1975, A study on the duration of strong earthquake ground motion: Seismological Society of America Bulletin, v. 65, no. 3, p. 581-626.

Trifunac, M. D., and Westermo, B., 1977, A note on the correlation of frequency-dependent duration of strong earthquake ground motion with the Modified Mercalli Intensity and the geologic conditions at the recording stations: Seismological Society of America Bulletin, v. 67, no. 3, p. 917-927.

U.S. Geological Survey, 1977, Western Hemisphere strong-motion accelerograph station list: U.S. Geological Survey Open-File Report 77-374, 112 p.

Vanmarcke, E. H., and Lai, S. P., 1977, Strong-motion duration of earthquakes: Massachusetts Institute of Technology, Department of Civil Engineering, Report R77-16, 32 p.

Symbols used in tables and figures

a_g - peak ground acceleration (cm/sec)

C - distance constant in attenuation equation

c_{1-5} - coefficient in attenuation equation

D_B - bracketed duration (Bolt, 1975)

D_F - fractional duration (Aptikayev, 1975)

D_{TB} - Trifunac-Brady (1975) duration

D_V - Vanmarcke and Lai (1977) duration

d_g - peak ground displacement (cm)

E_f - hysteretic energy (force times mm) absorbed by oscillator with initial frequency f

M - earthquake magnitude

MMI - modified Mercalli intensity

PSV_1 - peak pseudo-velocity (cm/sec) at linear oscillator with 1 hz frequency and 2% damping

R - distance (km)

$\mathcal{R}$ - multiple correlation coefficient

S - variable indicating soil conditions

SD_f - spectral displacement (cm) at linear oscillator with frequency f and 2% damping

σ - standard deviation of residuals

V - variable indicating component direction (horizontal or vertical)

v_g - peak ground velocity (cm/sec)

y - peak motion parameter (a_g, v_g, d_g, or PSV_1)

Table 1.--Strong motion records used.

RECORD NUMBER	MAGNITUDE	DISTANCE,km	SOIL CATEGORY	SITE MM INTENSITY
A001	6.4	12.0	ALLUV.	7.5
A002	6.0	53.0	ALLUV.	5.0
A003	7.2	109.0	ALLUV.	7.0
A004	7.2	42.0	ALLUV.	7.0
A005	7.2	85.0	ALLUV.	7.0
A006	7.2	107.0	ALLUV.	7.0
A007	7.2	107.0	ALLUV.	7.0
A008	6.6	24.0	ALLUV.	7.0
A009	6.6	40.0	ALLUV.	7.0
A010	5.8	9.6	ALLUV.	7.0
A014	5.3	14.0	ALLUV.	6.0
A015	5.3	8.0	ROCK	6.0
A016	5.3	12.0	ALLUV.	6.0
A017	5.3	24.0	ALLUV.	6.0
A018	5.6	11.0	ALLUV.	7.0
A019	6.5	45.0	ALLUV.	6.0
A020	6.5	105.0	ALLUV.	6.0
B021	6.3	53.0	ALLUV.	6.0
B024	6.5	64.0	ALLUV.	6.0
B026	5.5	55.0	ALLUV.	6.0
B027	6.6	104.0	ALLUV.	6.0
B030	5.4	43.0	ALLUV.	6.0
B034	5.3	9.3	ALLUV.	6.0
B035	5.3	13.0	ALLUV.	6.0
B036	5.3	17.3	ALLUV.	6.0
B037	5.3	16.0	ROCK	6.0
B038	5.3	63.6	ROCK	6.0
B039	5.8	51.0	ALLUV.	5.0
B040	6.5	122.0	ROCK	5.0
C048	6.4	7.7	ALLUV.	7.0
D056	6.4	26.0	ROCK	6.0
E071	6.4	82.0	ALLUV.	5.0
M183	6.4	59.0	ROCK	5.0
P221	6.4	26.0	ROCK	6.0
U299	5.9	16.0	ALLUV.	8.0
U307	5.0	11.0	ALLUV.	6.0
V314	6.3	59.0	ROCK	7.0
V315	6.3	6.0	ALLUV.	8.0
V316	5.4	6.0	ALLUV.	6.0
V317	5.4	27.0	ALLUV.	6.0
V319	6.0	77.0	ROCK	6.0
V329	5.0	6.0	ALLUV.	6.0
V331	4.5	18.0	ROCK	5.0
W334	5.4	15.0	ROCK	6.0
W335	5.4	18.0	ROCK	5.5
W336	5.4	18.0	ROCK	5.5
W342	5.4	57.0	ALLUV.	5.0
Y371	6.5	157.0	ALLUV.	5.0
Y377	6.5	218.0	ROCK	5.0
Y378	6.5	203.0	ROCK	5.0

Table 2.--Coefficients from regression analyses for peak acceleration (a_g), velocity (v_g), and displacement (d_g).

$$\ln y = c_1 + c_2 M + c_3 S + c_4 V + c_5 \ln(R+C)$$

y	c_1	c_2	c_3	c_4	$c_5 \ln(R+C)$	$\sigma_{\ln y}$	$\mathscr{R}$
a_g	2.2	0.89	-0.21	-0.72	-0.90 $\ln R$	0.70	0.75
a_g	3.6	0.97	-0.23	-0.72	-1.30 $\ln(R+10)$	0.66	0.78
a_g	5.7	0.99	-0.25	-0.72	-1.70 $\ln(R+25)$	0.64	0.79
a_g	7.8	0.99	-0.25	-0.72	-2.10 $\ln(R+40)$	0.63	0.80
v_g	-2.6	1.2	0.061	-0.82	-0.73 $\ln R$	0.66	0.77
v_g	-1.5	1.2	0.058	-0.82	-1.0 $\ln(R+10)$	0.65	0.78
v_g	0.16	1.2	0.055	-0.82	-1.3 $\ln(R+25)$	0.65	0.78
v_g	1.70	1.2	0.054	-0.82	-1.6 $\ln(R+40)$	0.65	0.78
d_g	-4.4	1.2	0.18	-0.54	-0.54 $\ln R$	0.65	0.75
d_g	-3.5	1.2	0.19	-0.54	-0.74 $\ln(R+10)$	0.64	0.75
d_g	-2.3	1.2	0.18	-0.54	-0.97 $\ln(R+25)$	0.64	0.75
d_g	-1.2	1.2	0.18	-0.54	-1.20 $\ln(R+40)$	0.65	0.75

a_g, v_g, and d_g are in units of cm and sec; R is in km.

Table 3.--Coefficients from regression analyses for spectral displacement (SD_f).

$$\ell n\ y = c_1 + c_2M + c_3S + c_4V + c_5\ell n(R+C)$$

y	c_1	c_2	c_3	c_4	$c_5\ \ell n(R+C)$	$\sigma_{\ell n\ y}$	$\mathcal{R}$
SD_{10}	-4.4	0.81	-0.41	-0.34	-1.0 ℓnR	0.80	0.71
SD_{10}	-2.8	0.91	-0.44	-0.34	-1.5 ℓn(R+10)	0.74	0.76
SD_{10}	-0.33	0.95	-0.47	-0.34	-2.0 ℓn(R+25)	0.70	0.78
SD_{10}	+2.1	0.96	-0.48	-0.34	-2.5 ℓn(R+40)	0.69	0.80
SD_4	-3.3	0.90	-0.07	-0.77	-0.90 ℓnR	0.74	0.73
SD_4	-1.9	0.98	-0.10	-0.77	-1.3 ℓn(R+10)	0.69	0.77
SD_4	+0.29	1.0	-0.12	-0.77	-1.8 ℓn(R+25)	0.67	0.79
SD_4	+2.5	1.0	-0.13	-0.77	-2.2 ℓn(R+40)	0.65	0.80
SD_2	-3.6	1.0	0.18	-0.89	-0.72 ℓnR	0.72	0.73
SD_2	-2.5	1.1	0.17	-0.89	-1.0 ℓn(R+10)	0.70	0.75
SD_2	-0.80	1.1	0.16	-0.89	-1.4 ℓn(R+25)	0.69	0.76
SD_2	+0.86	1.1	0.15	-0.89	-1.7 ℓn(R+40)	0.69	0.76
SD_1	-4.9	1.3	0.37	-0.87	-0.66 ℓnR	0.73	0.77
SD_1	-3.9	1.3	0.37	-0.87	-0.91 ℓn(R+10)	0.73	0.77
SD_1	-2.4	1.3	0.37	-0.87	-1.2 ℓn(R+25)	0.73	0.77
SD_1	-1.0	1.3	0.36	-0.87	-1.5 ℓn(R+40)	0.73	0.77
$SD_{.5}$	-5.5	1.4	0.36	-0.76	-0.60 ℓnR	0.82	0.75
$SD_{.5}$	-4.6	1.4	0.37	-0.76	-0.80 ℓn(R+10)	0.82	0.74
$SD_{.5}$	-3.3	1.4	0.37	-0.76	-1.0 ℓn(R+25)	0.83	0.74
$SD_{.5}$	-2.2	1.4	0.38	-0.76	-1.2 ℓn(R+40)	0.83	0.73
$SD_{.25}$	-4.9	1.4	0.26	-0.69	-0.57 ℓnR	0.77	0.75
$SD_{.25}$	-4.0	1.4	0.27	-0.69	-0.77 ℓn(R+10)	0.77	0.75
$SD_{.25}$	-2.8	1.4	0.27	-0.69	-0.99 ℓn(R+25)	0.78	0.75
$SD_{.25}$	-1.7	1.4	0.27	-0.69	-1.2 ℓn(R+40)	0.78	0.74

SD_f is in cm; R is in km

Table 4.--Coefficients from regression analysis for duration (D).

$$\ell n D = c_1 + c_2 M + c_3 S + c_4 V + c_5 \ell n R$$

D	c_1	c_2	c_3	c_4	c_5	$\sigma_{\ell n D}$	$\mathscr{R}$
D_B*	-7.7	2.0	.20	-.16	-1.27	2.0	0.49
D_F	-4.5	.74	.36	.31	.37	.99	0.49
D_{TB}	0.19	.15	.73	.23	.35	.47	0.75
D_V	-3.0	.56	.47	.21	.34	.71	0.70

* Only 82 nonzero components of motion used

Table 5.--Coefficients from regression analysis for MM intensity

$$MMI = c_1 + c_2 \ln y + c_3 S + c_4 V + c_5 D$$

y	c_1	c_2	c_3	c_4	c_5 D	σ_{MMI}	$\mathscr{R}$
a_g	4.0	0.42	0.54	0.30		0.62	0.63
a_g	4.2	0.34	0.52	0.29	0.022 D_B	0.61	0.64
a_g	3.6	0.49	0.49	0.30	0.017 D_F	0.61	0.66
a_g	3.7	0.46	0.47	0.30	0.007 D_{TB}	0.62	0.64
a_g	3.5	0.51	0.46	0.31	0.020 D_V	0.60	0.67
v_g	4.9	0.49	0.39	0.40		0.59	0.67
v_g	4.9	0.44	0.39	0.39	0.010 D_B	0.59	0.67
v_g	4.9	0.48	0.39	0.41	-0.0021 D_F	0.60	0.67
v_g	5.0	0.47	0.46	0.42	-0.0061 D_{TB}	0.59	0.68
v_g	4.9	0.49	0.39	0.40	-0.0017 D_V	0.60	0.67
d_g	5.4	0.44	0.38	0.24		0.63	0.61
d_g	5.4	0.34	0.40	0.23	0.024 D_B	0.62	0.63
d_g	5.4	0.45	0.39	0.27	-0.0093 D_F	0.63	0.62
d_g	5.5	0.44	0.51	0.30	-0.013 D_{TB}	0.61	0.64
d_g	5.4	0.45	0.40	0.27	-0.0098 D_V	0.63	0.62
PSV_1	4.8	0.45	0.27	0.39		0.60	0.67
PSV_1	4.8	0.39	0.29	0.37	0.016 D_B	0.59	0.67
PSV_1	4.8	0.45	0.28	0.41	-0.0051 D_F	0.60	0.67
PSV_1	4.9	0.44	0.37	0.42	-0.0088 D_{TB}	0.59	0.68
PSV_1	4.9	0.45	0.29	0.41	-0.0060 D_V	0.60	0.67

a_g, v_g, d_g, and PSV_1 are in units of cm and sec.

Table 6.--Coefficients from regression analysis for hysteretic energy (E) using peak parameters.

$$\ell n\ E = c_1 + c_2\ \ell n\ y$$

No. of Records	E	c_1	$c_2\ \ell n\ y$	σ	$\mathscr{R}$
63	E_{10}	0.93	1.6 $\ell n\ a_g$	1.1	0.69
63	E_{10}	7.0	0.80 $\ell n\ v_g$	1.3	0.45
63	E_{10}	8.1	0.61 $\ell n\ d_g$	1.4	0.38
63	E_{10}	7.2	0.61 $\ell n\ PSV_1$	1.4	0.41
63	E_4	-0.81	2.1 $\ell n\ a_g$	1.2	0.69
63	E_4	6.5	1.3 $\ell n\ v_g$	1.4	0.57
63	E_4	8.6	0.74 $\ell n\ d_g$	1.6	0.38
63	E_4	7.2	0.84 $\ell n\ PSV_1$	1.5	0.43
47	E_2	1.2	1.8 $\ell n\ a_g$	1.3	0.62
47	E_2	5.9	1.6 $\ell n\ v_g$	1.3	0.63
47	E_2	9.3	0.64 $\ell n\ d_g$	1.5	0.32
47	E_2	5.1	1.6 $\ell n\ PSV_1$	1.3	0.57
47	E_1	5.1	1.0 $\ell n\ a_g$	1.5	0.39
47	E_1	4.8	1.9 $\ell n\ v_g$	1.3	0.63
47	E_1	7.6	1.4 $\ell n\ d_g$	1.4	0.55
47	E_1	-2.9	3.7 $\ell n\ PSV_1$	0.81	0.87
54	$E_{1/2}$	5.2	1.0 $\ell n\ a_g$	1.8	0.45
54	$E_{1/2}$	4.5	2.1 $\ell n\ v_g$	1.4	0.69
54	$E_{1/2}$	6.1	2.2 $\ell n\ d_g$	1.3	0.73
54	$E_{1/2}$	4.1	1.8 $\ell n\ PSV_1$	1.6	0.61
80	$E_{1/4}$	5.8	0.72 $\ell n\ a_g$	1.7	0.35
80	$E_{1/4}$	5.2	1.7 $\ell n\ v_g$	1.4	0.66
80	$E_{1/4}$	5.6	2.1 $\ell n\ d_g$	1.1	0.81
80	$E_{1/4}$	5.1	1.3 $\ell n\ PSV_1$	1.5	0.56

E is in units of force times mm; a_g, v_g, d_g, and PSV_1 are in cm and sec.

Table 7.--Coefficients from regression analysis for hysteretic energy (E) using peak parameters and duration.

$$\ell n\ E=c_1+c_2\ \ell n\ y+c_3\ D$$

E	c_1	$c_2\ \ell n$ Y	c_3 D	σ	$\mathscr{R}$
E_{10}	2.11	1.33 $\ell n\ a_g$	0.52 D_B	1.04	0.72
E_{10}	-0.13	1.8 $\ell n\ a_g$	0.077 D_F	1.01	0.74
E_{10}	1.6	1.6 $\ell n\ a_g$	-0.027 D_{TB}	1.06	0.71
E_{10}	-0.17	1.8 $\ell n\ a_g$	0.061 D_V	1.04	0.72
E_1	-3.2	3.8 $\ell n\ PSV_1$	.017 D_B	0.79	0.88
E_1	-1.7	3.3 $\ell n\ PSV_1$	.037 D_F	0.81	0.88
E_1	-3.2	3.7 $\ell n\ PSV_1$	.022 D_{TB}	0.78	0.89
E_1	-3.2	3.8 $\ell n\ PSV_1$	.016 D_V	0.81	0.88
$E_{1/4}$	3.7	2.1 $\ell n\ d_g$	.010 D_B	1.07	0.81
$E_{1/4}$	- .70	1.4 $\ell n\ d_g$	.033 D_F	1.06	0.81
$E_{1/4}$	2.9	2.2 $\ell n\ d_g$	.026 D_{TB}	1.01	0.83
$E_{1/4}$	3.3	2.2 $\ell n\ d_g$	.025 D_V	1.04	0.82

E is in units of force times mm; a_g, PSV_1, and d_g are in cm and sec.

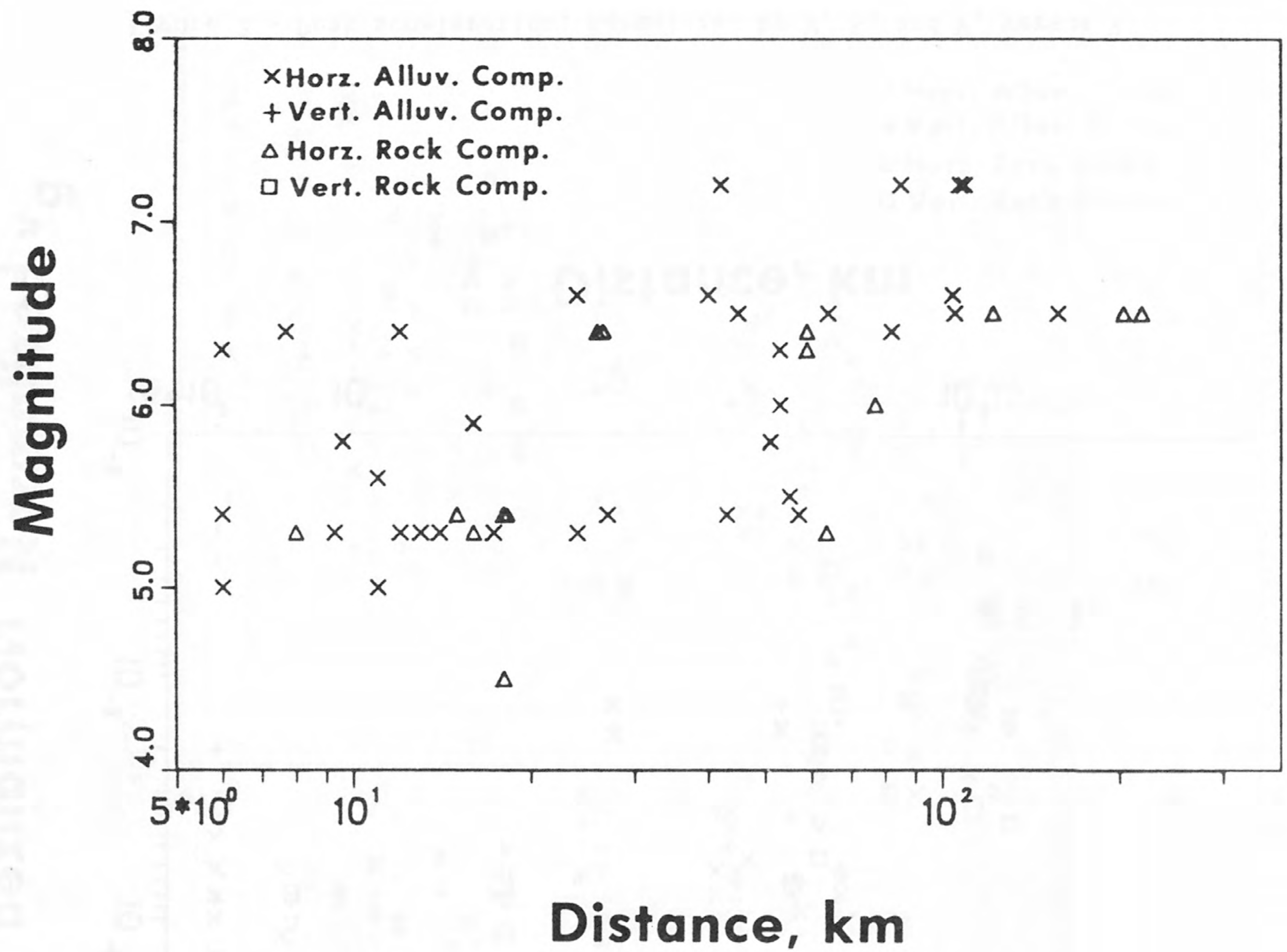

Figure 1.--Magnitudes and distances of strong motion records.

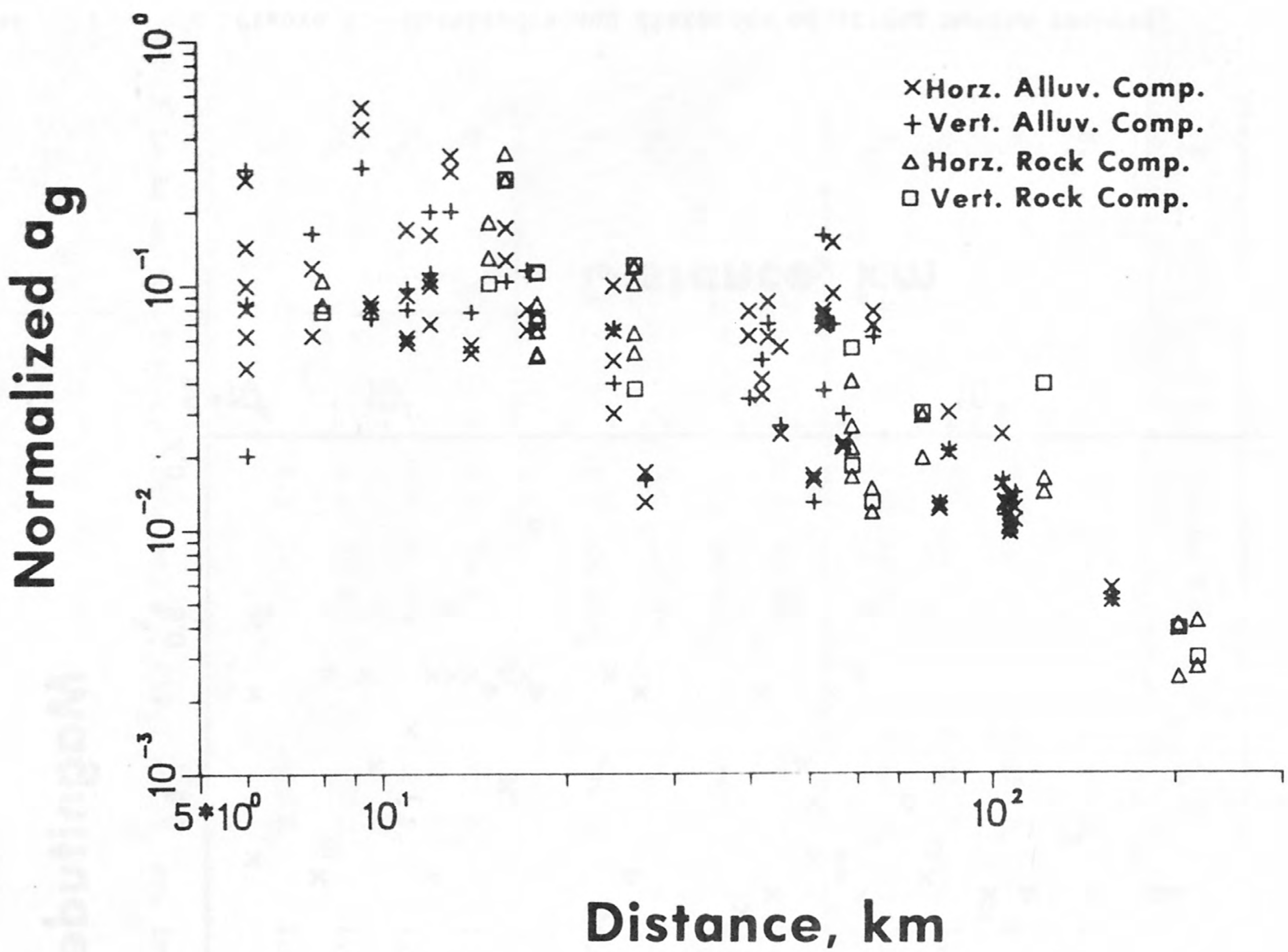

Figure 2.--Peak acceleration, normalized by M, S, and V, versus R.

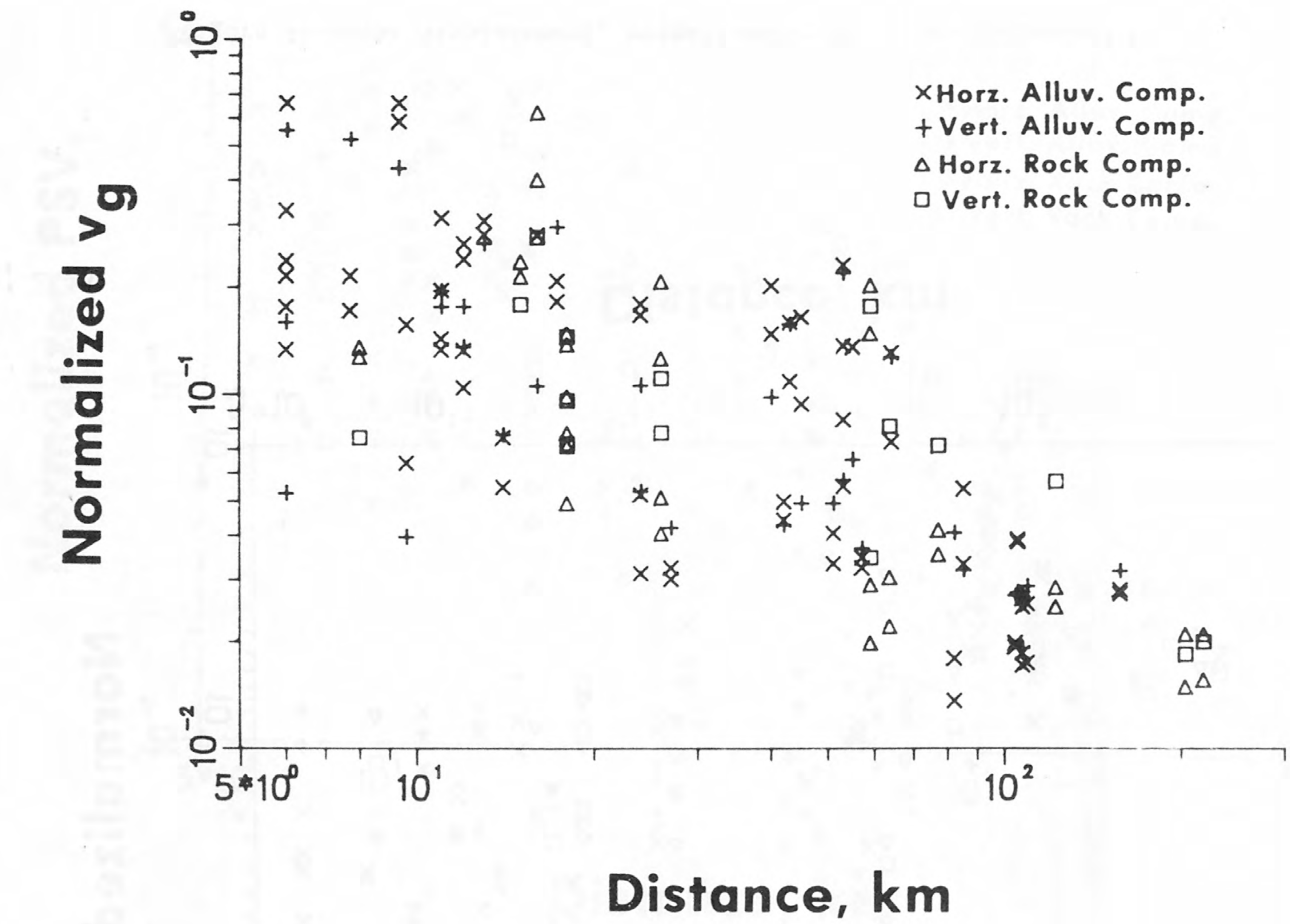

Figure 3.--Peak velocity, normalized by M, S, and V, versus R.

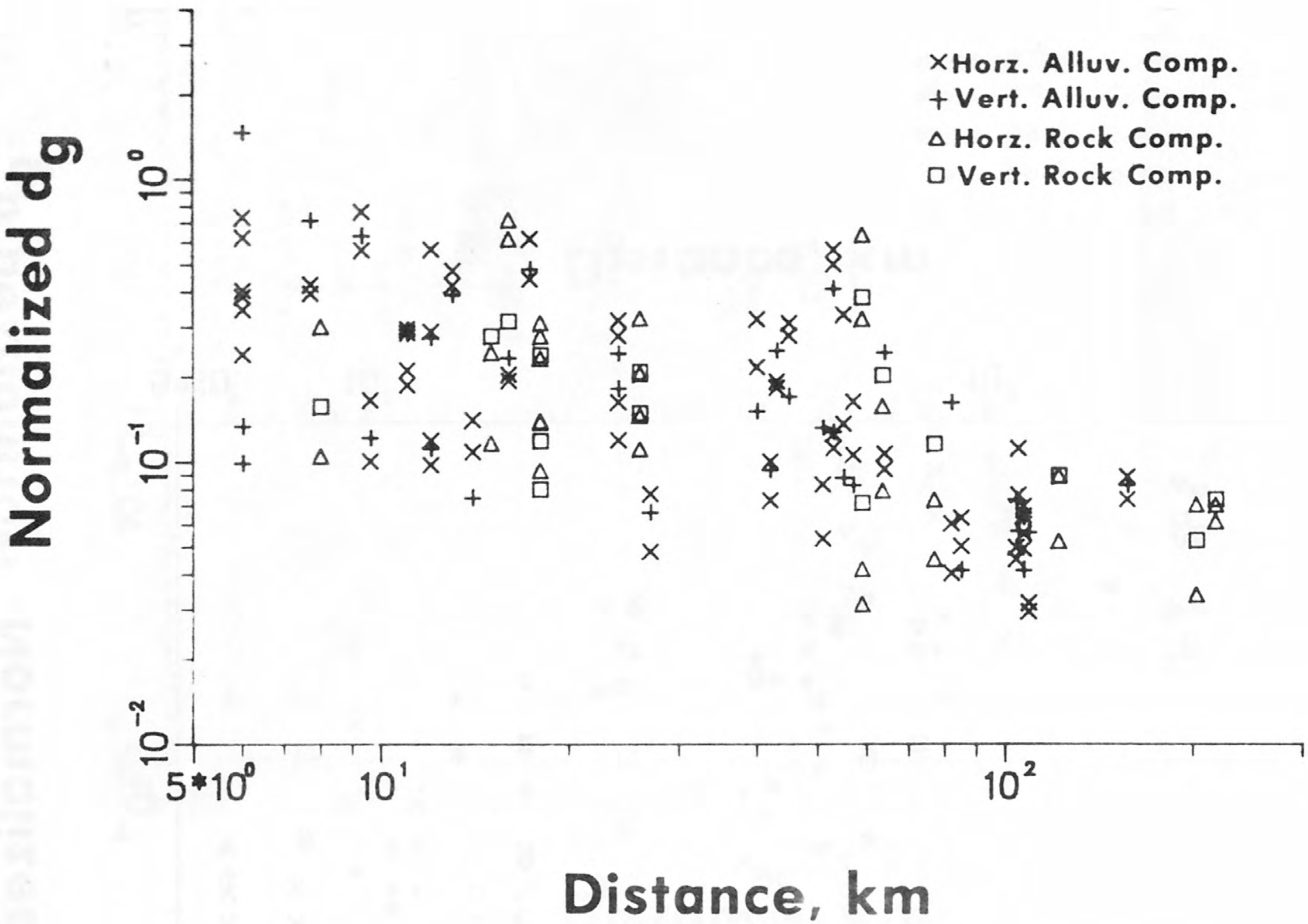

Figure 4.--Peak displacement, normalized by M, S, and V, versus R.

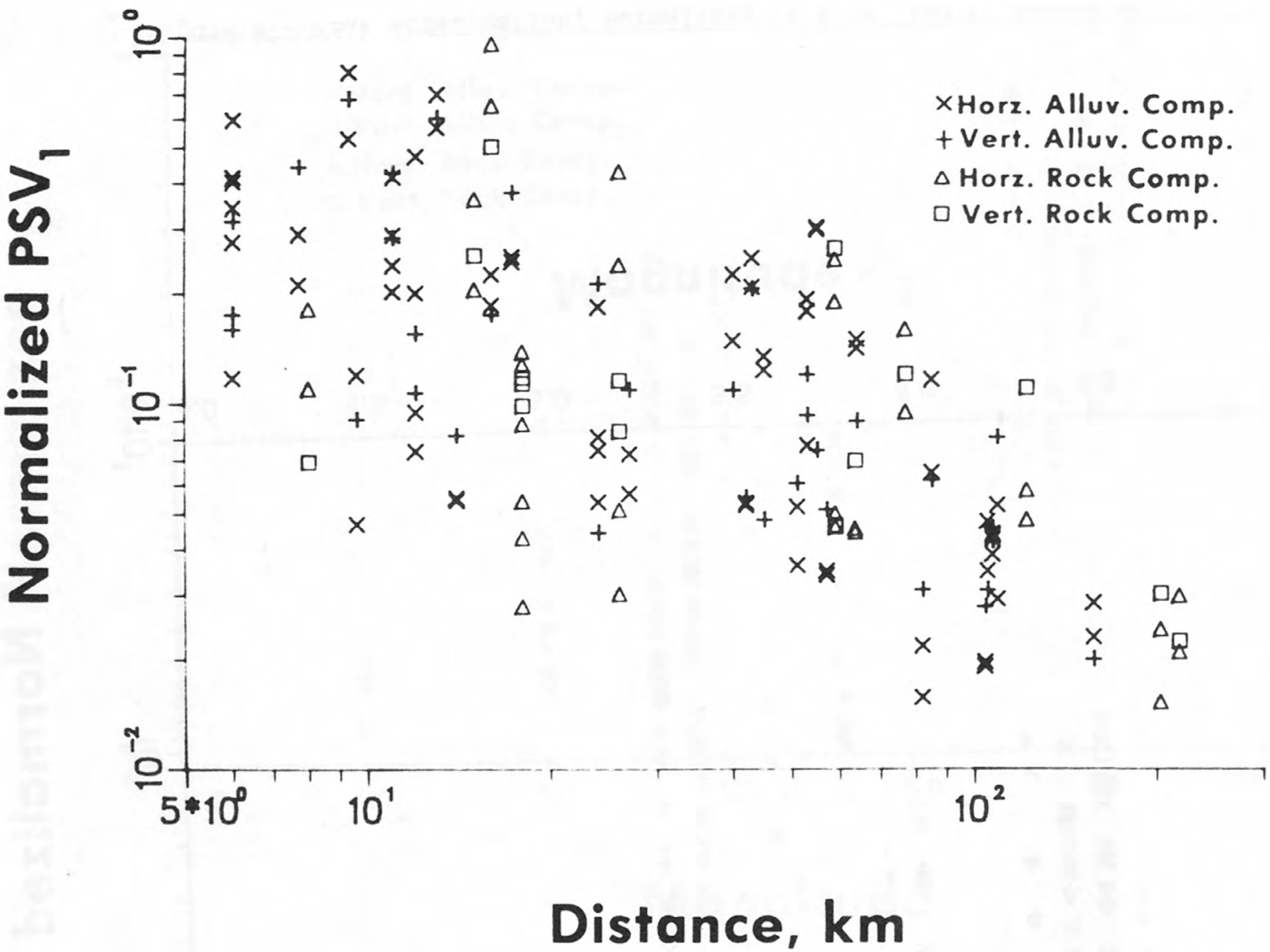

Figure 5.--Spectral velocity PSV_1, normalized by M, S, and V, versus R.

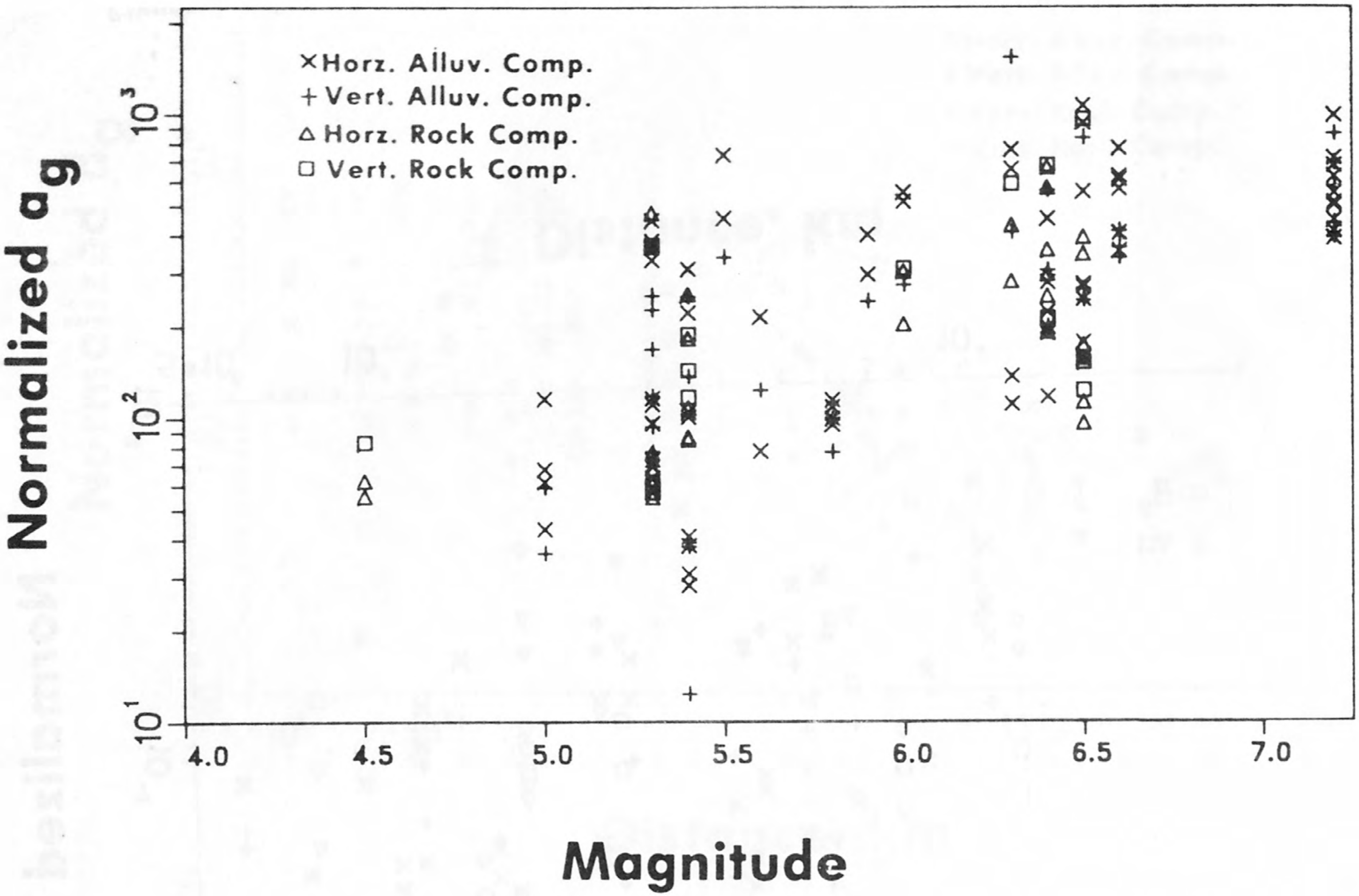

Figure 6.--Peak acceleration, normalized by R, S, and V, versus M.

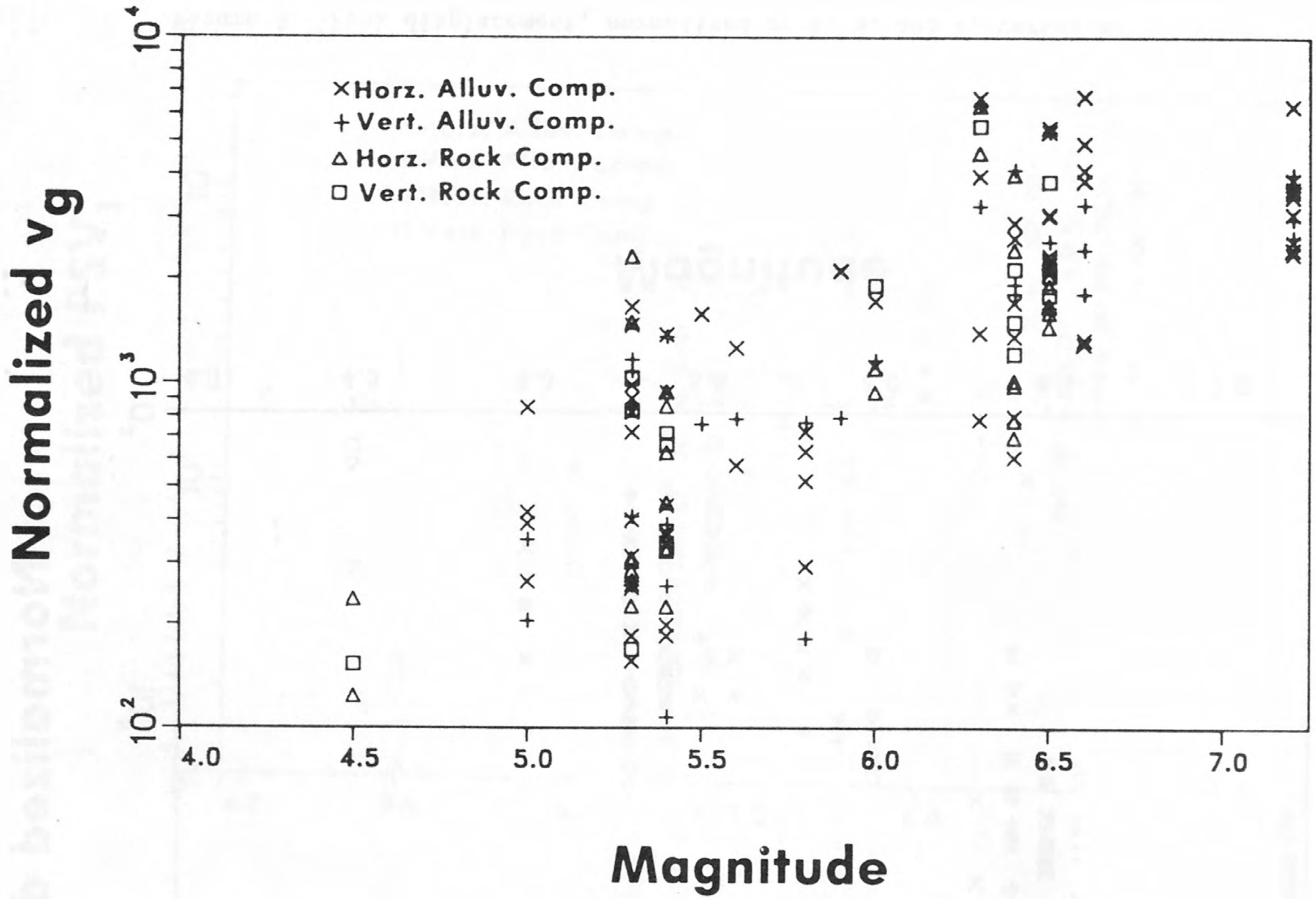

Figure 7.--Peak velocity, normalized by R, S, and V, versus M.

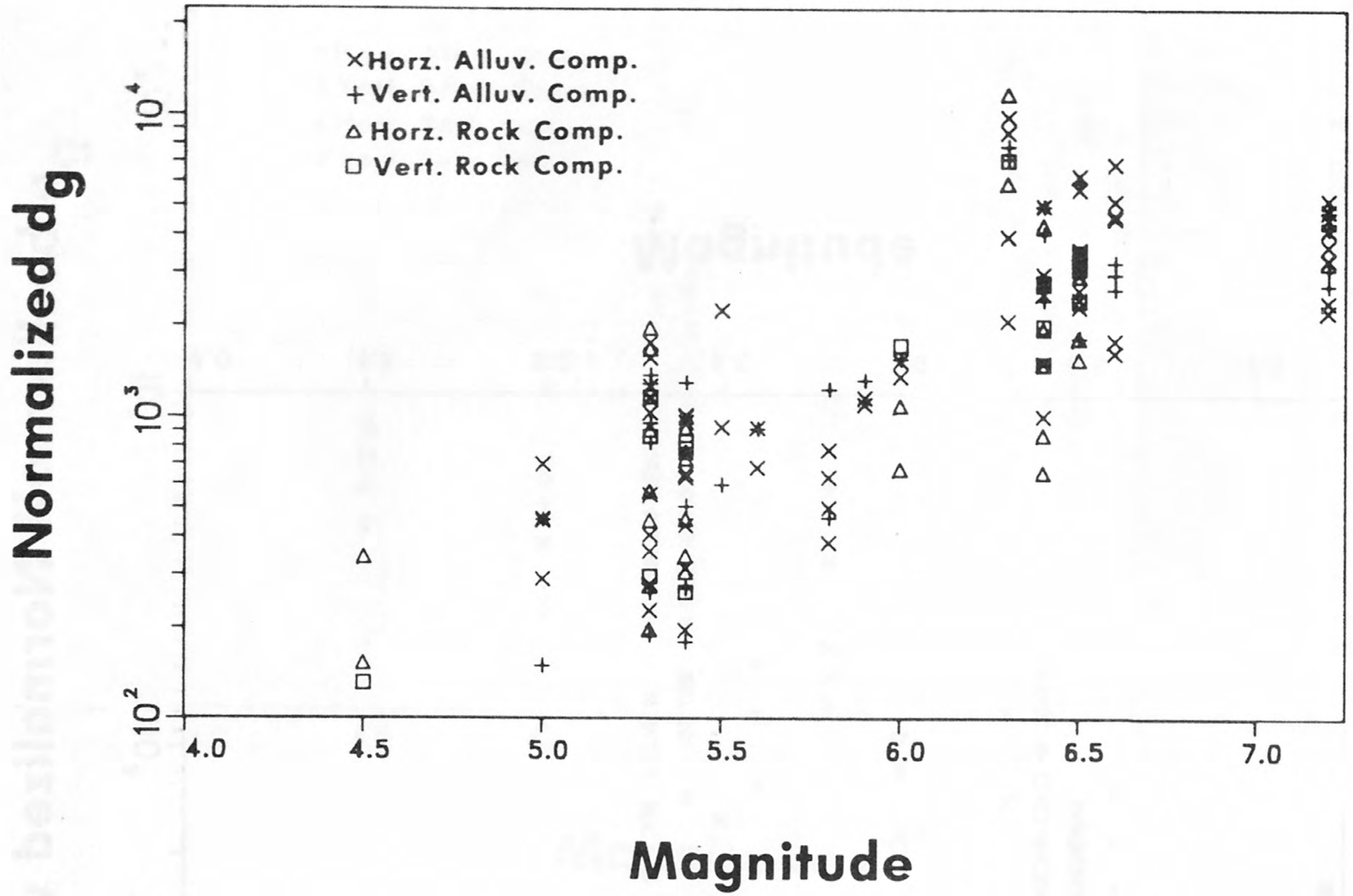

Figure 8.--Peak displacement, normalized by R, S, and V, versus M.

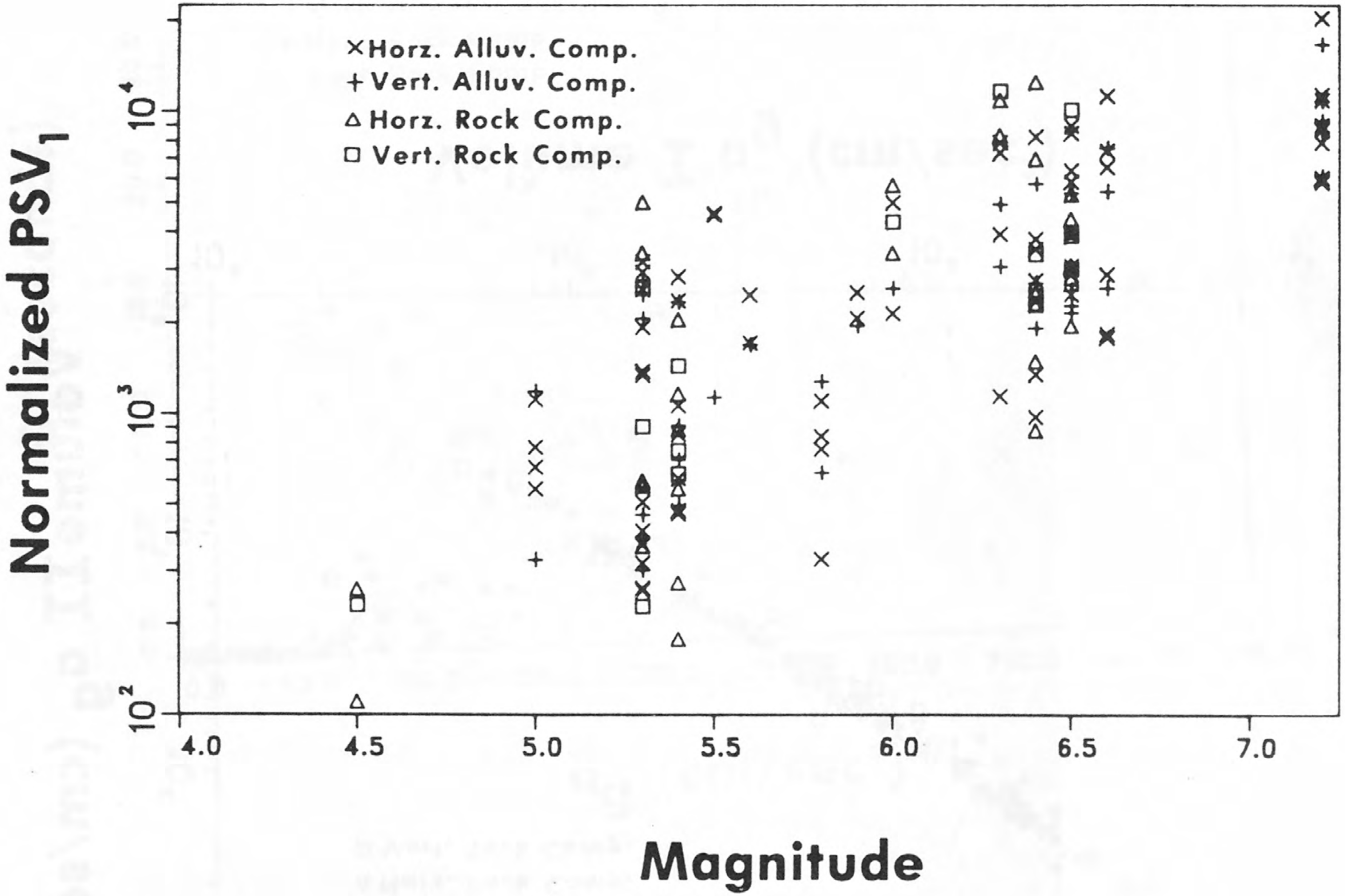

Figure 9.--Spectral velocity PSV_1, normalized by R, S, and V, versus M.

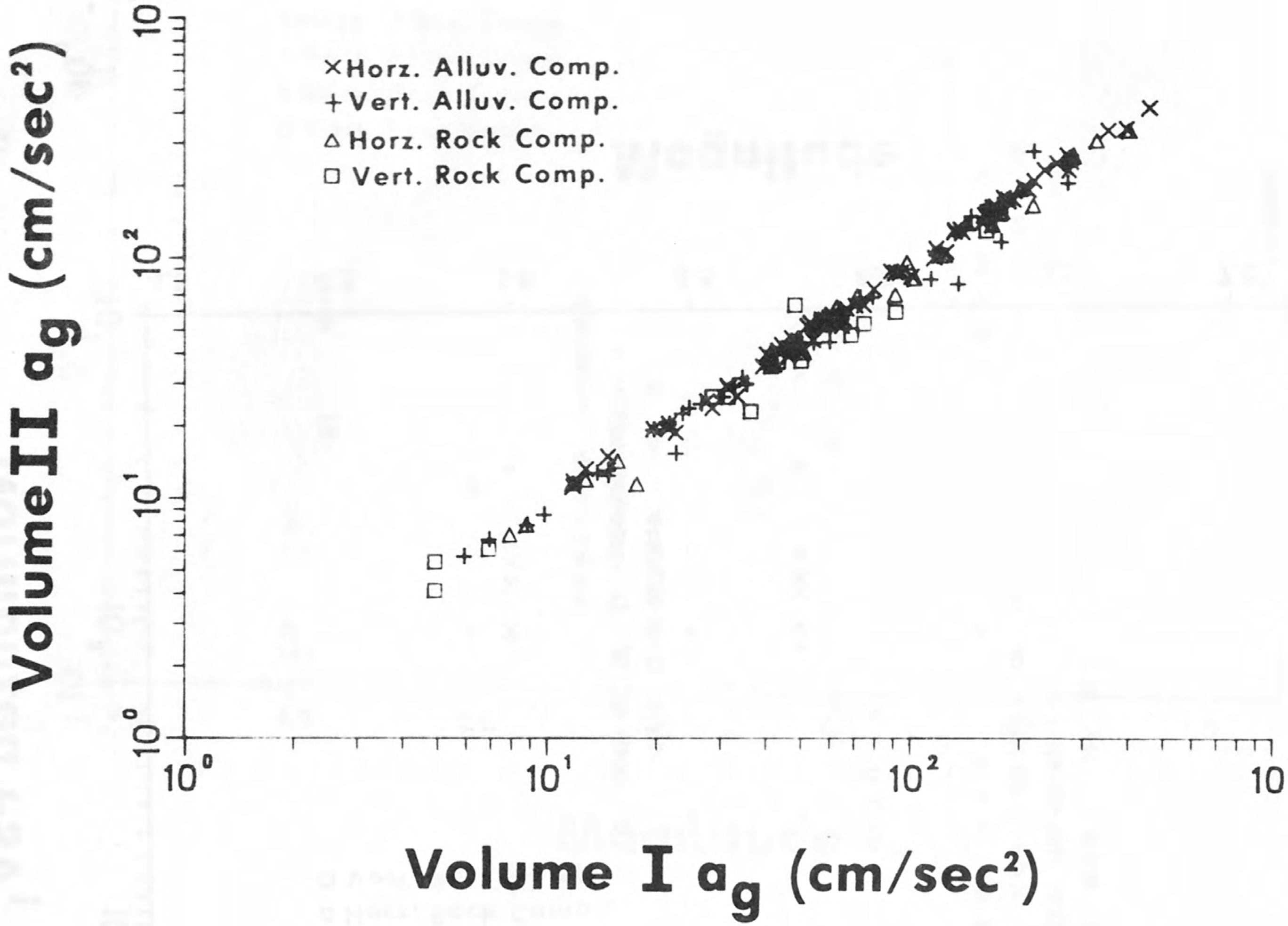

Figure 10.--Volume II value of a_g plotted versus Volume I value.

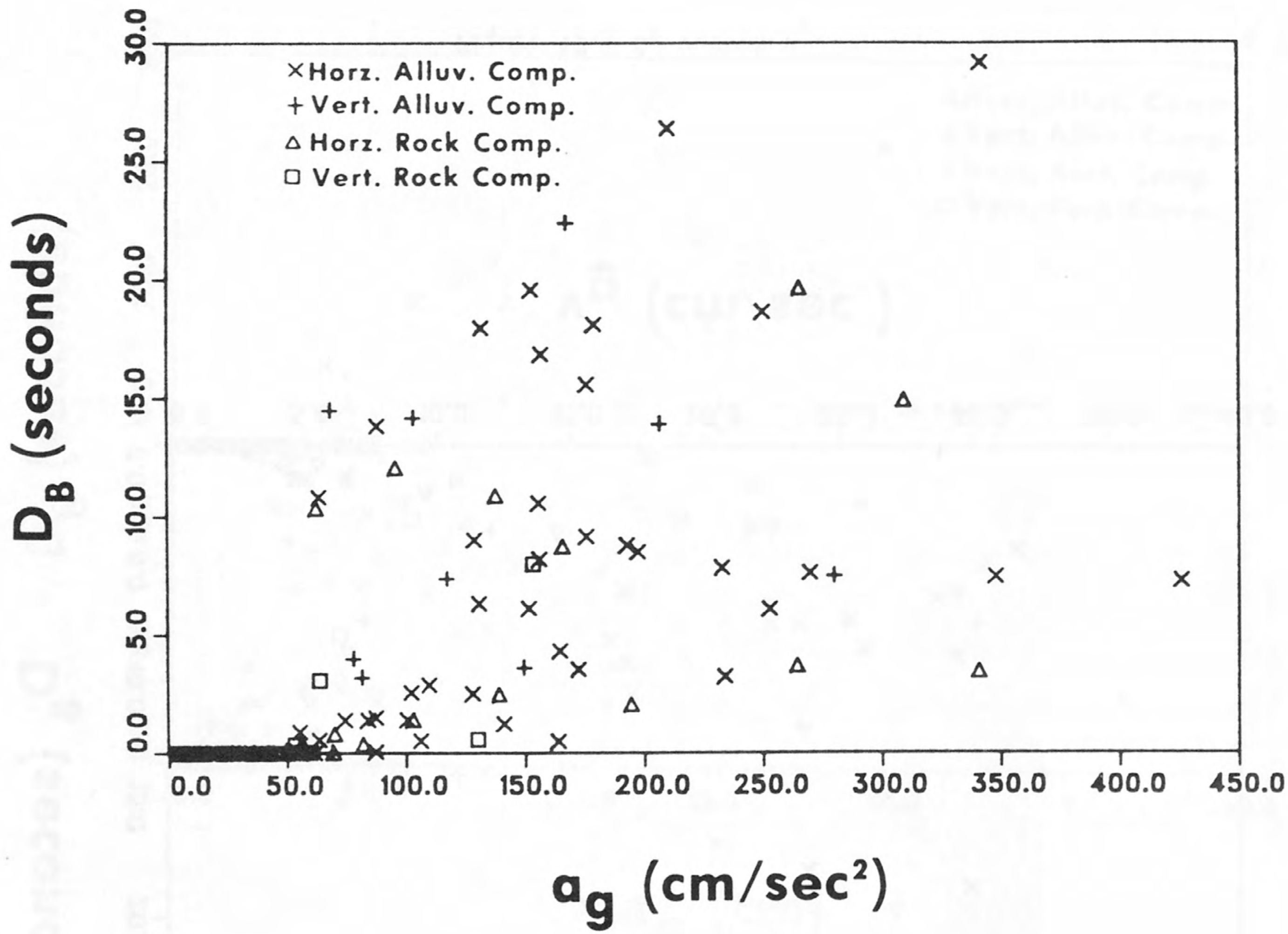

Figure 11.--D_B versus a_g.

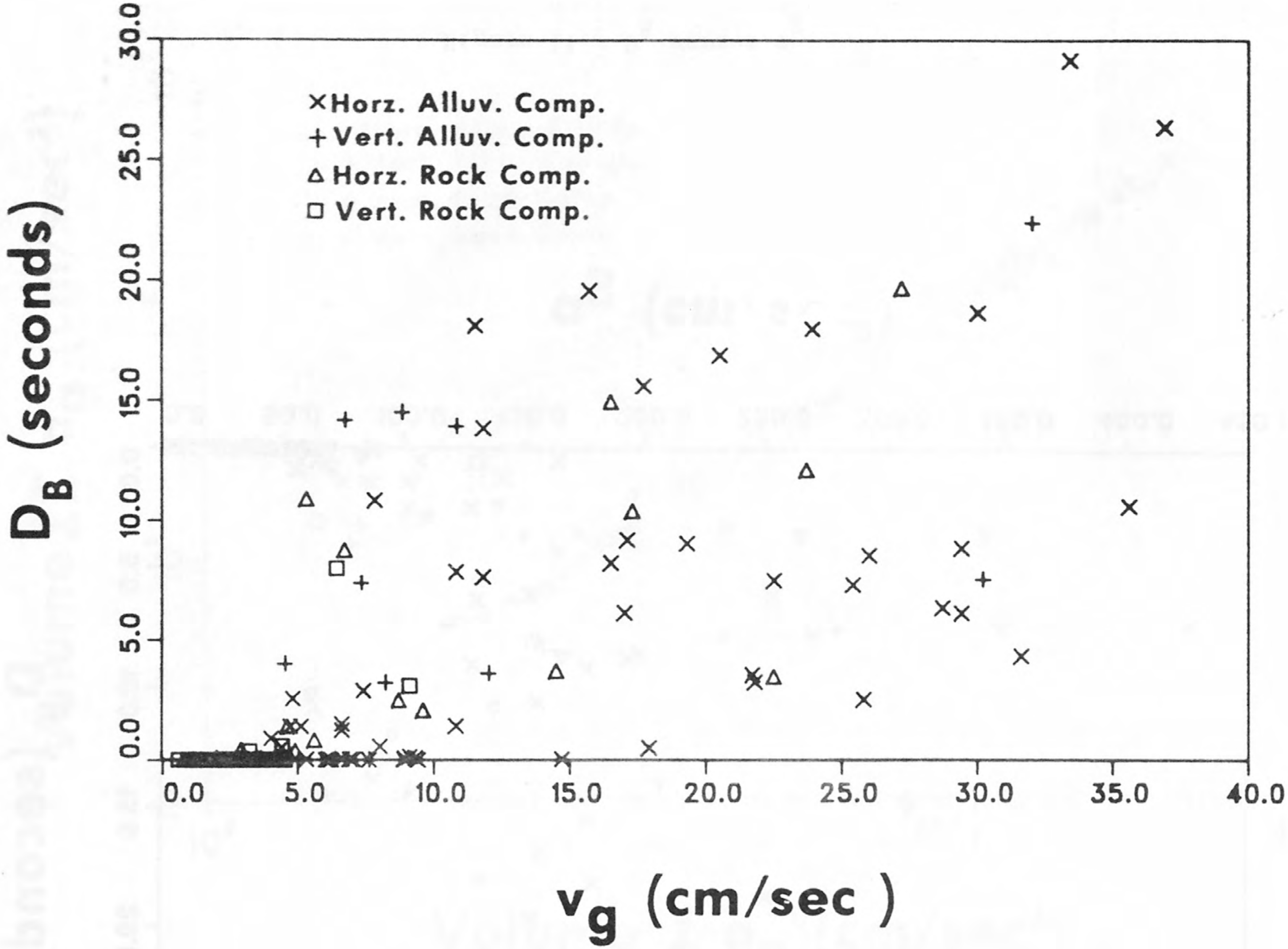

Figure 12.--D_B versus v_g.

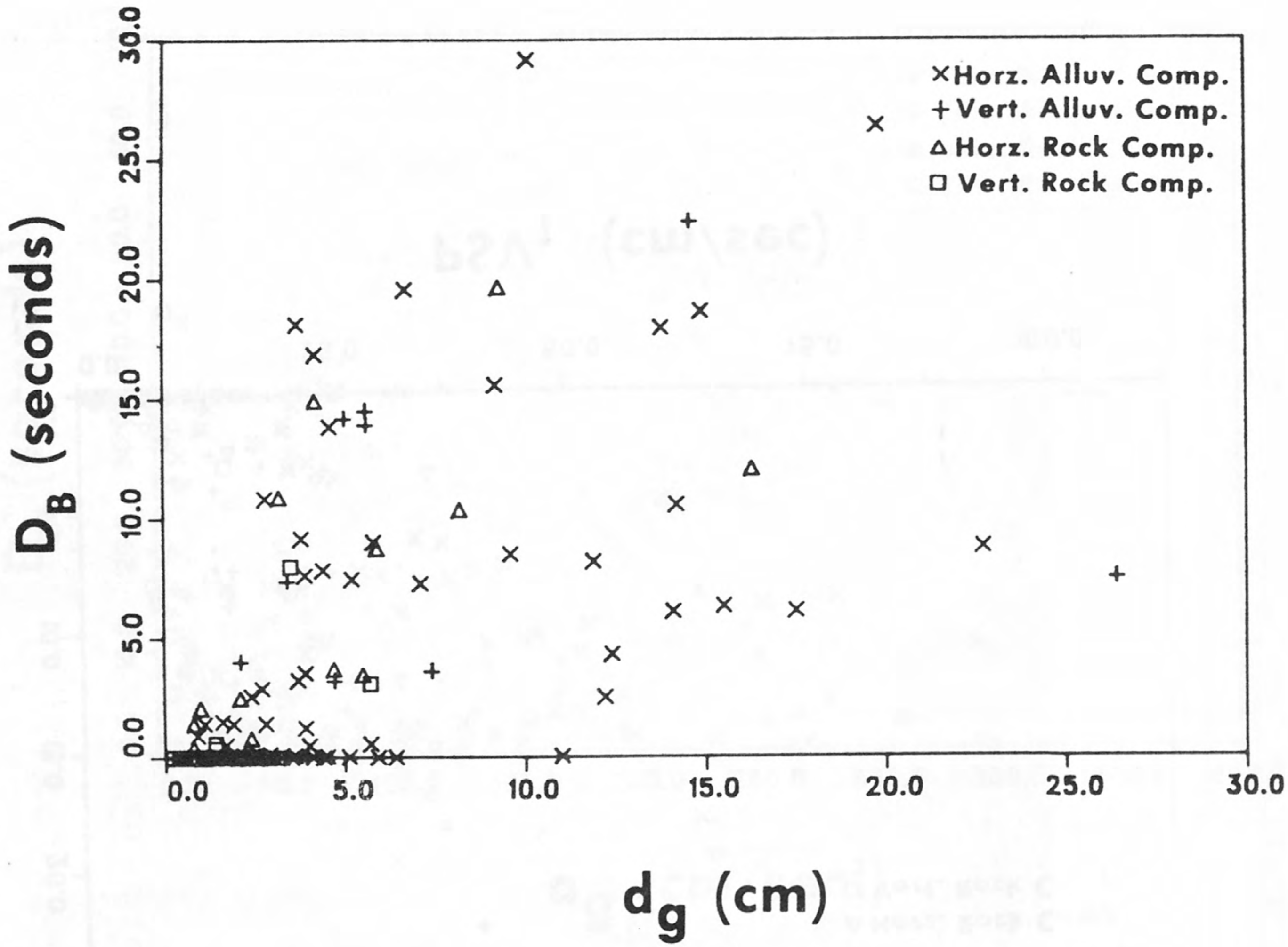

Figure 13.--D_B versus d_g.

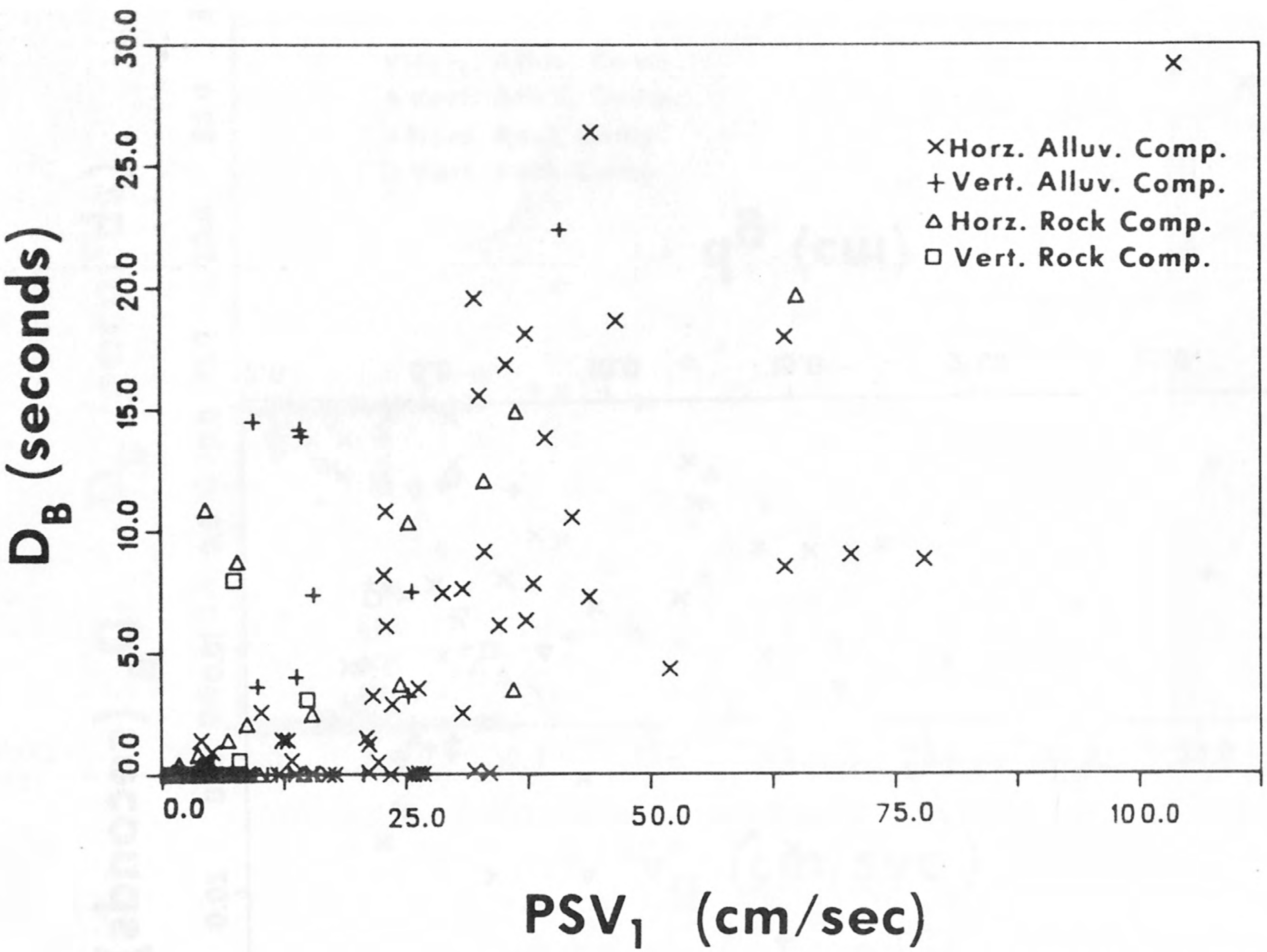

Figure 14.--D_B versus PSV_1.

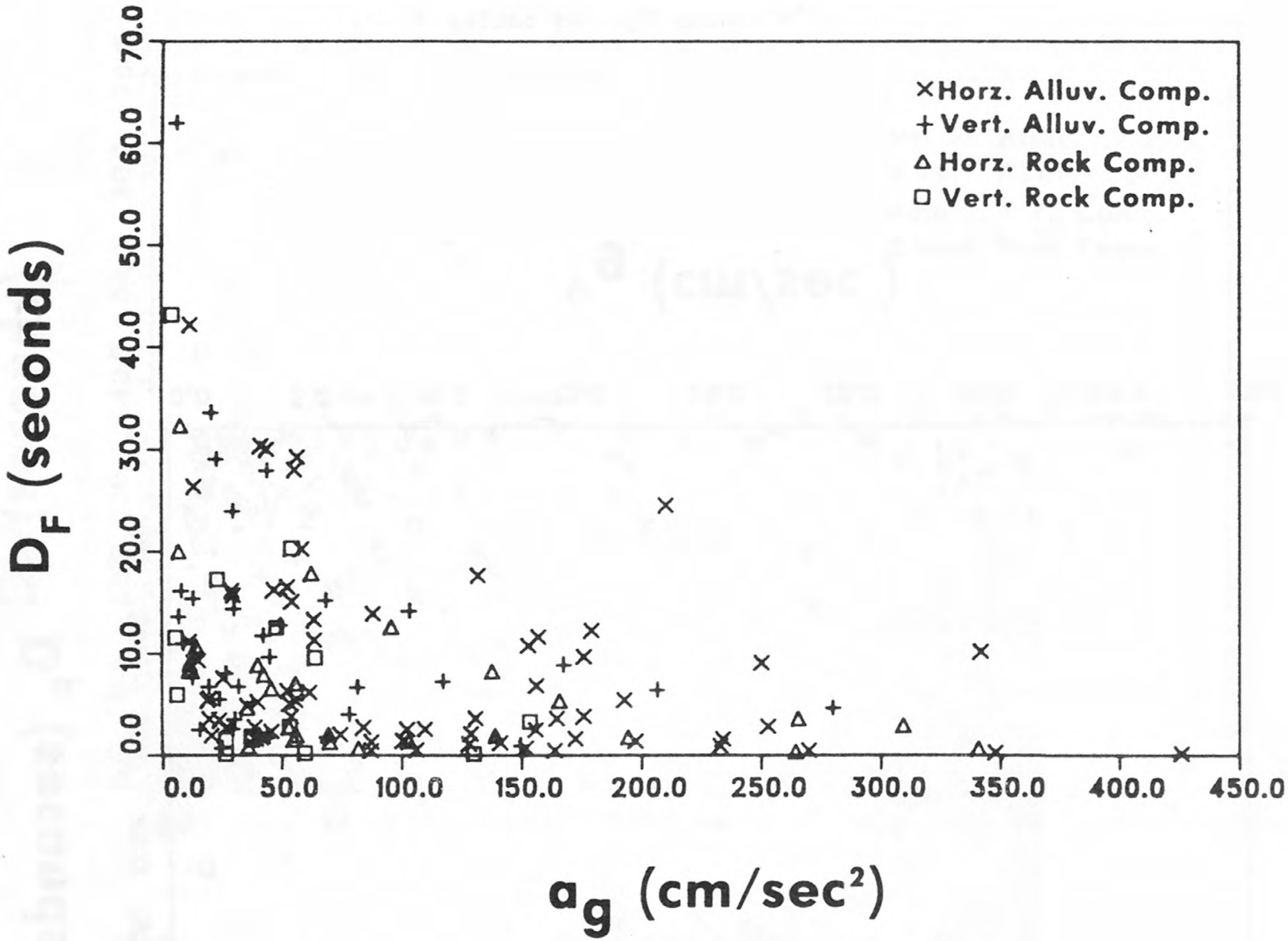

Figure 15.--D_F versus a_g.

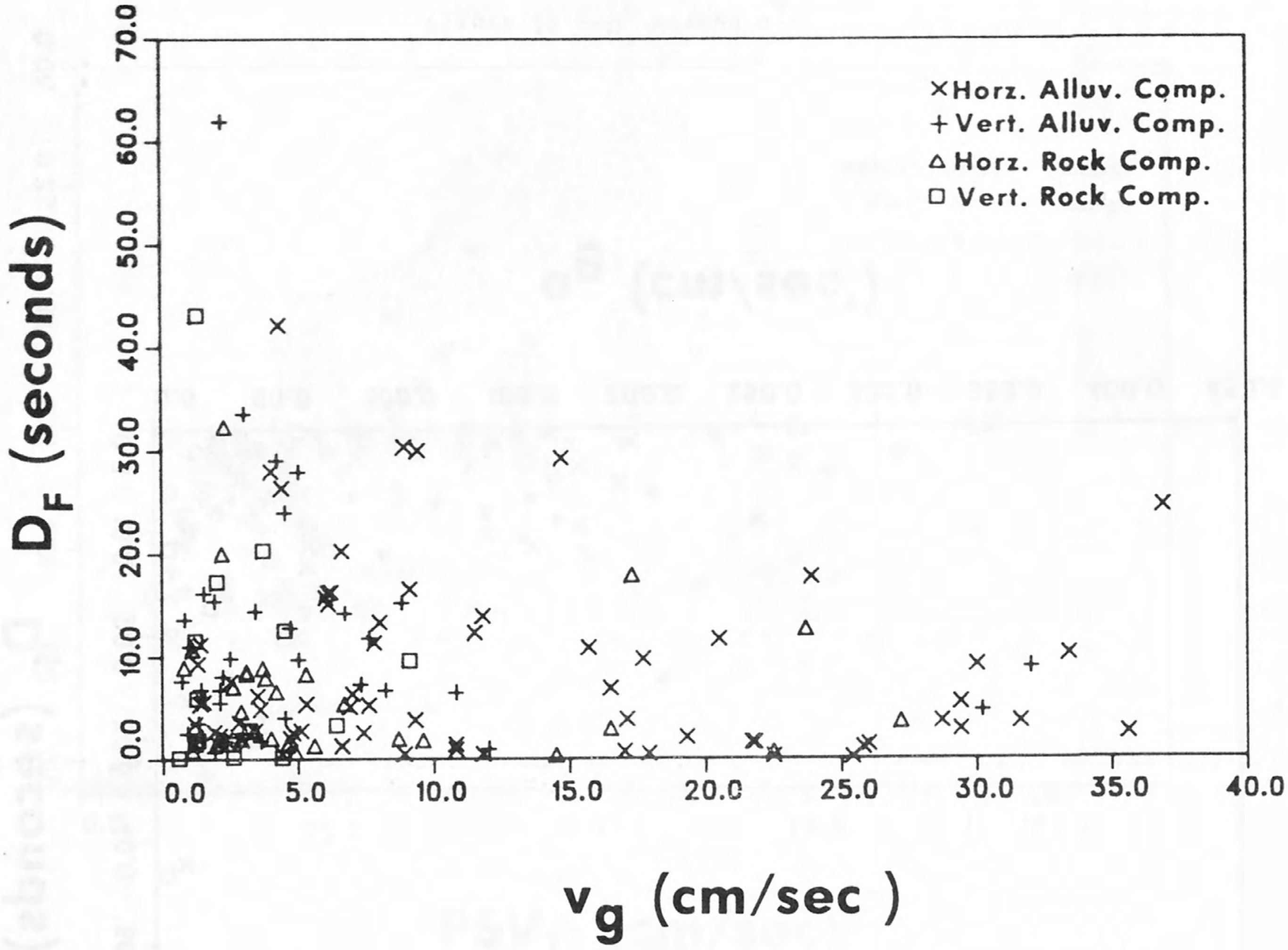

Figure 16.--D_F versus v_g.

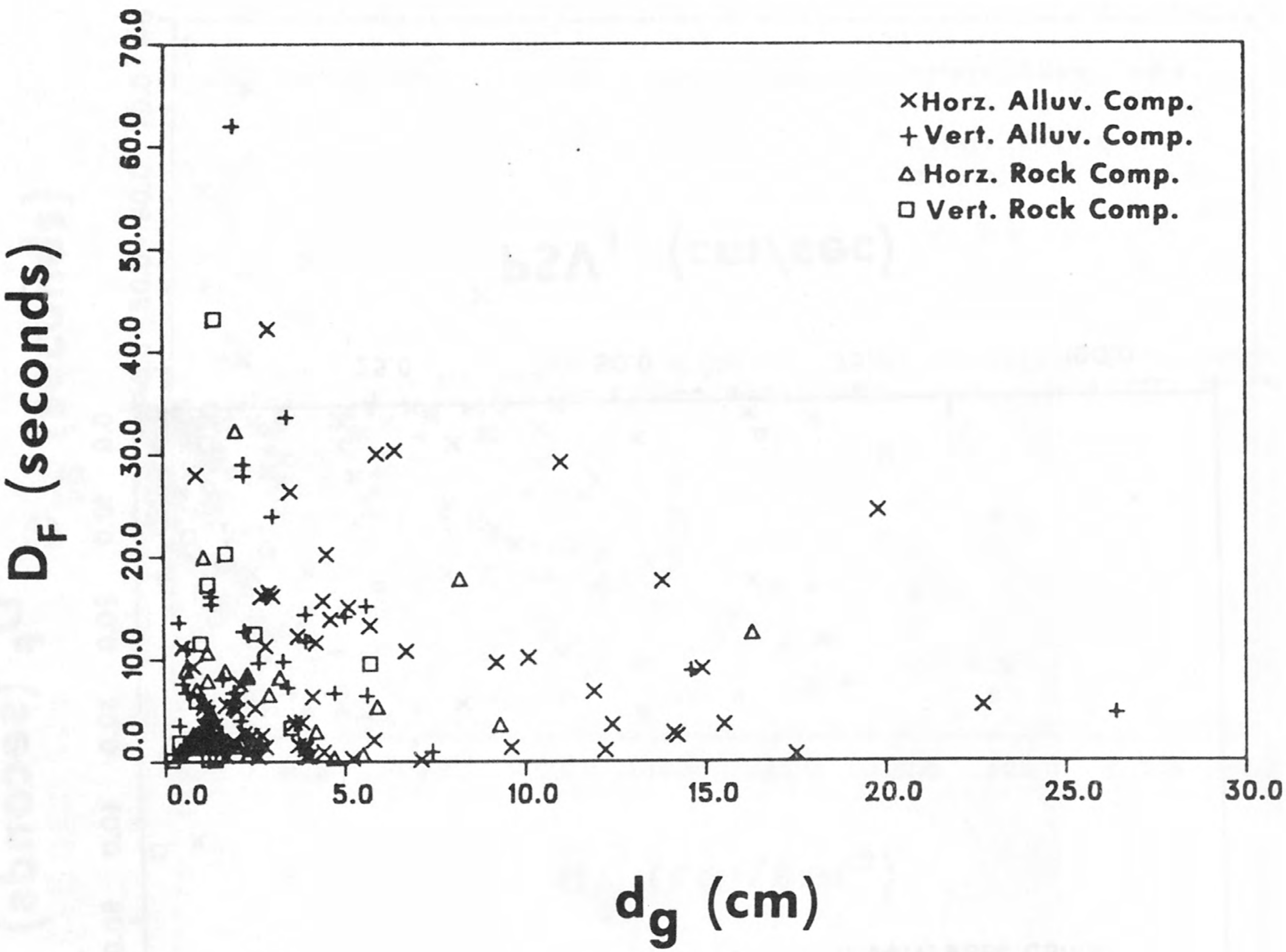

Figure 17.--D_F versus d_g.

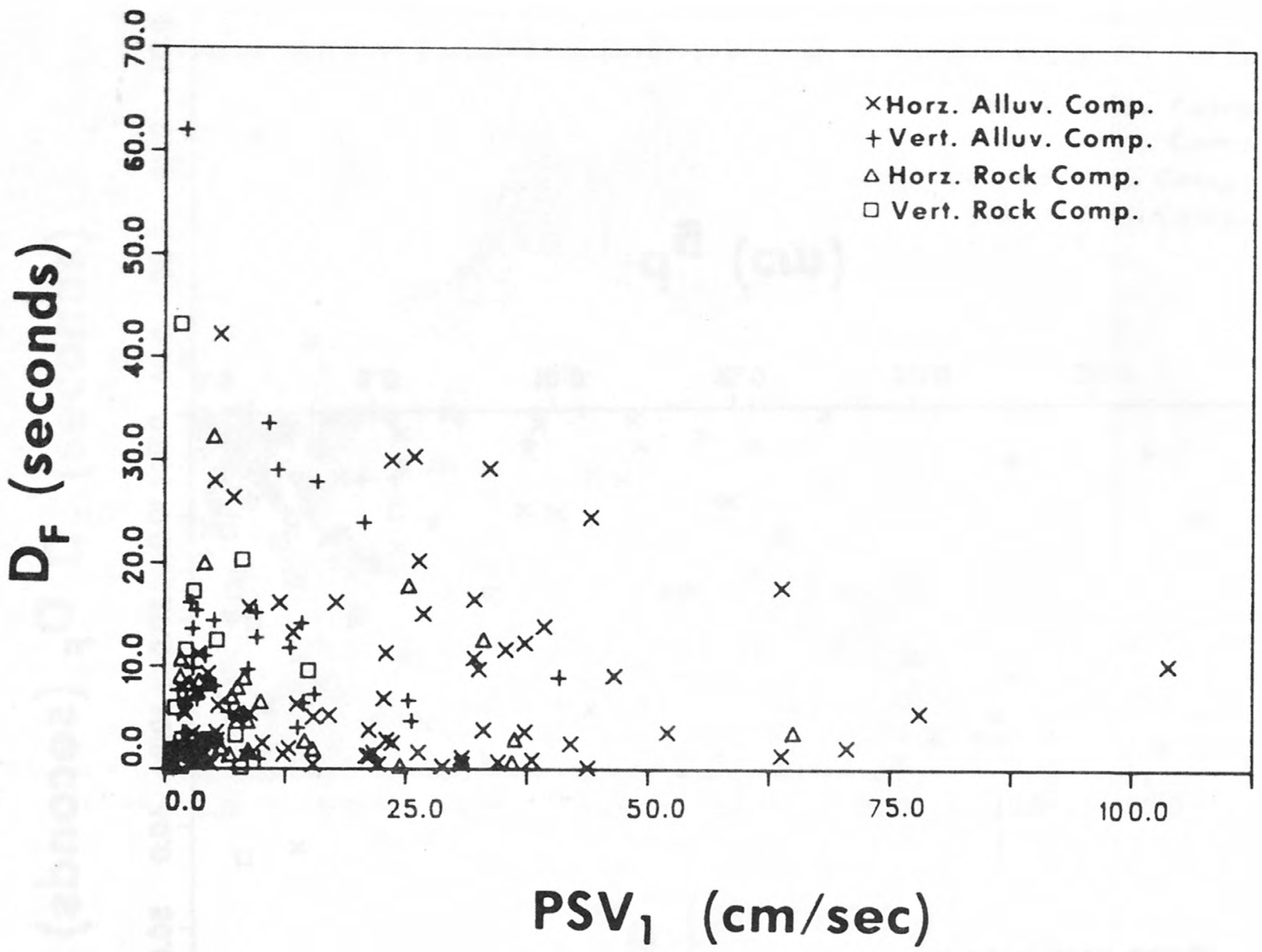

Figure 18.--D_F versus PSV_1.

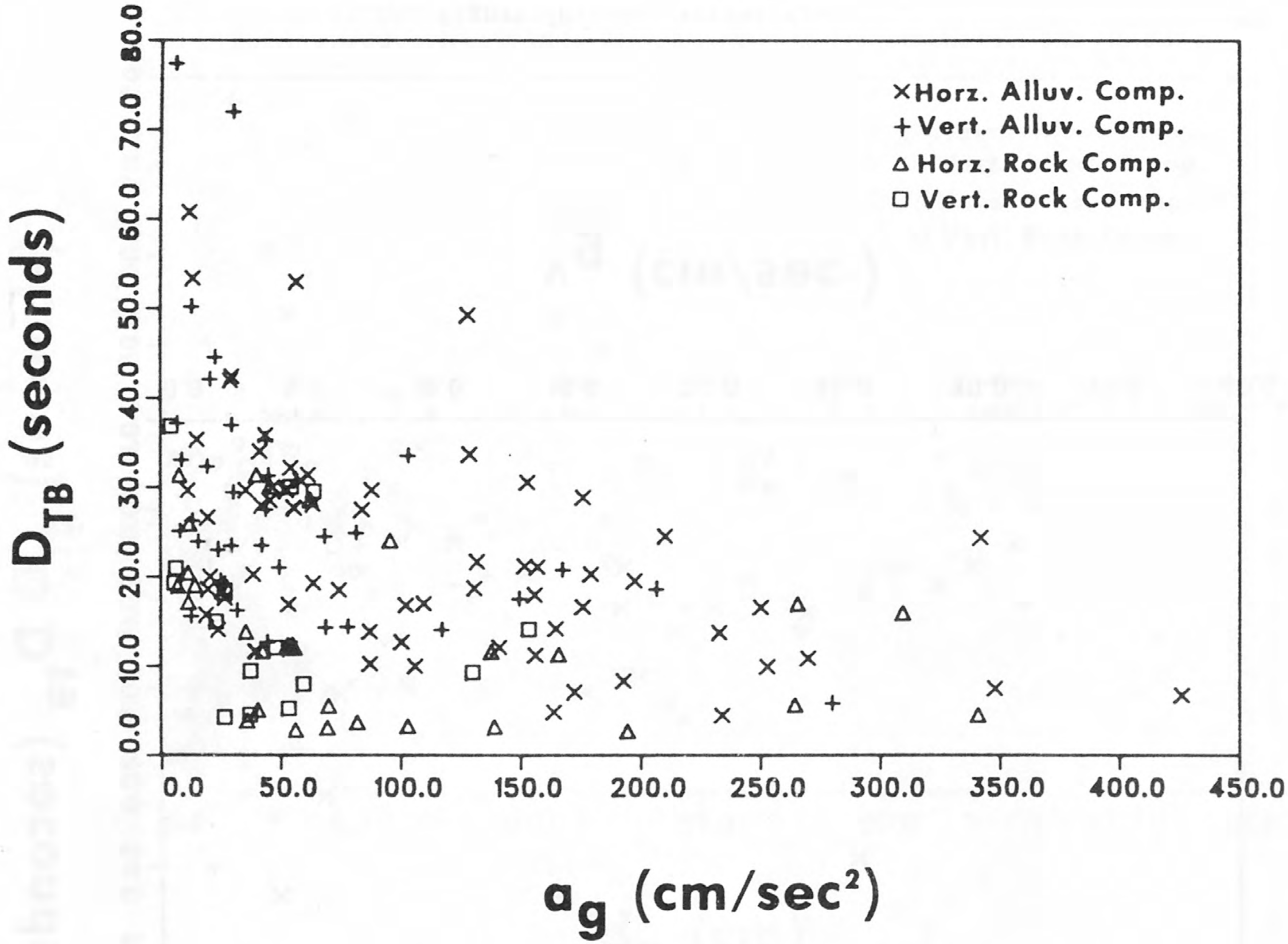

Figure 19.--D_{TB} versus a_g.

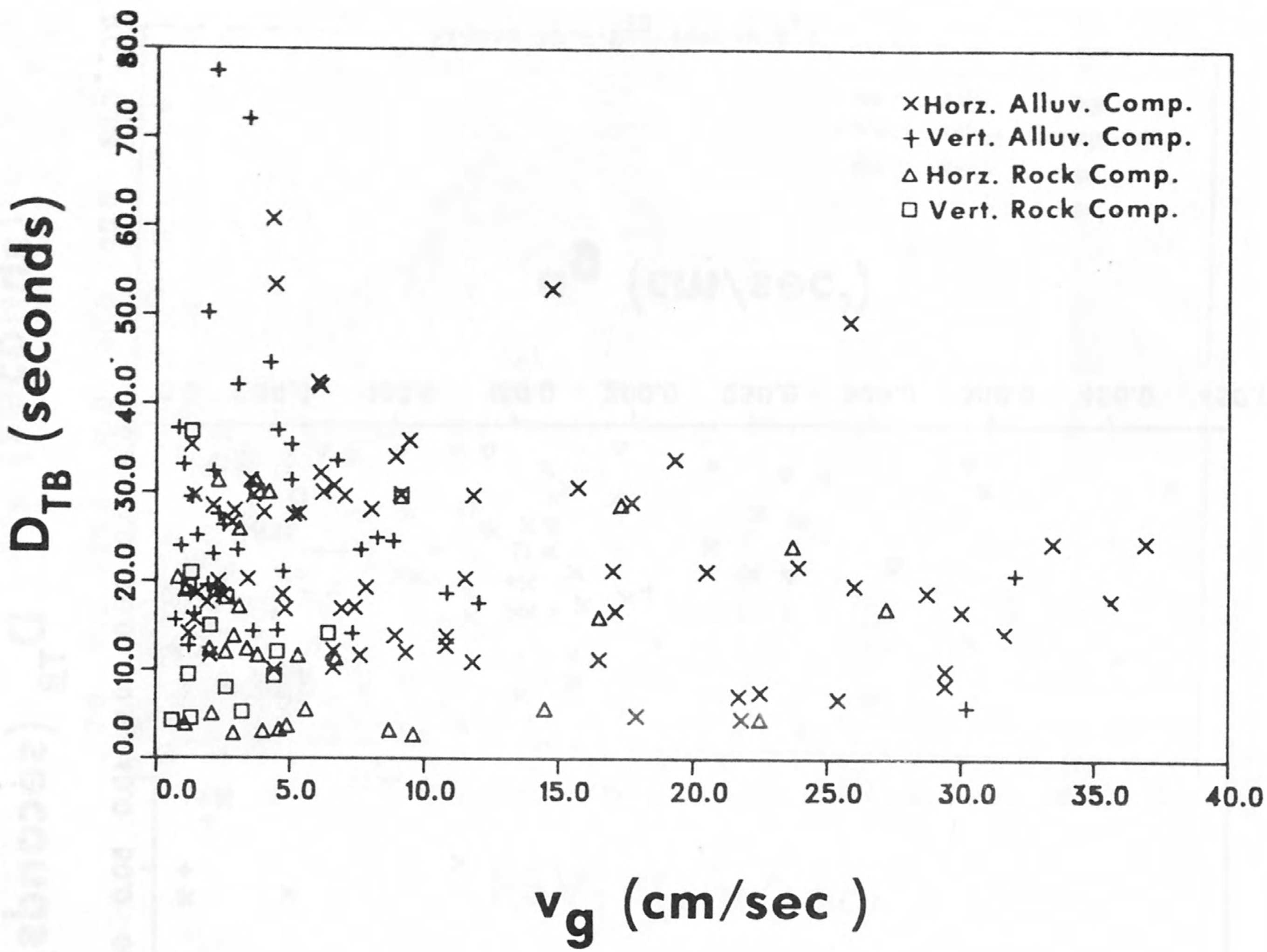

Figure 20.--D_{TB} versus v_g.

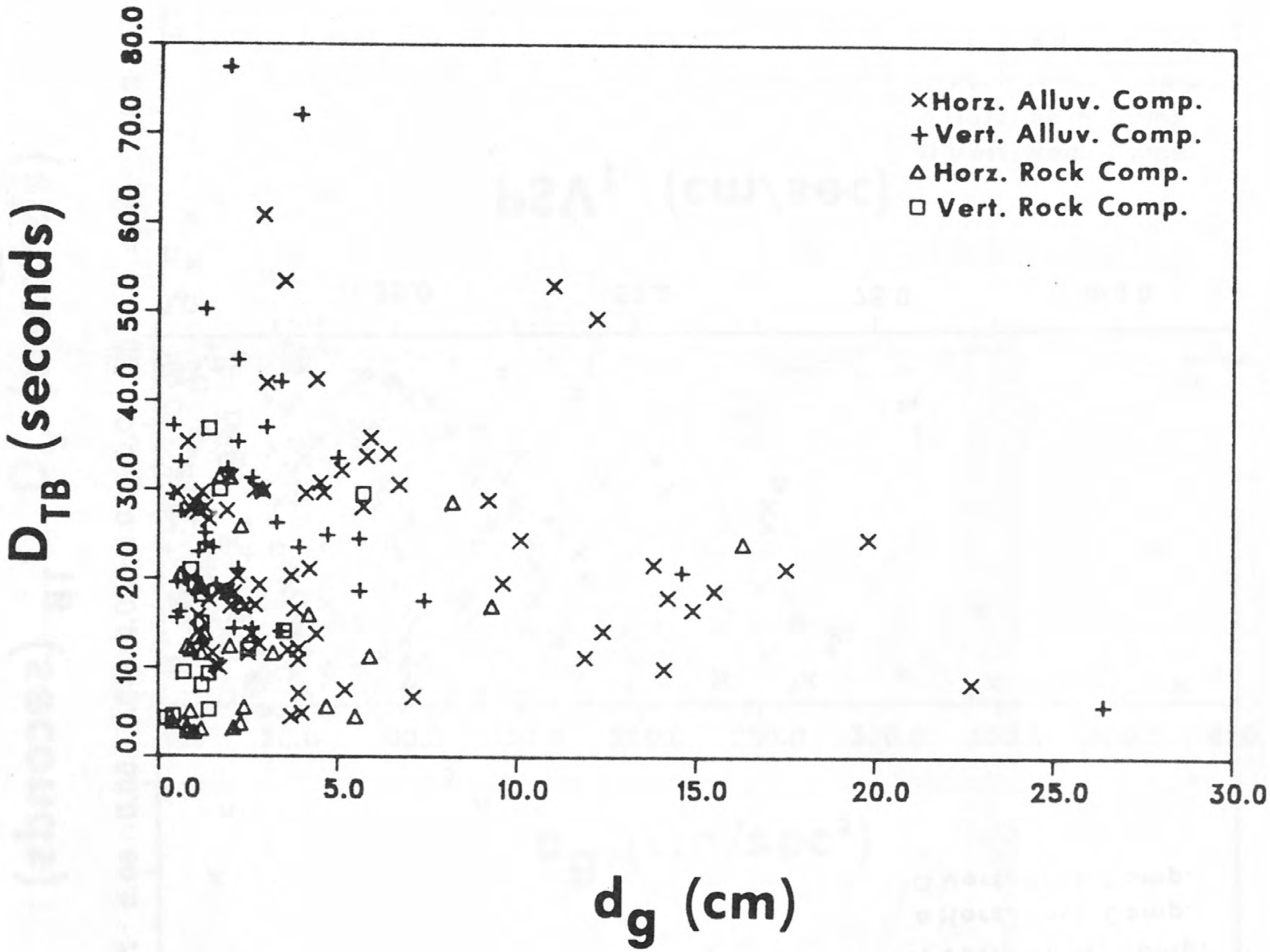

Figure 21.--D_{TB} versus d_g.

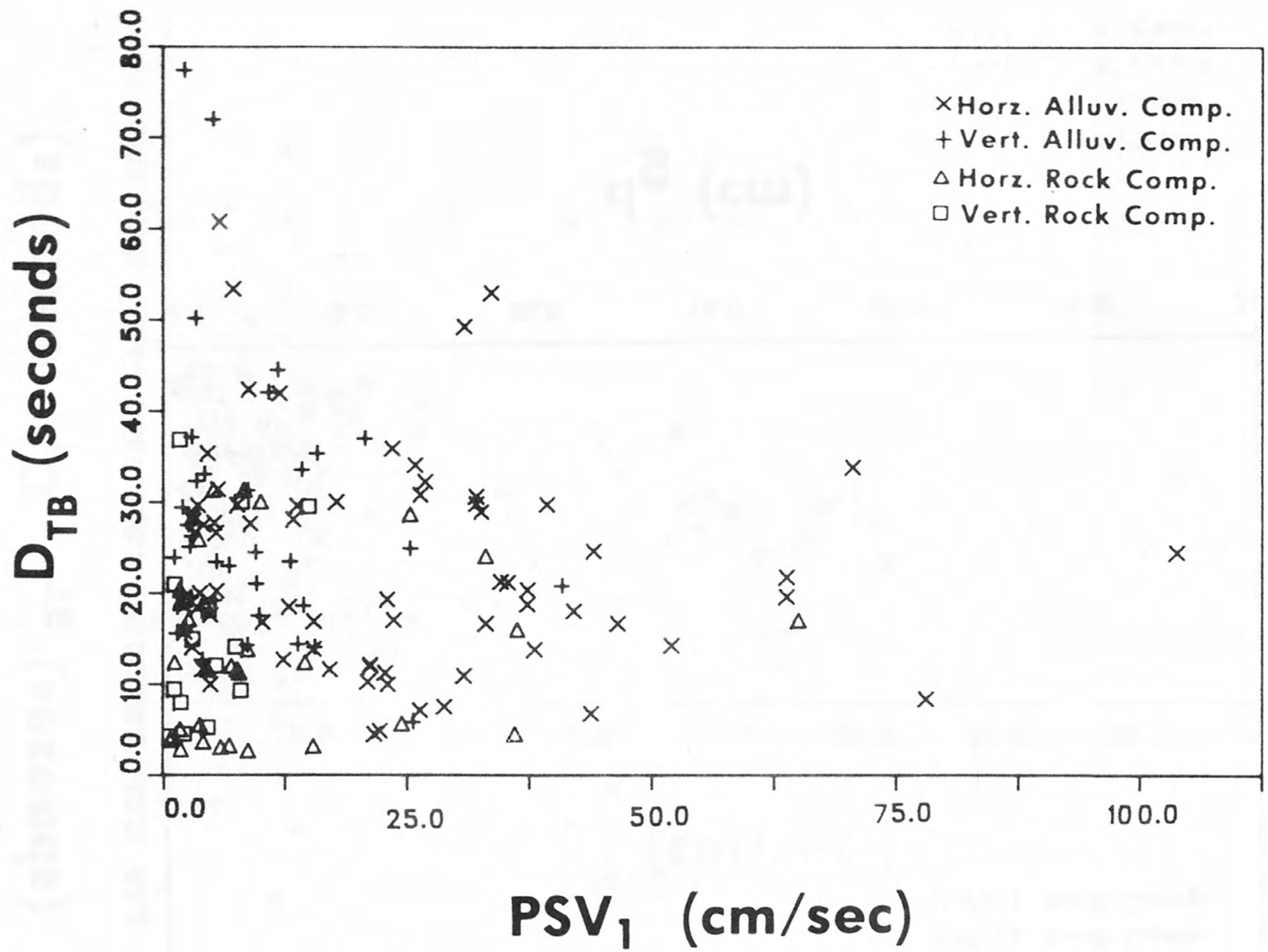

Figure 22.--D_{TB} versus PSV_1.

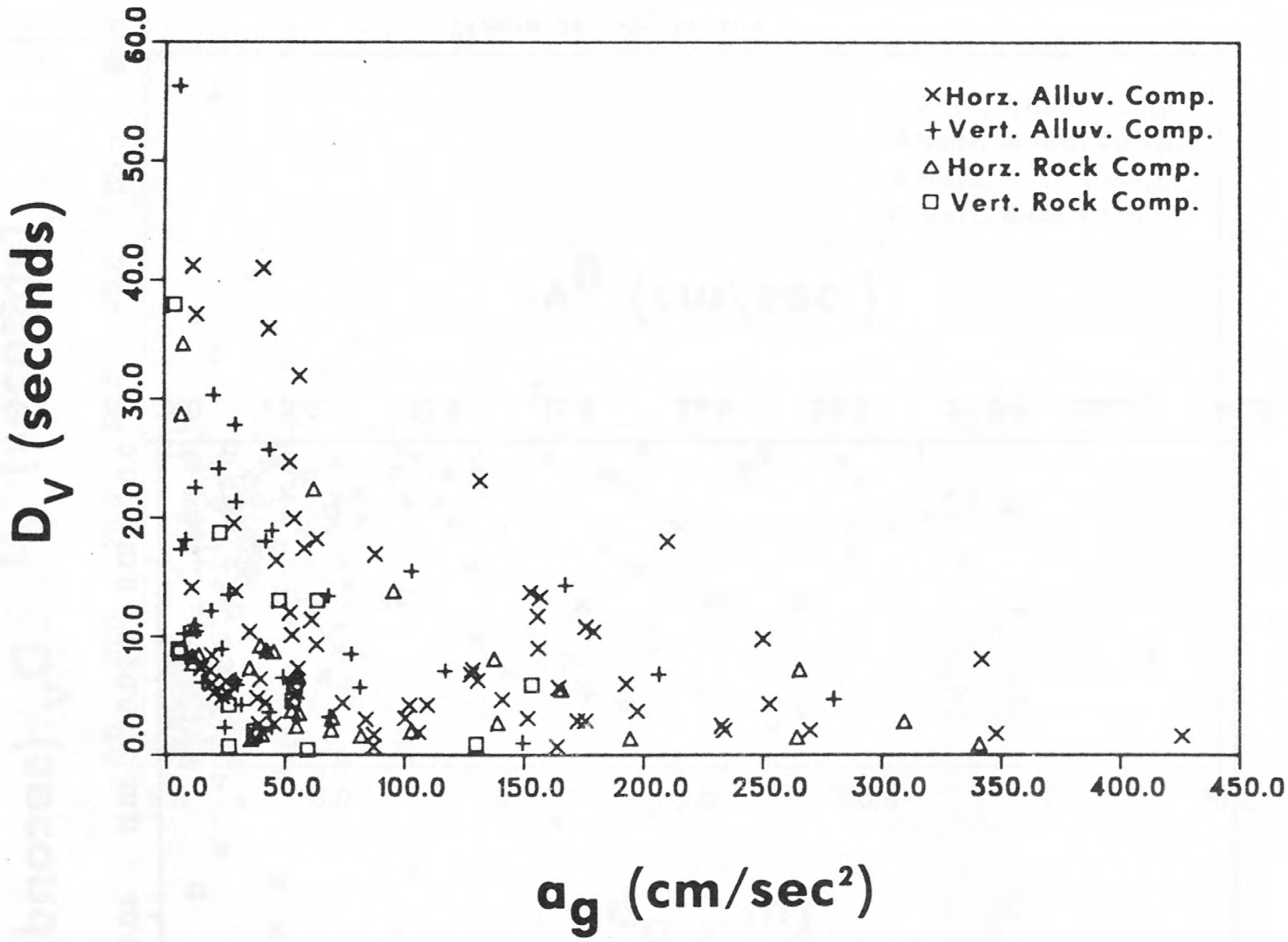

Figure 23.--D_V versus a_g.

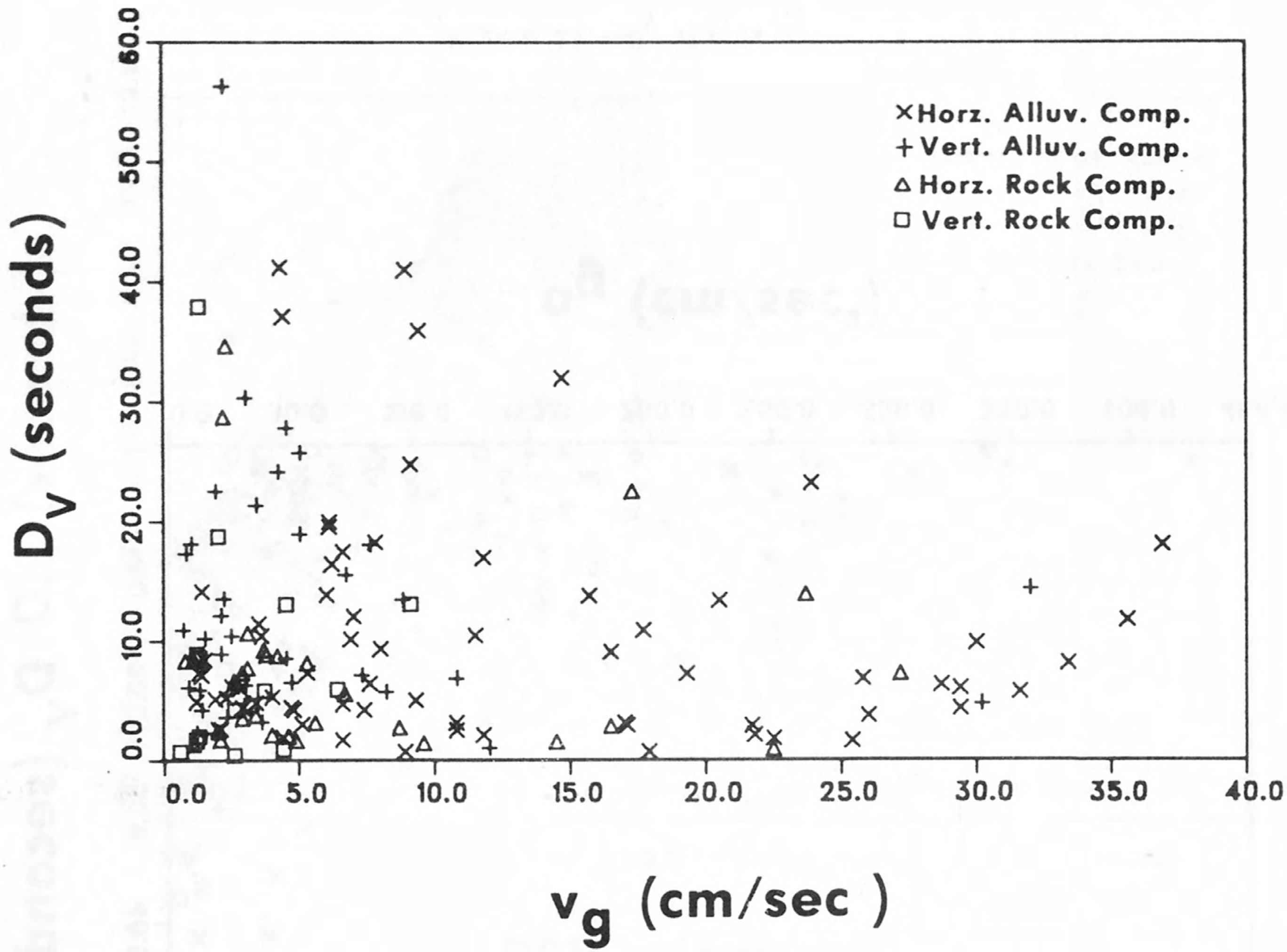

Figure 24.--D_V versus v_g.

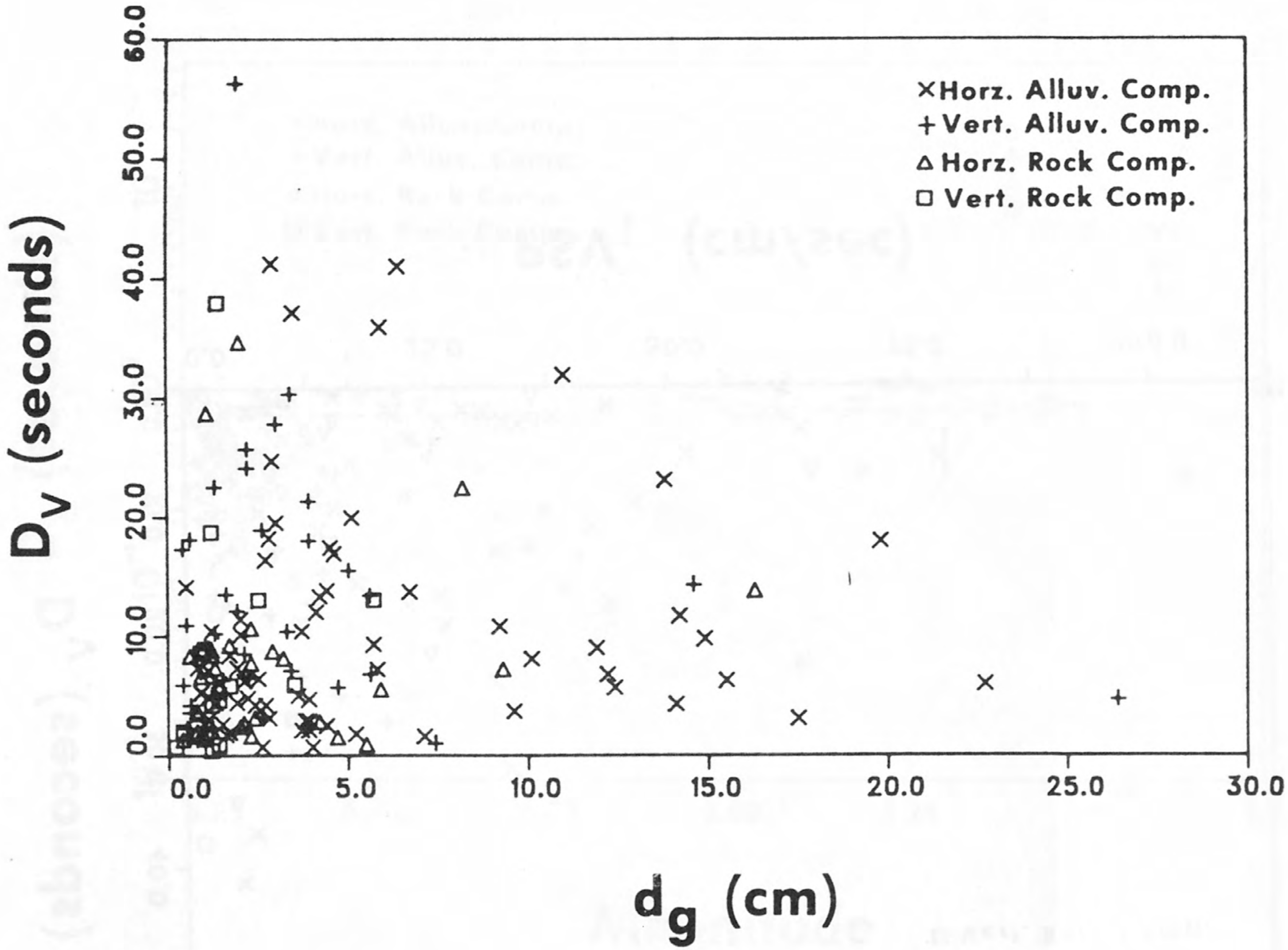

Figure 25.--D_V versus d_g.

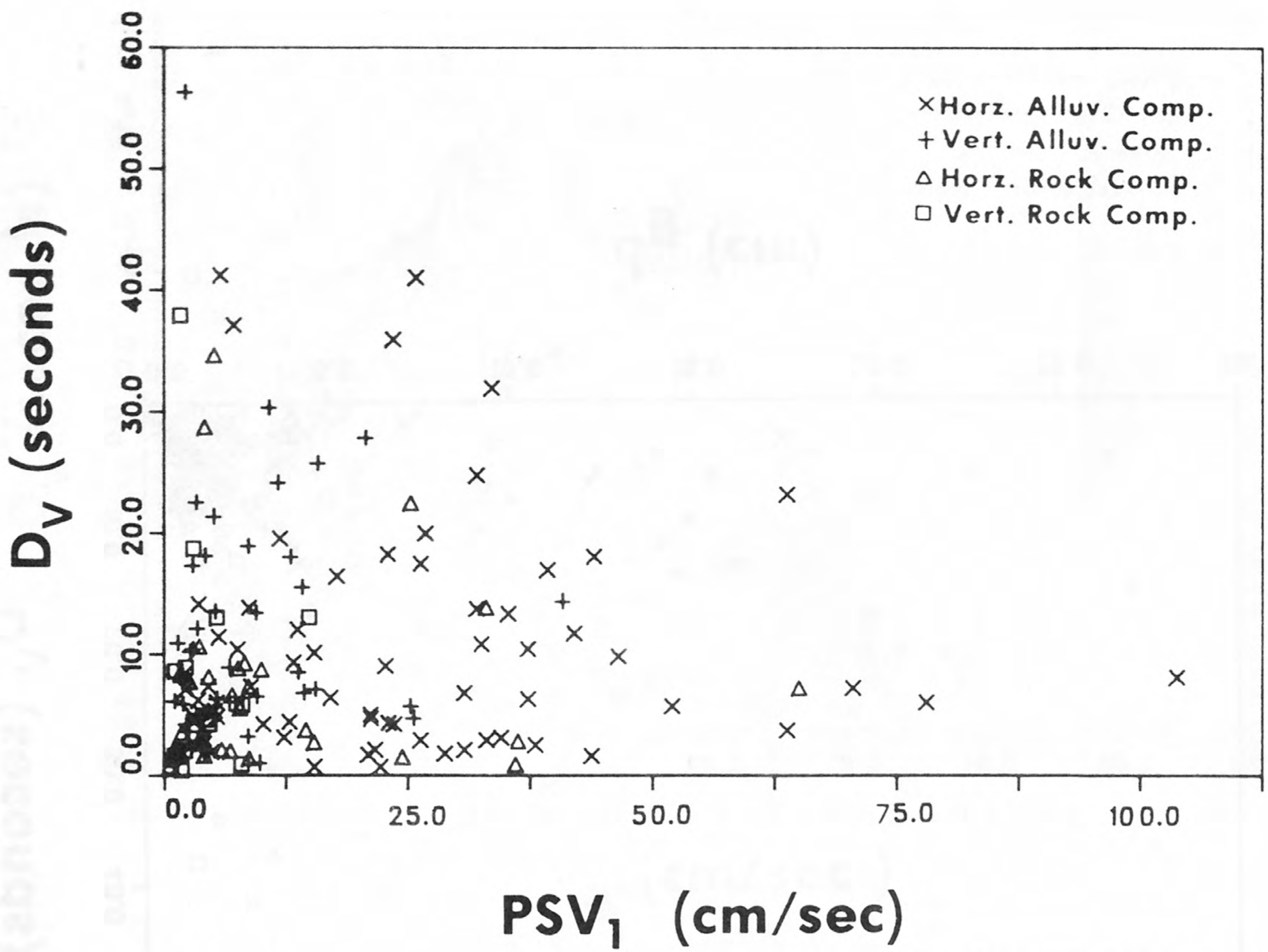

Figure 26.--D_V versus PSV_1.

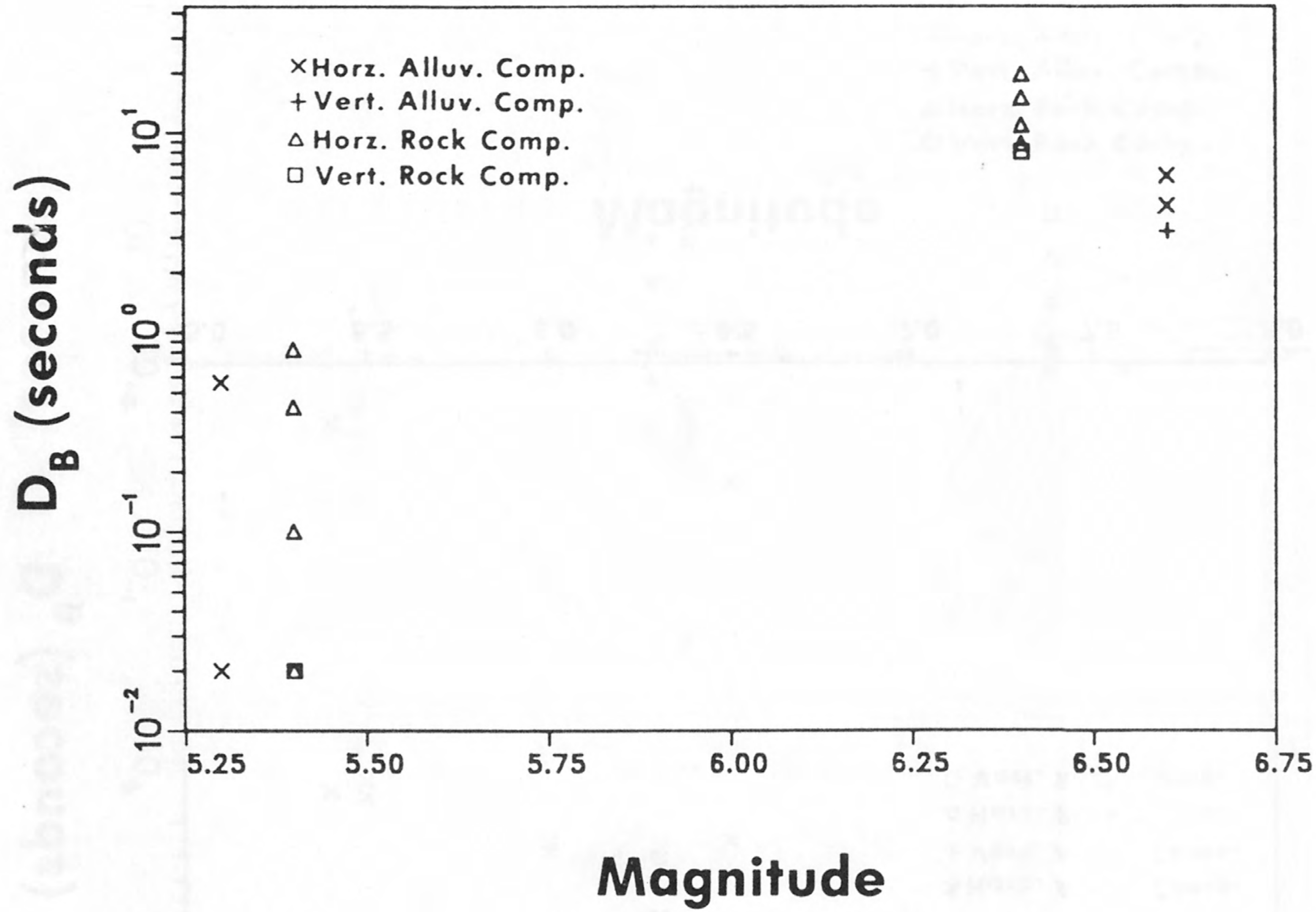

Figure 27.--D_B versus M for records with $17 \leq R \leq 27$ km.

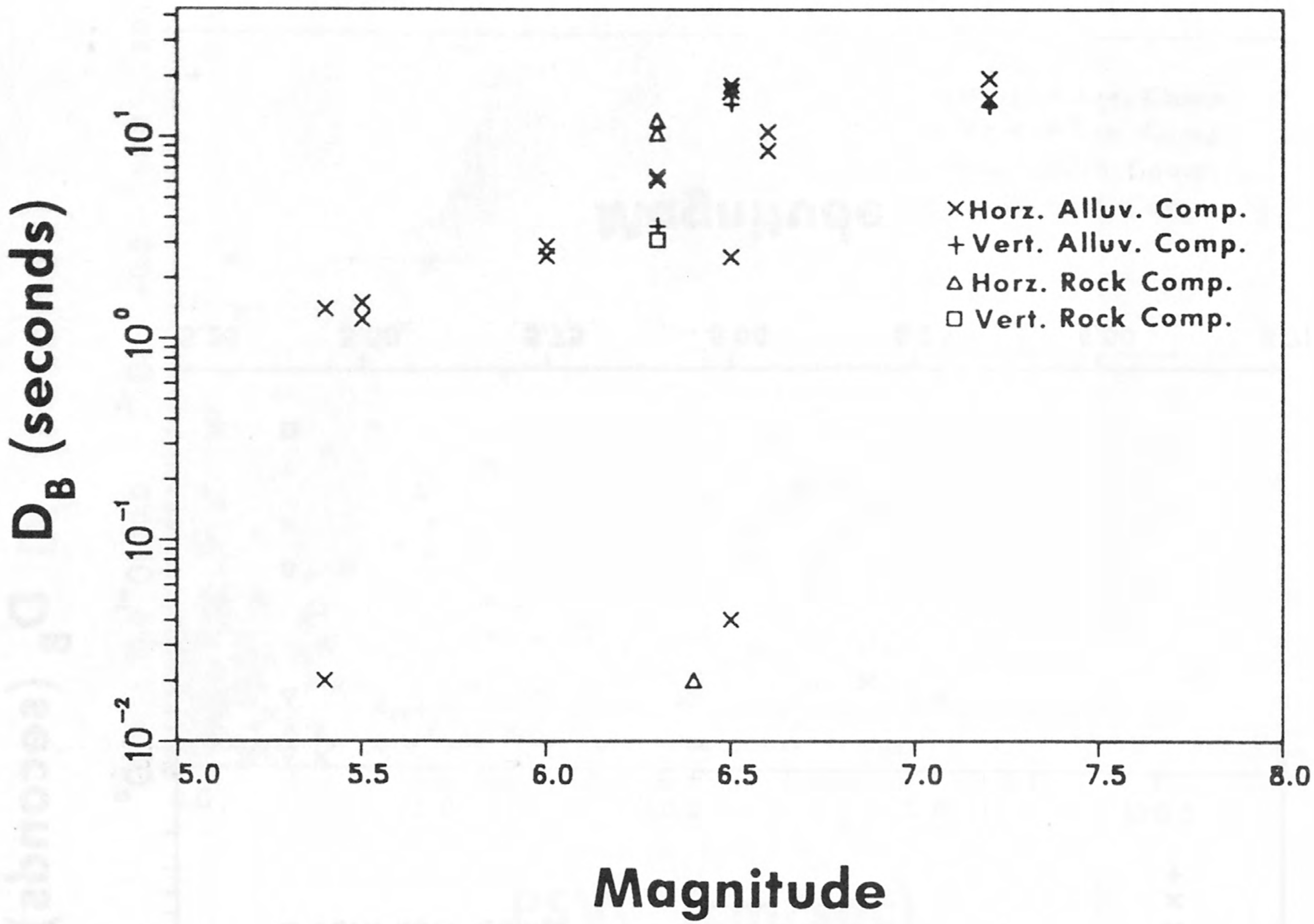

Figure 28.--D_B versus M for records with $40 \leq R \leq 65$ km.

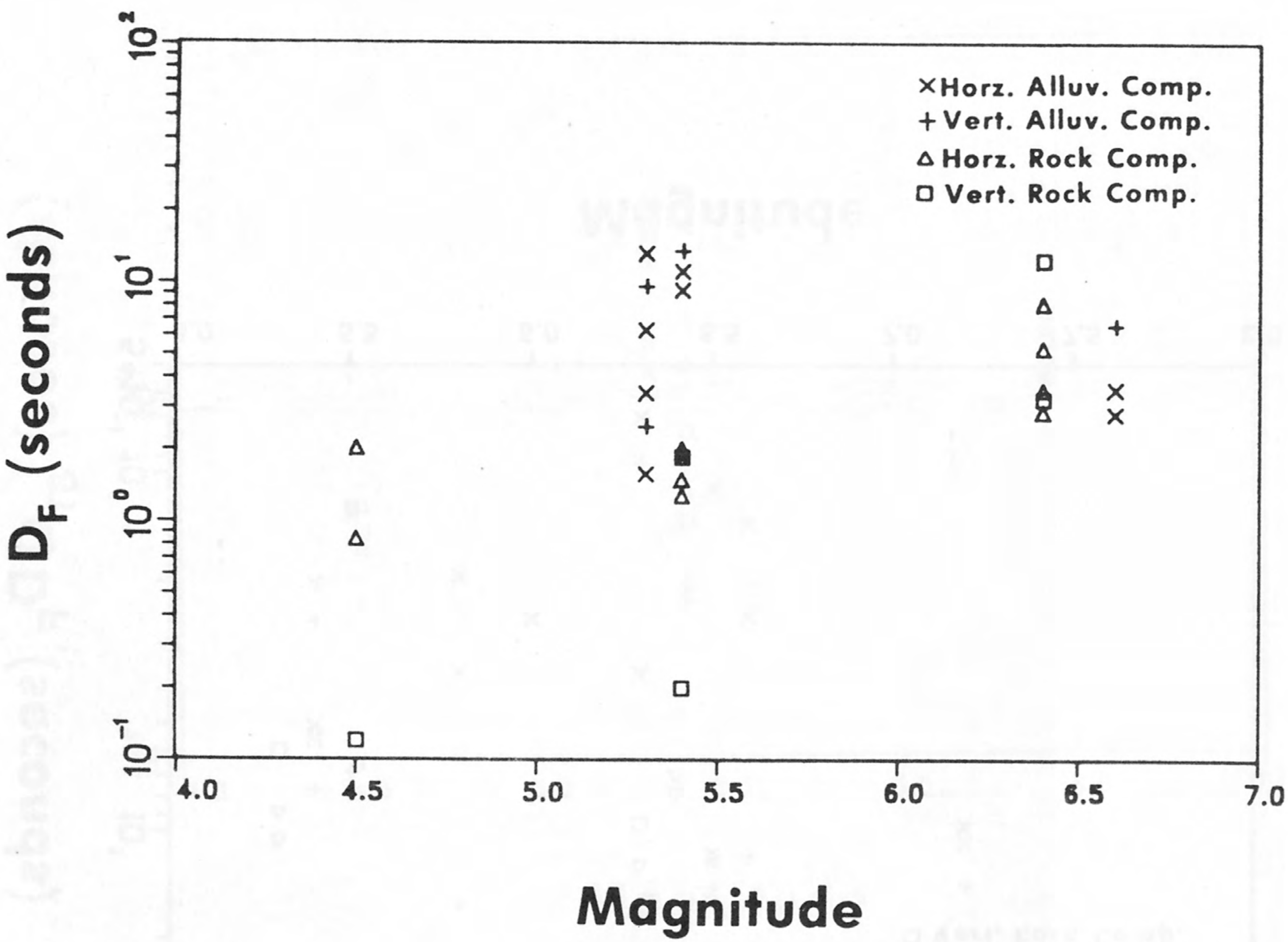

Figure 29.--D_F versus M for records with $17 \leq R \leq 27$ km.

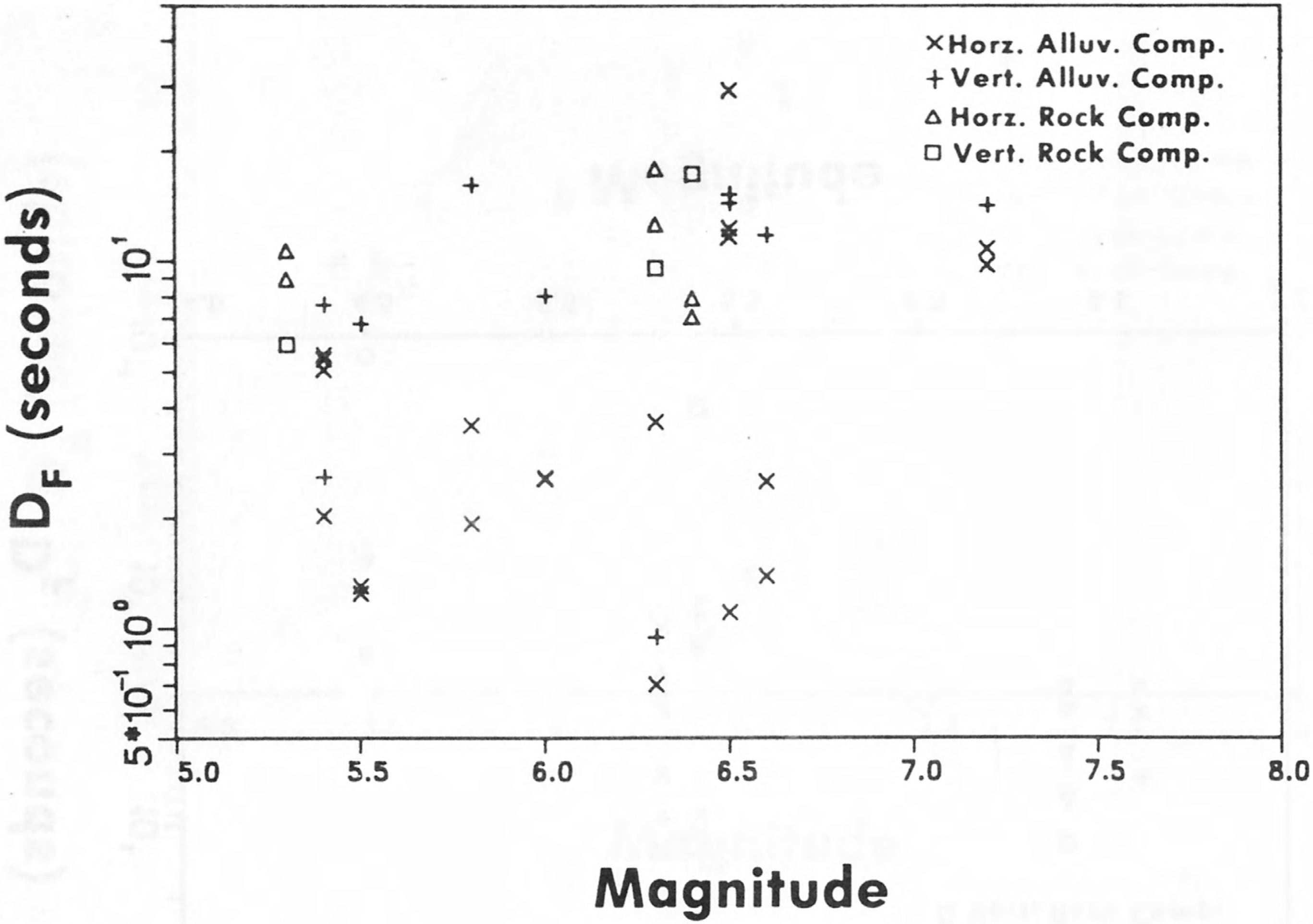

Figure 30.--D_F versus M for records with 40 ≤ R ≤ 65 km.

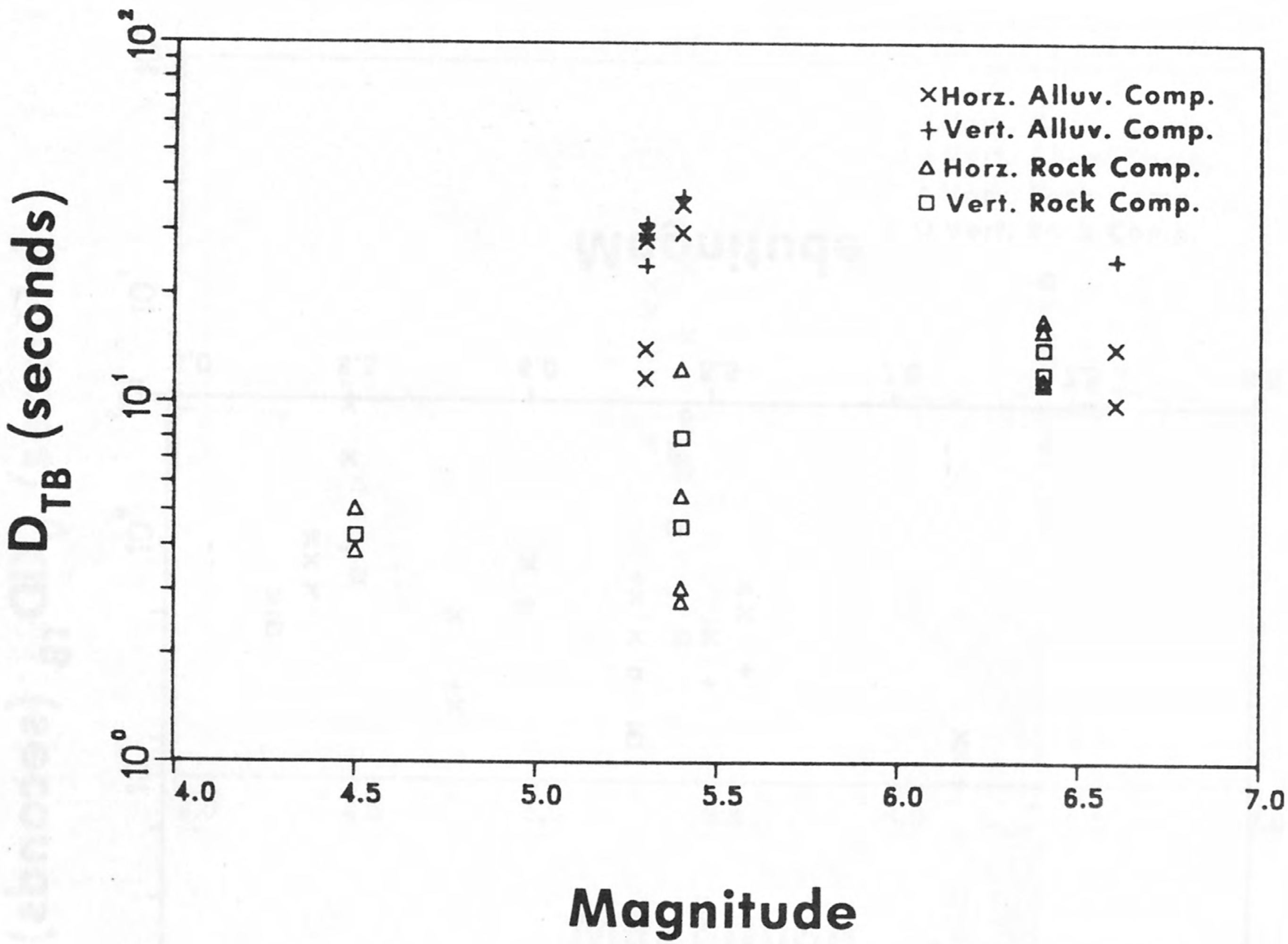

Figure 31.--D_{TB} versus M for records with 17 $\leq$ R $\leq$ 27 km.

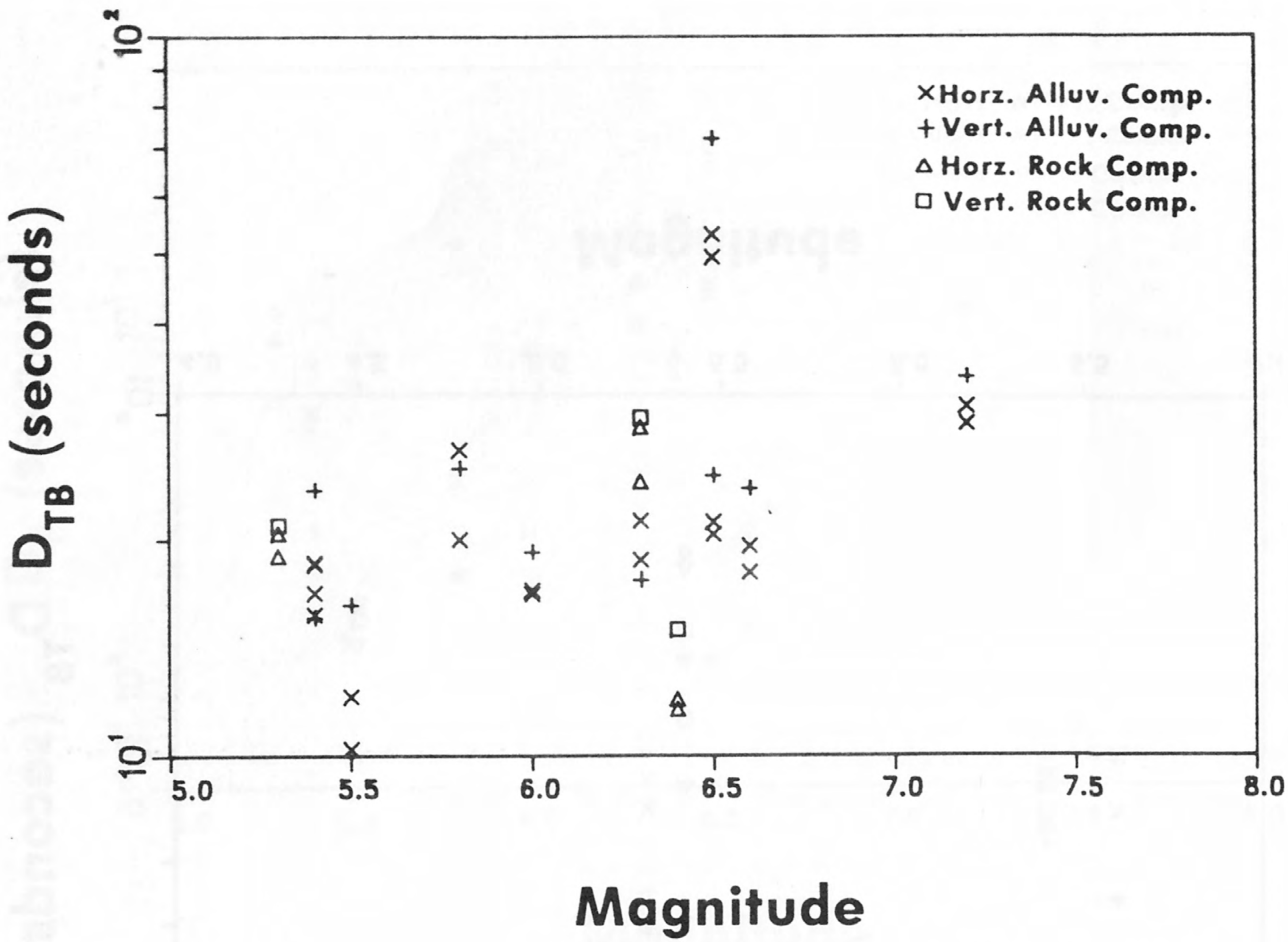

Figure 32.--D_{TB} versus M for records with $40 \leq R \leq 65$ km.

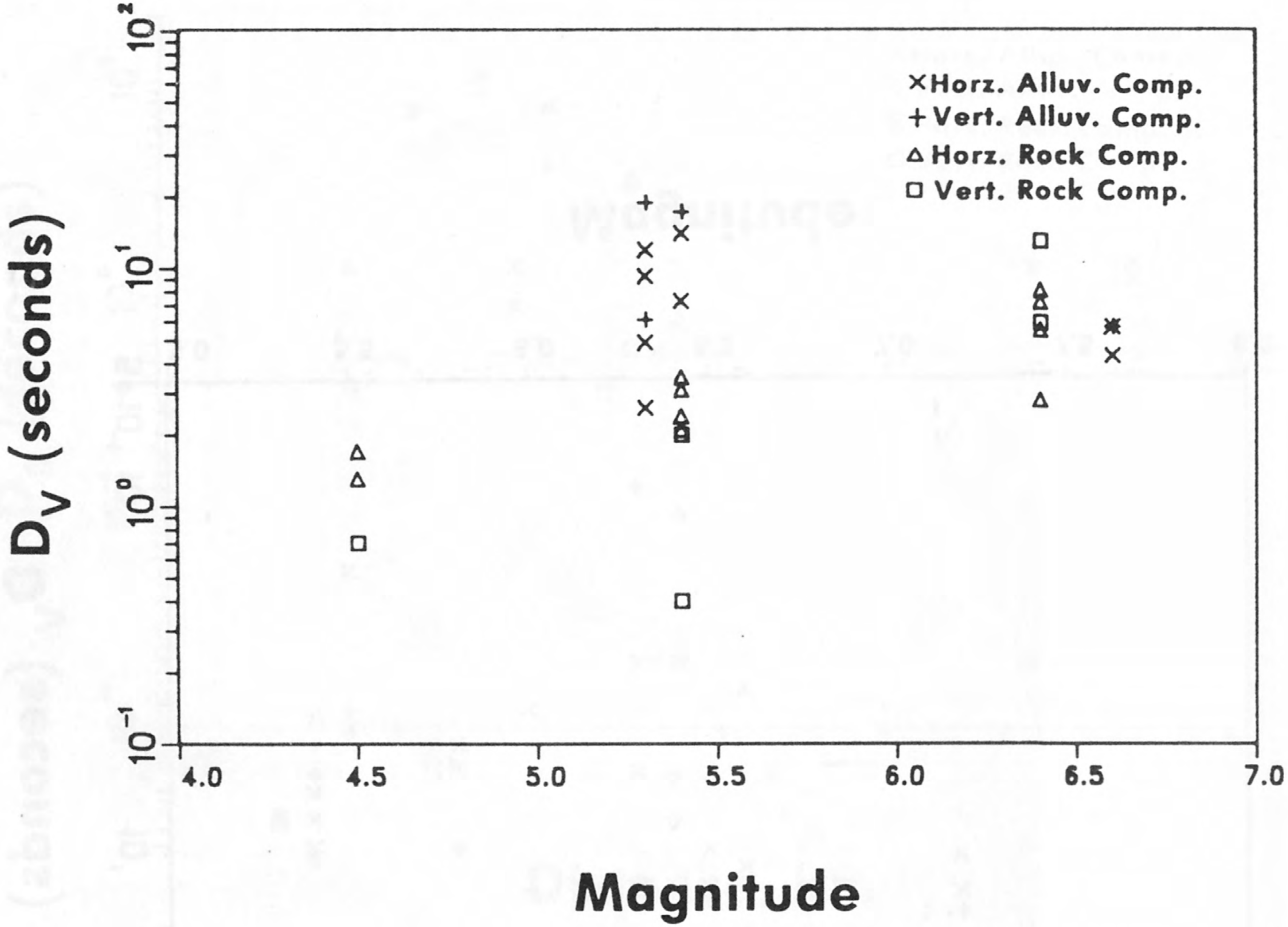

Figure 33.--D_V versus M for records with 17 $\leq$ R $\leq$ 27 km.

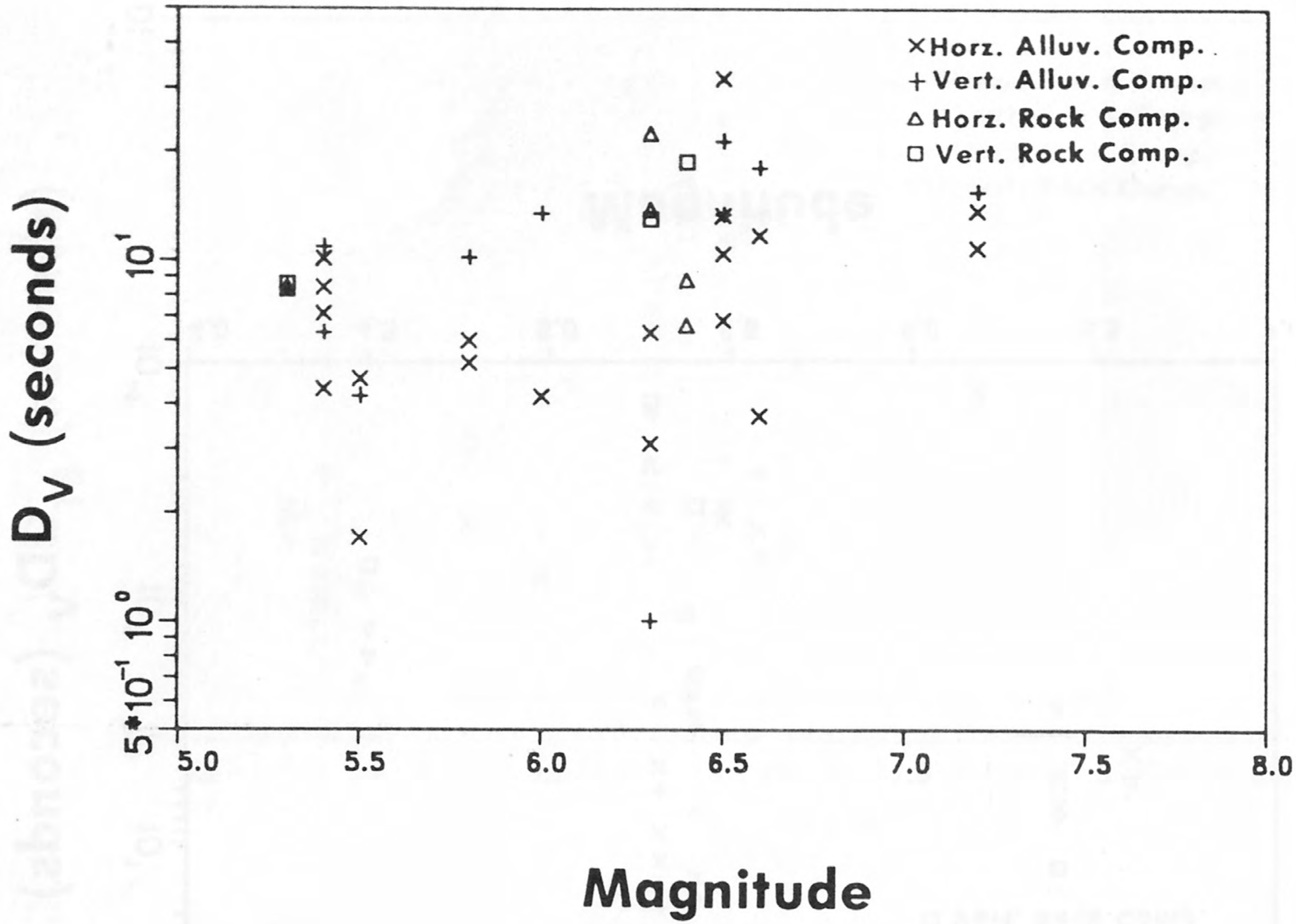

Figure 34.--D_V versus M for records with $40 \leq R \leq 65$ km.

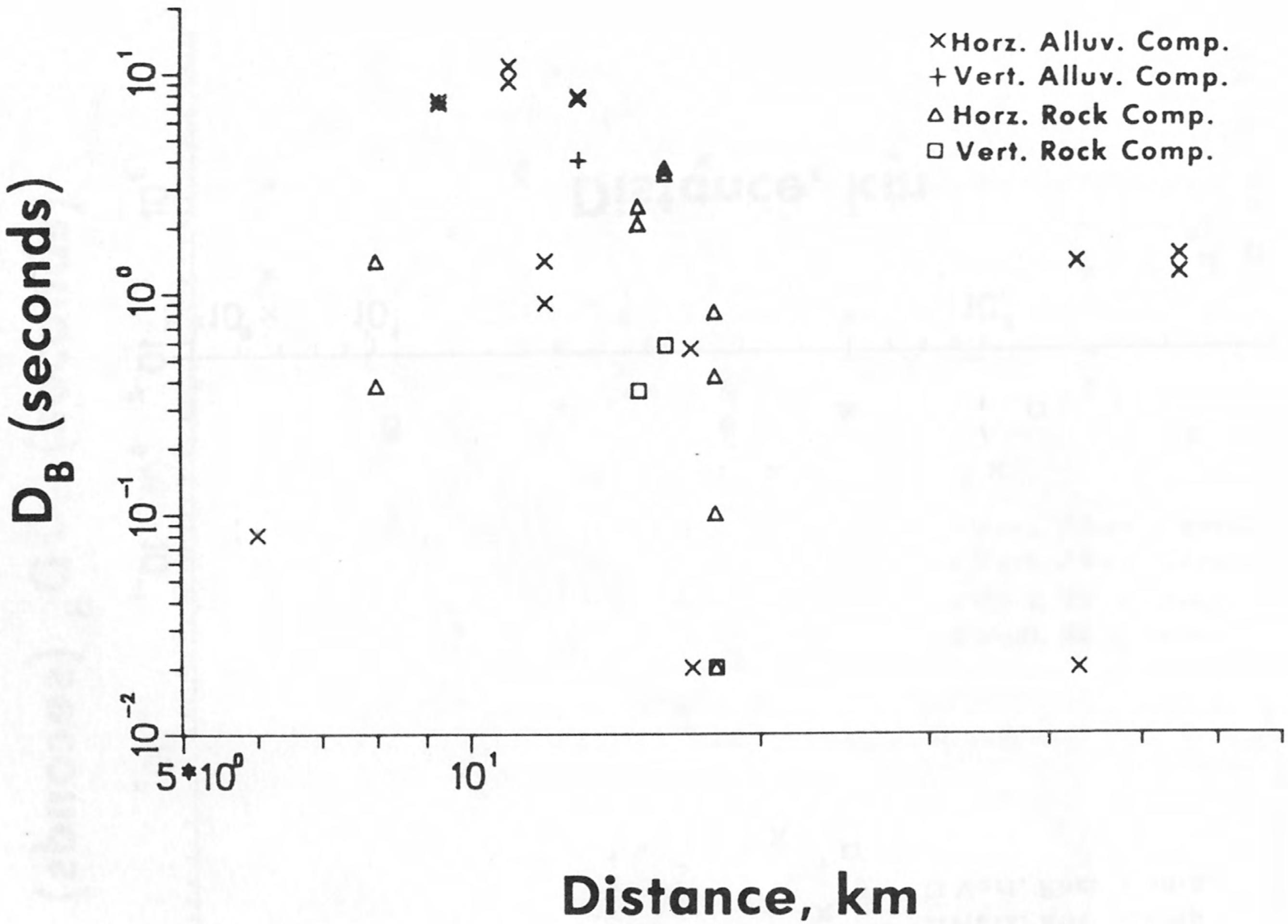

Figure 35.--D_B versus R for records with $5.3 \leq M \leq 5.6$.

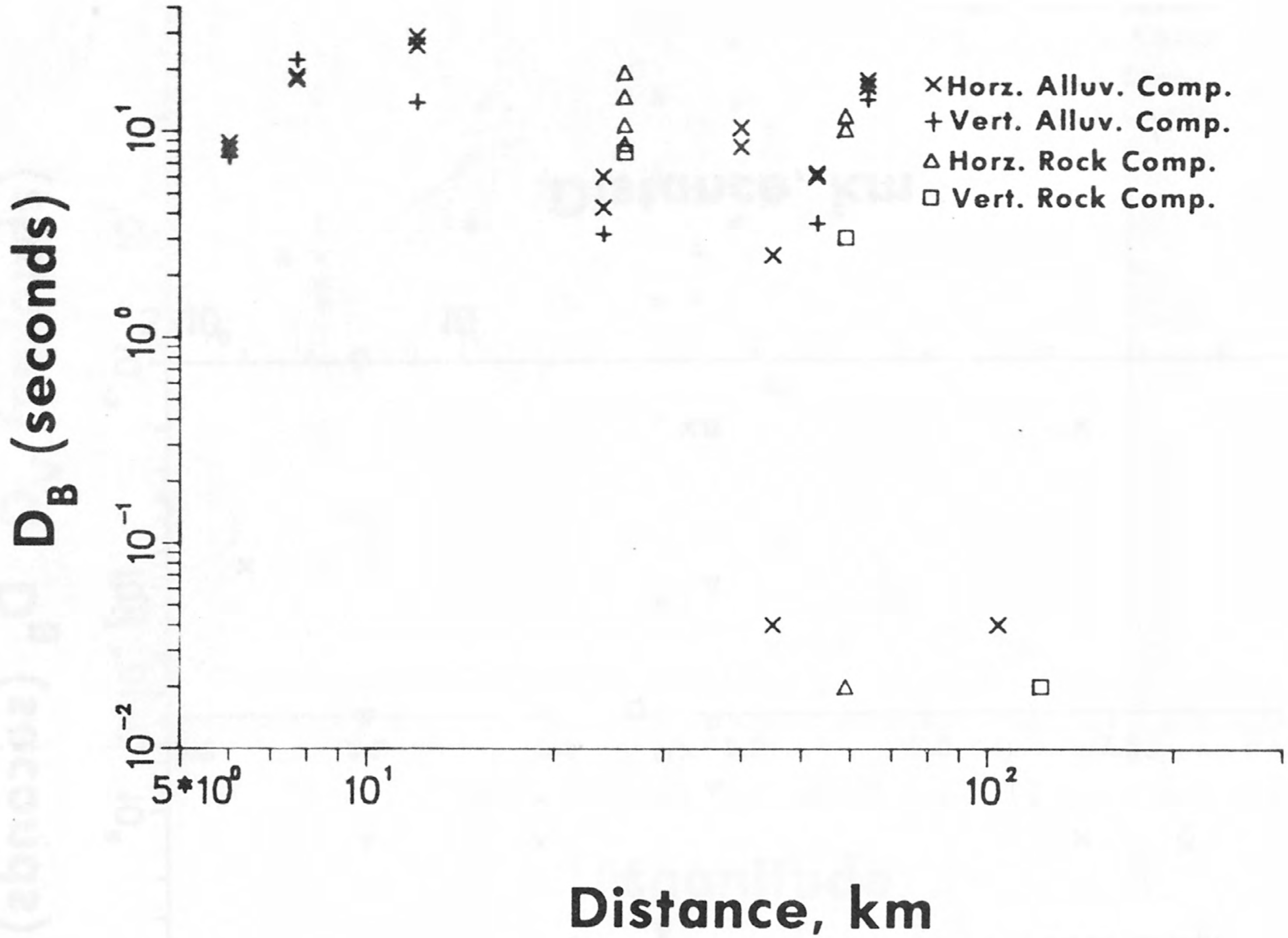

Figure 36.--D_B versus R for records with $6.3 \leq M \leq 6.6$.

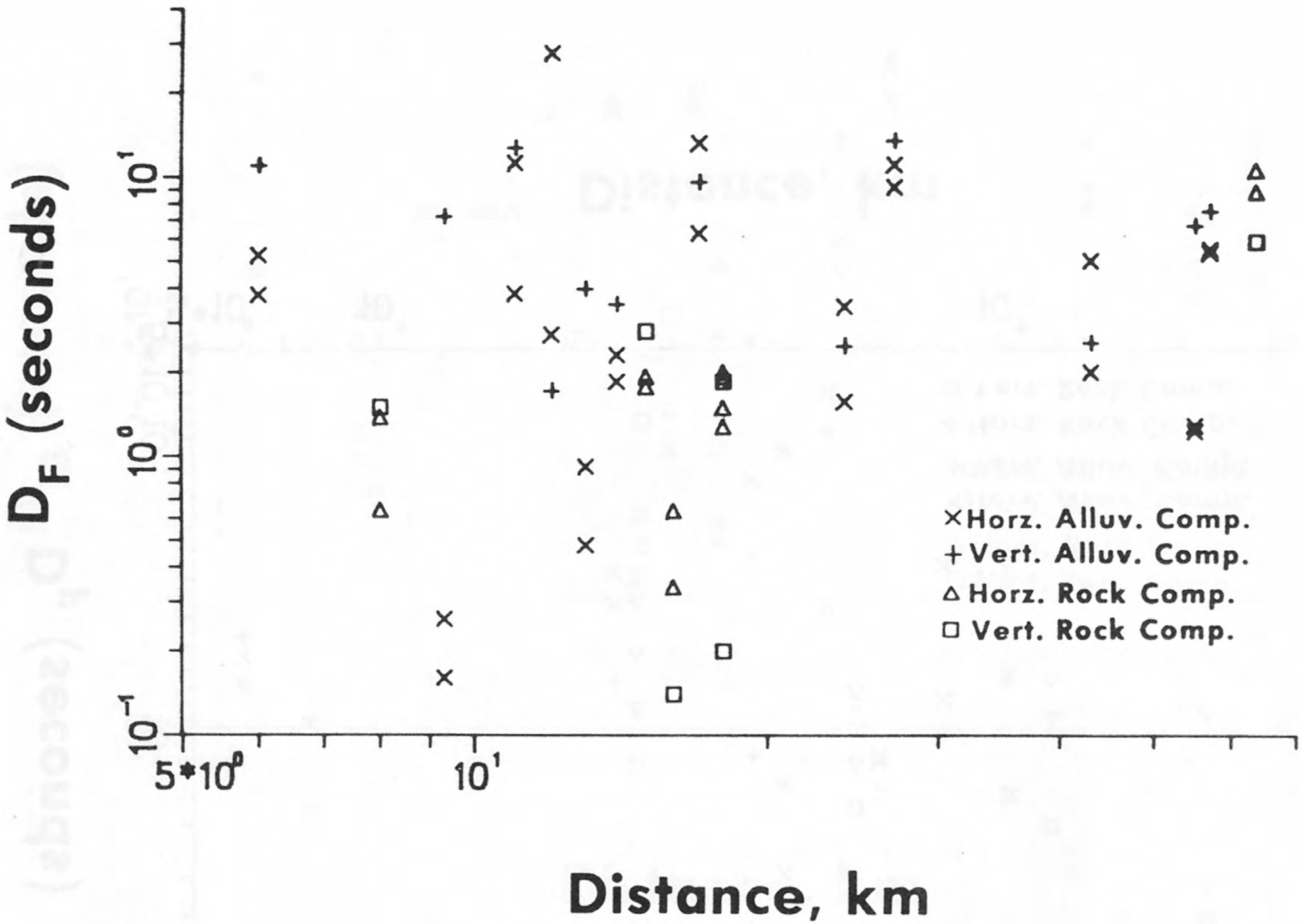

Figure 37.--D_F versus R for records with $5.3 \leq M \leq 5.6$.

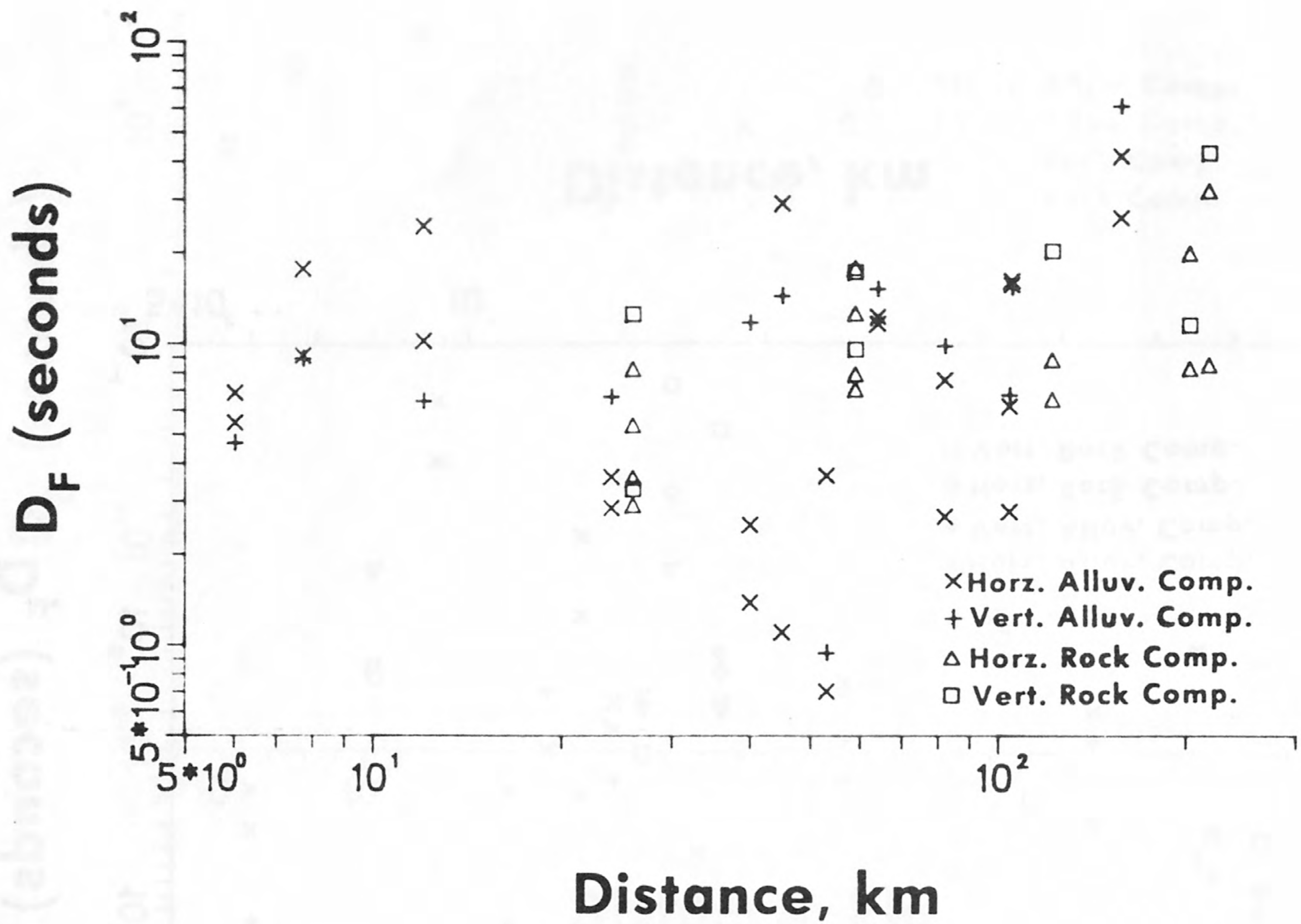

Figure 38.--D_F versus R for records with $6.3 \leq M \leq 6.6$.

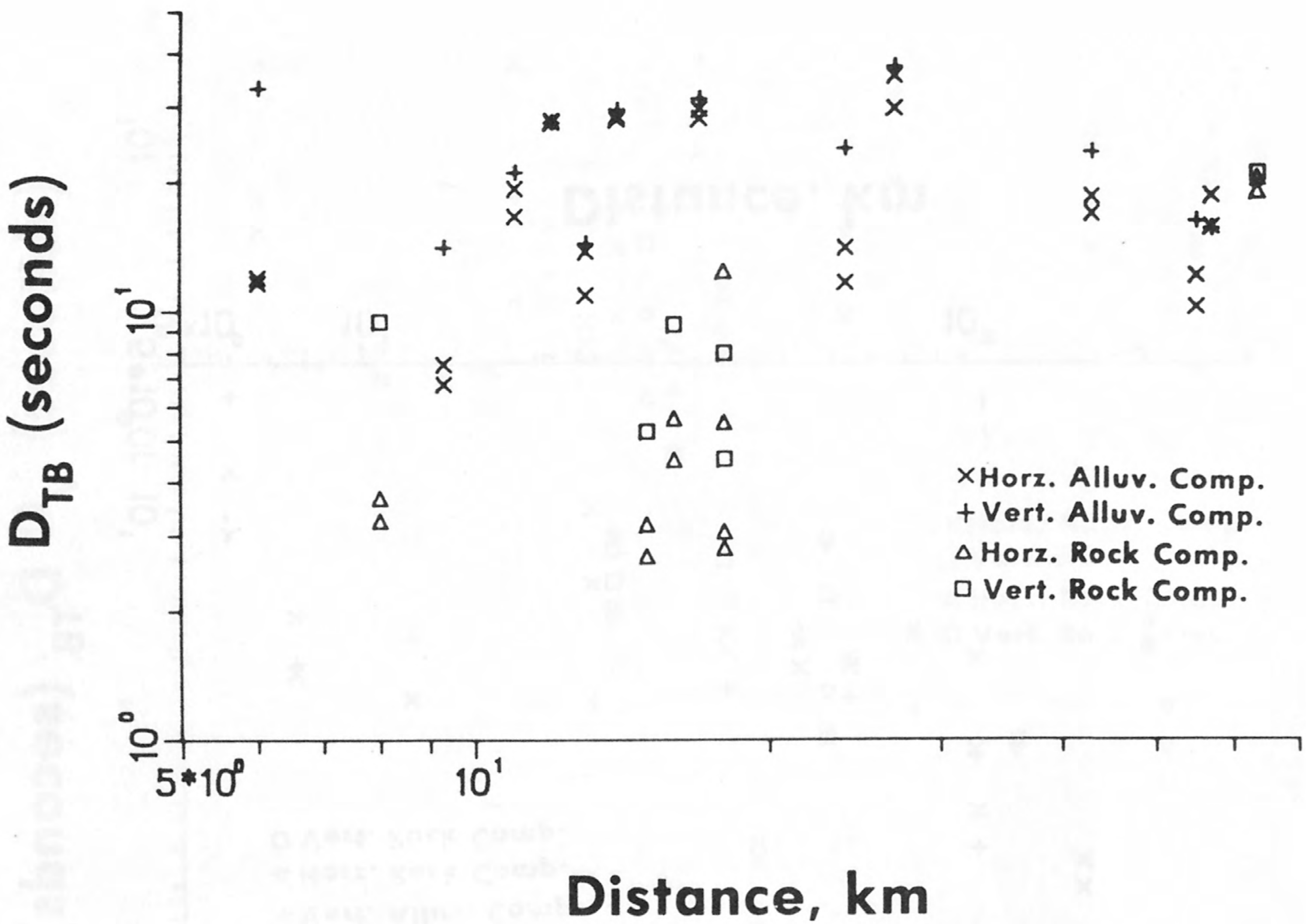

Figure 39.--D_{TB} versus R for records with $5.3 \leq M \leq 5.6$.

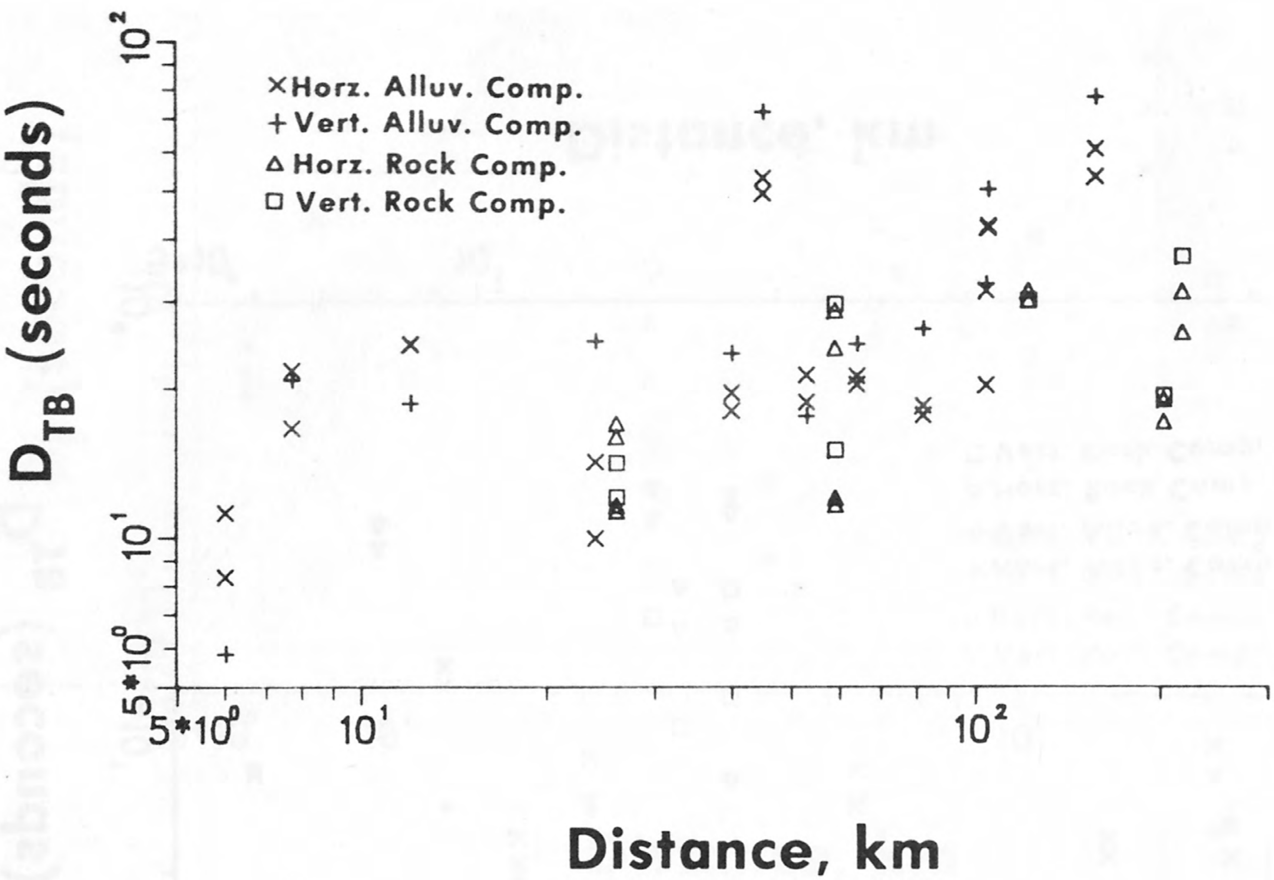

Figure 40.-- D_{TB} versus R for records with $6.3 \leq M \leq 6.6$.

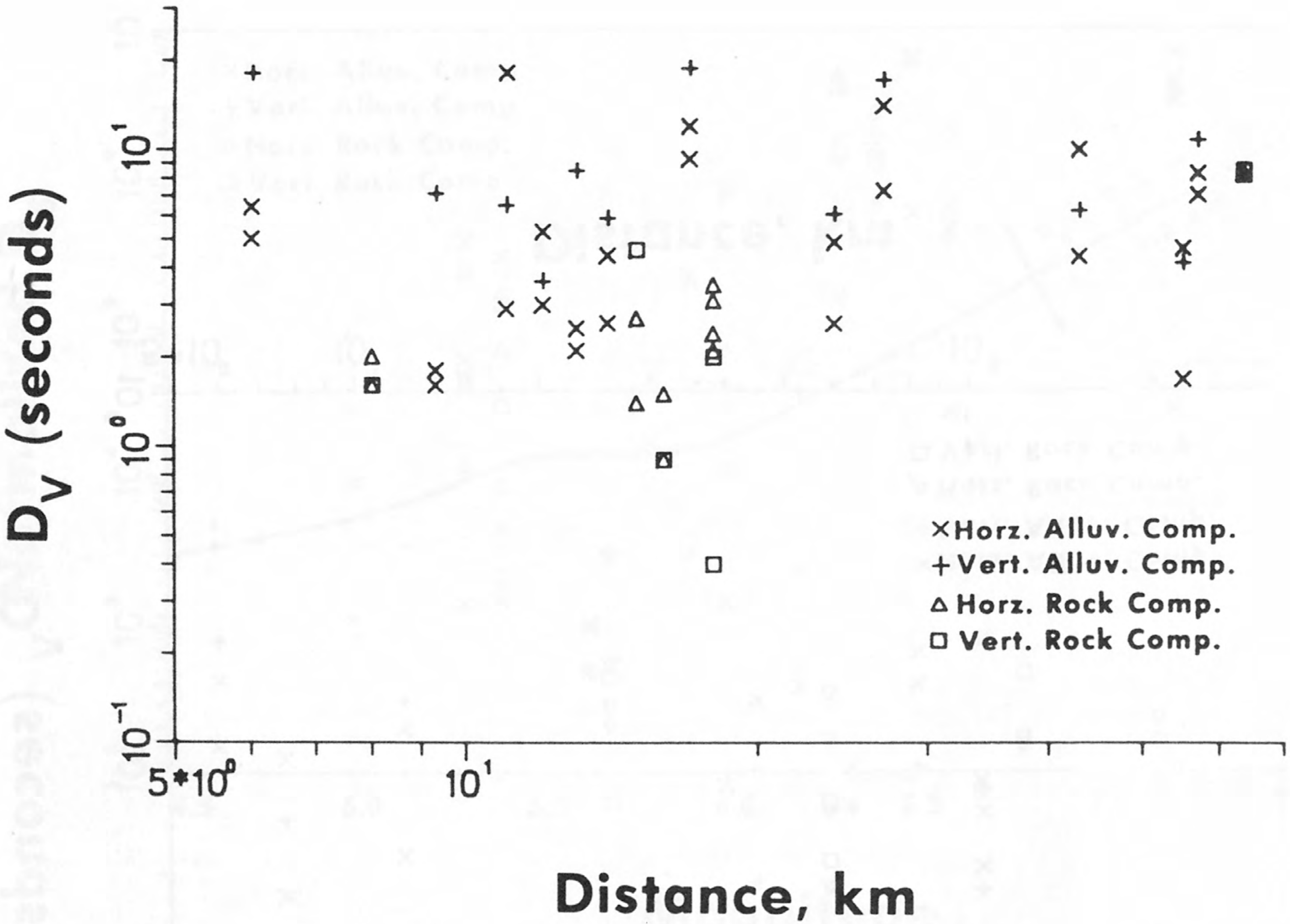

Figure 41.--D_V versus R for records with $5.3 \leq M \leq 5.6$.

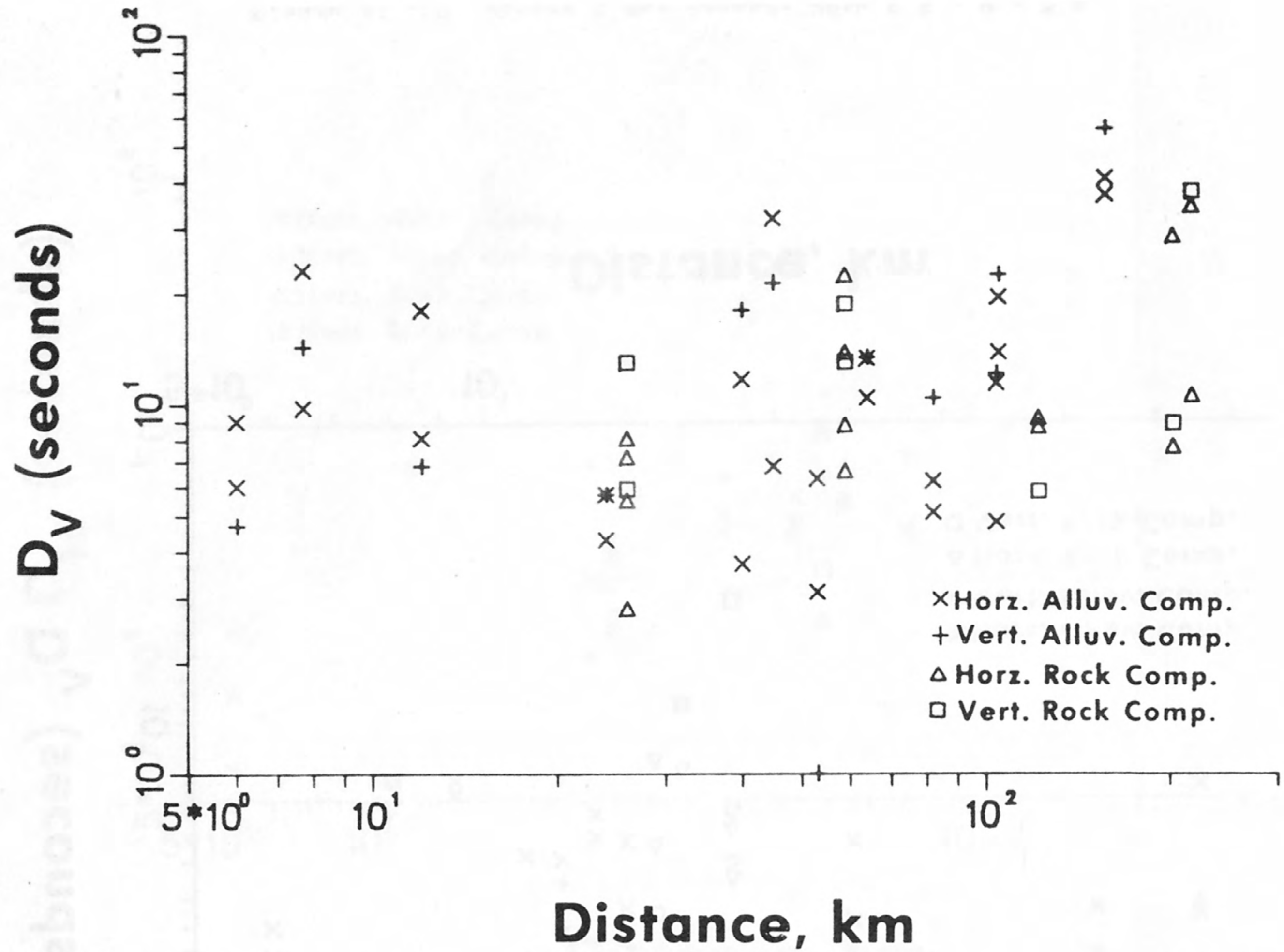

Figure 42.--D_V versus R for records with $6.3 \leq M \leq 6.6$.

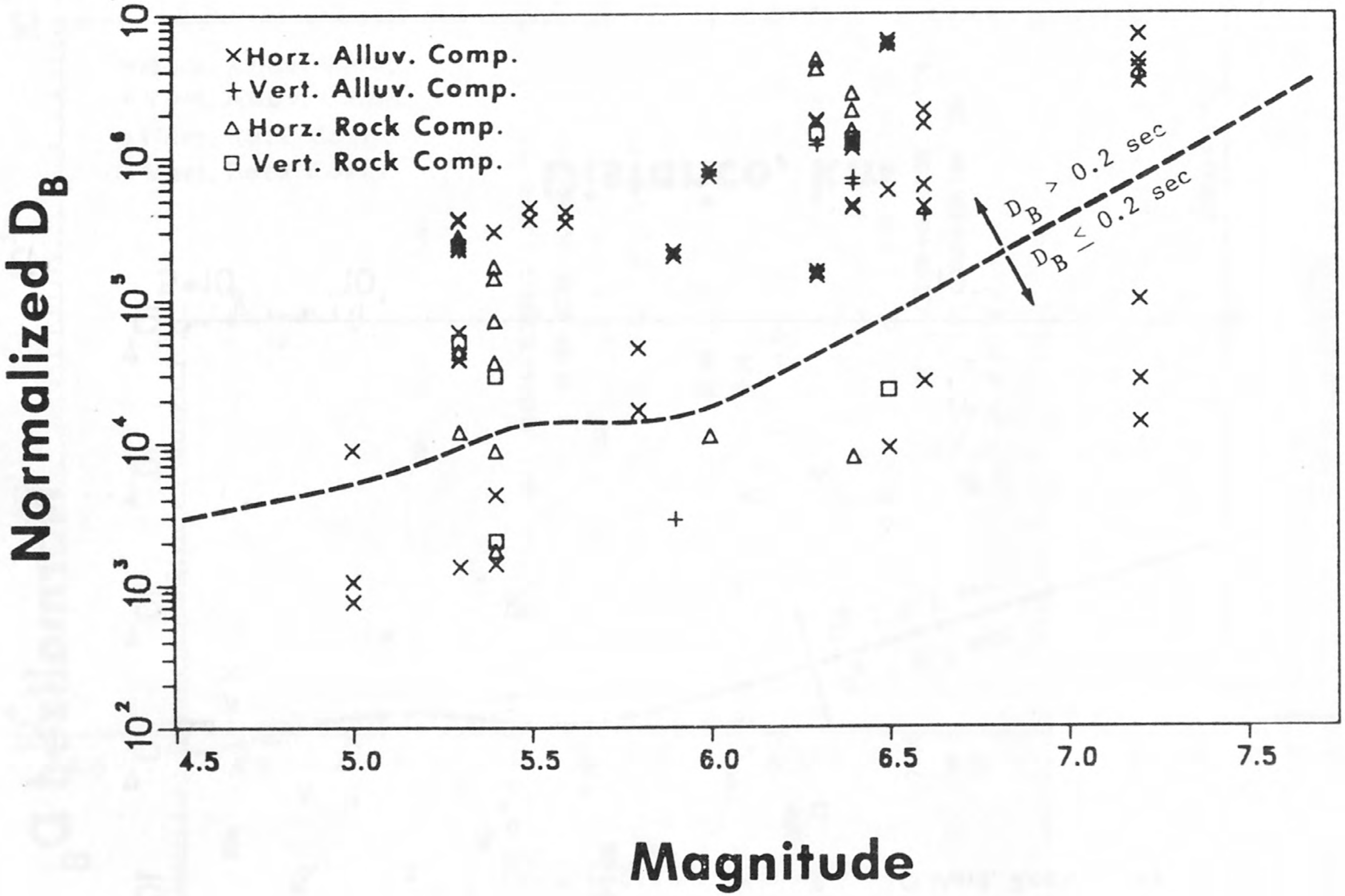

Figure 43.--D_B normalized by R, S, and V versus M.

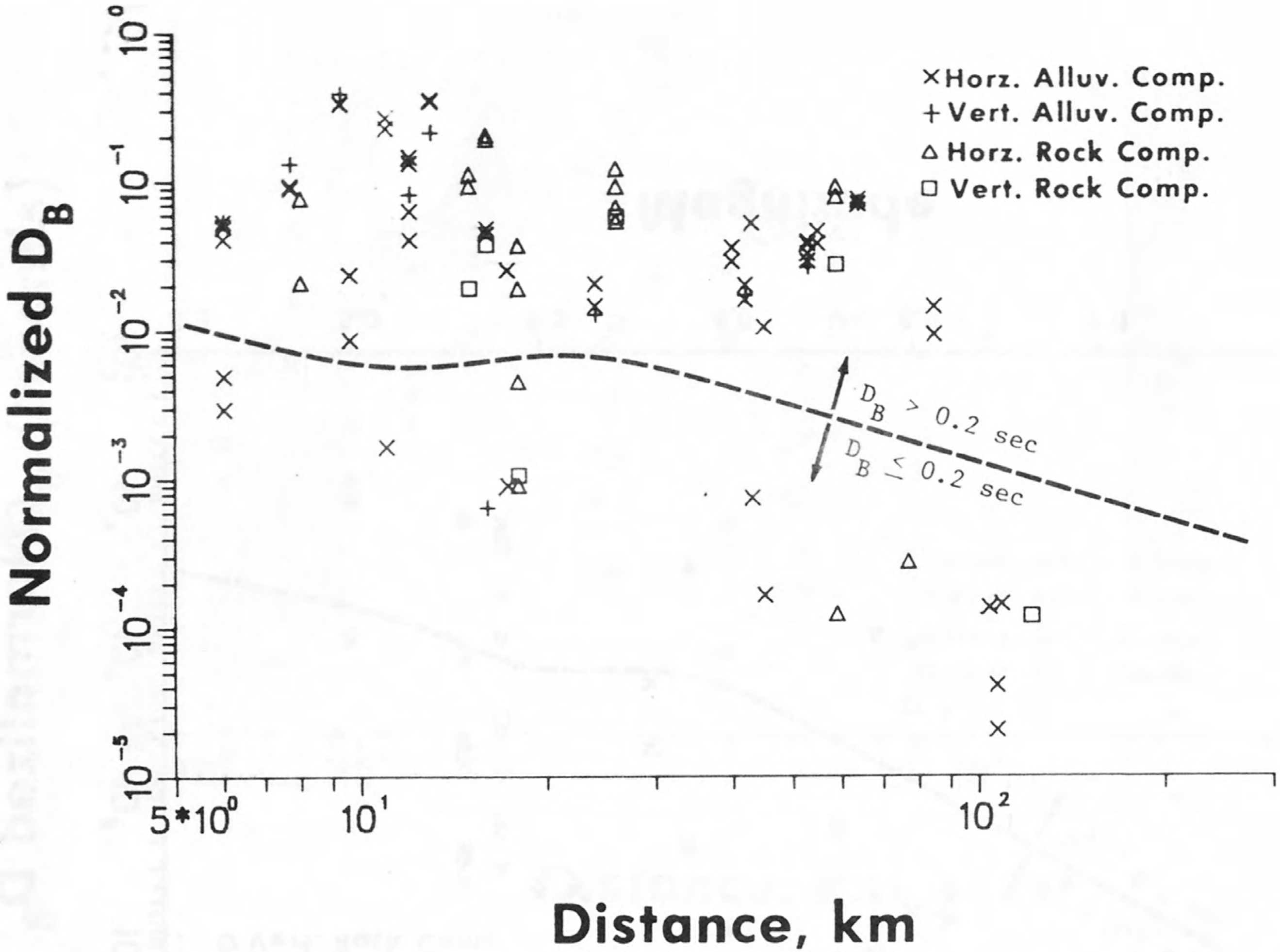

Figure 44.--D_B normalized by M, S, and V versus R.

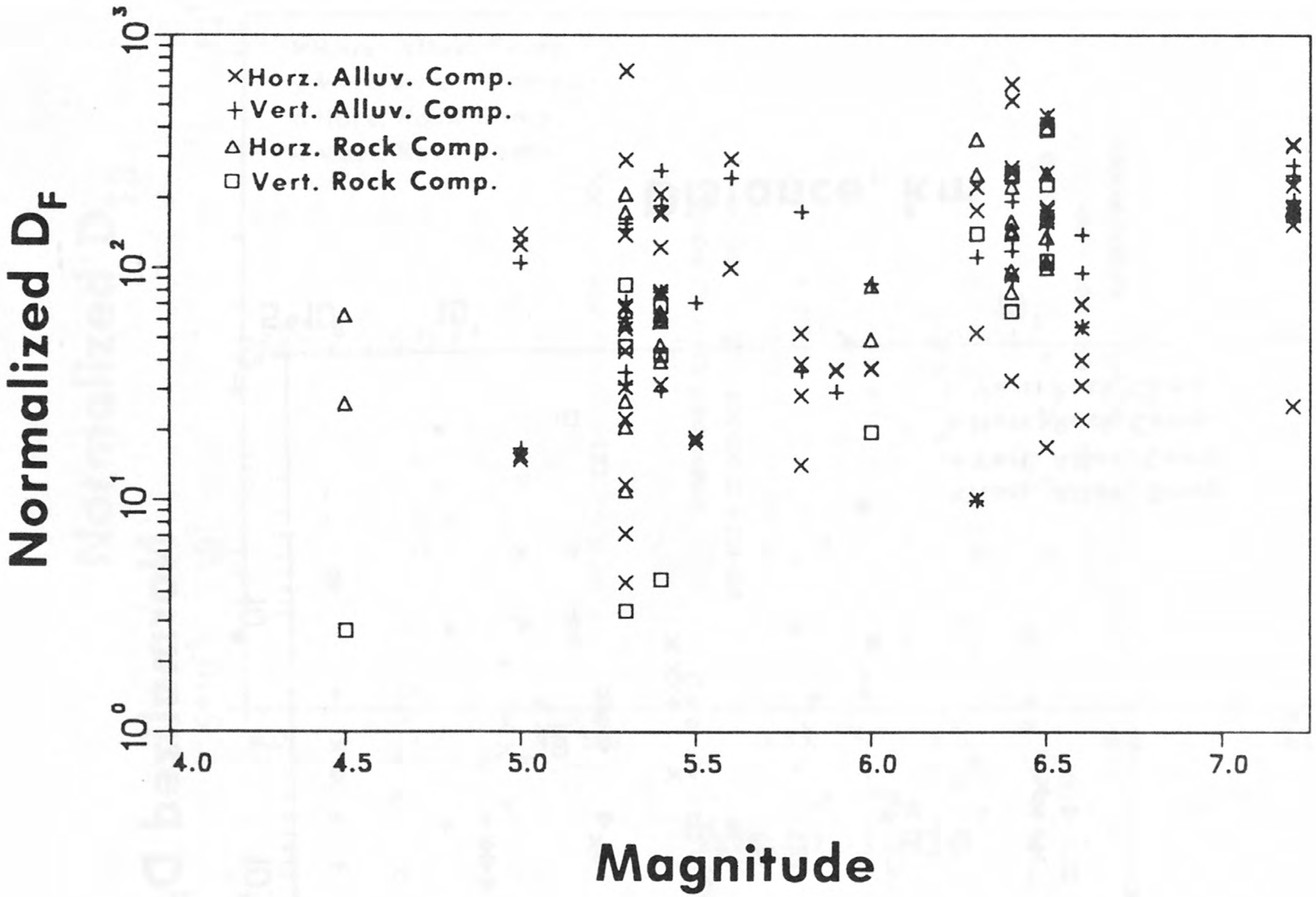

Figure 45.--D_F normalized by R, S, and V versus M.

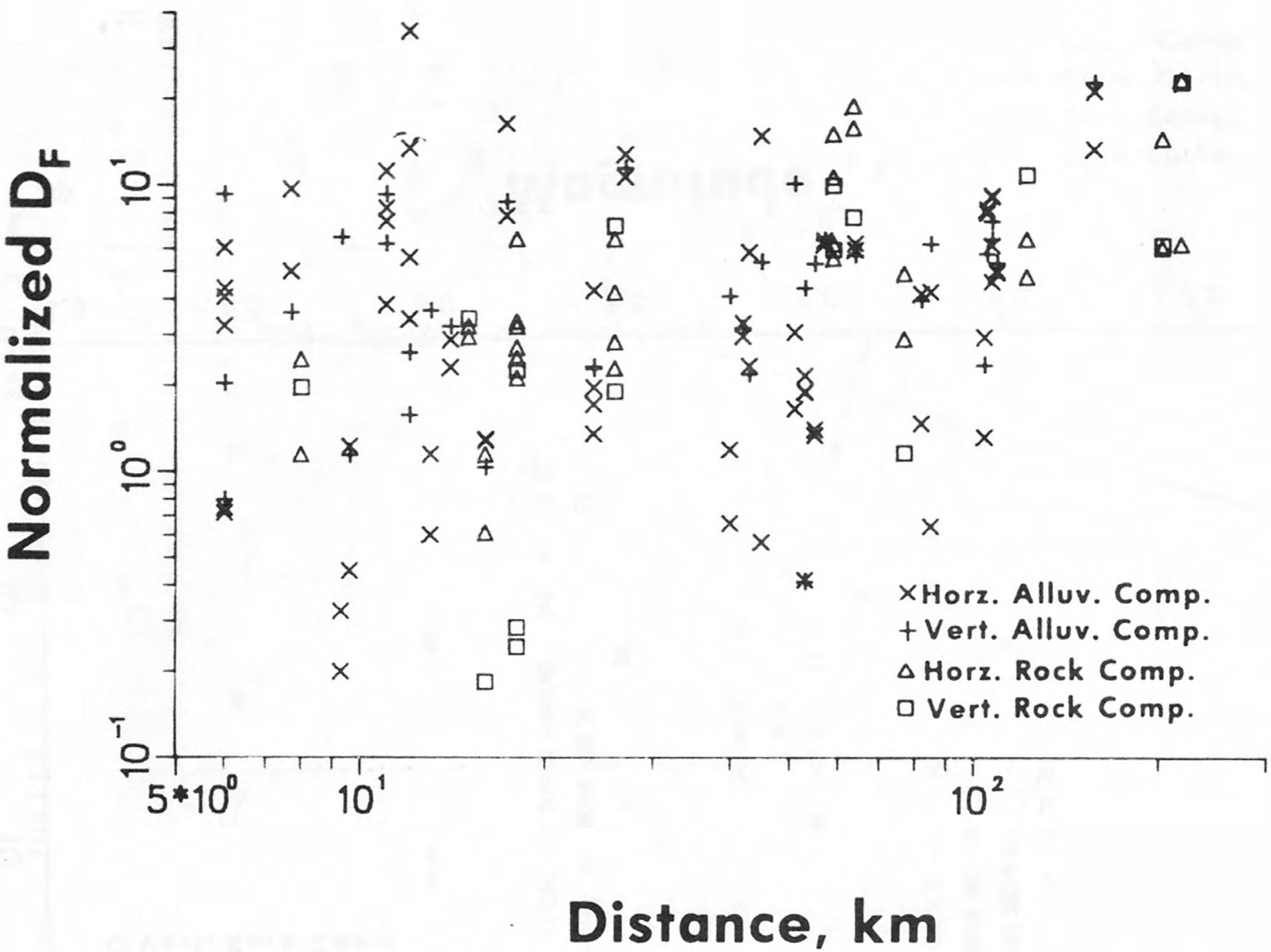

Figure 46.--D_F normalized by M, S, and V versus R.

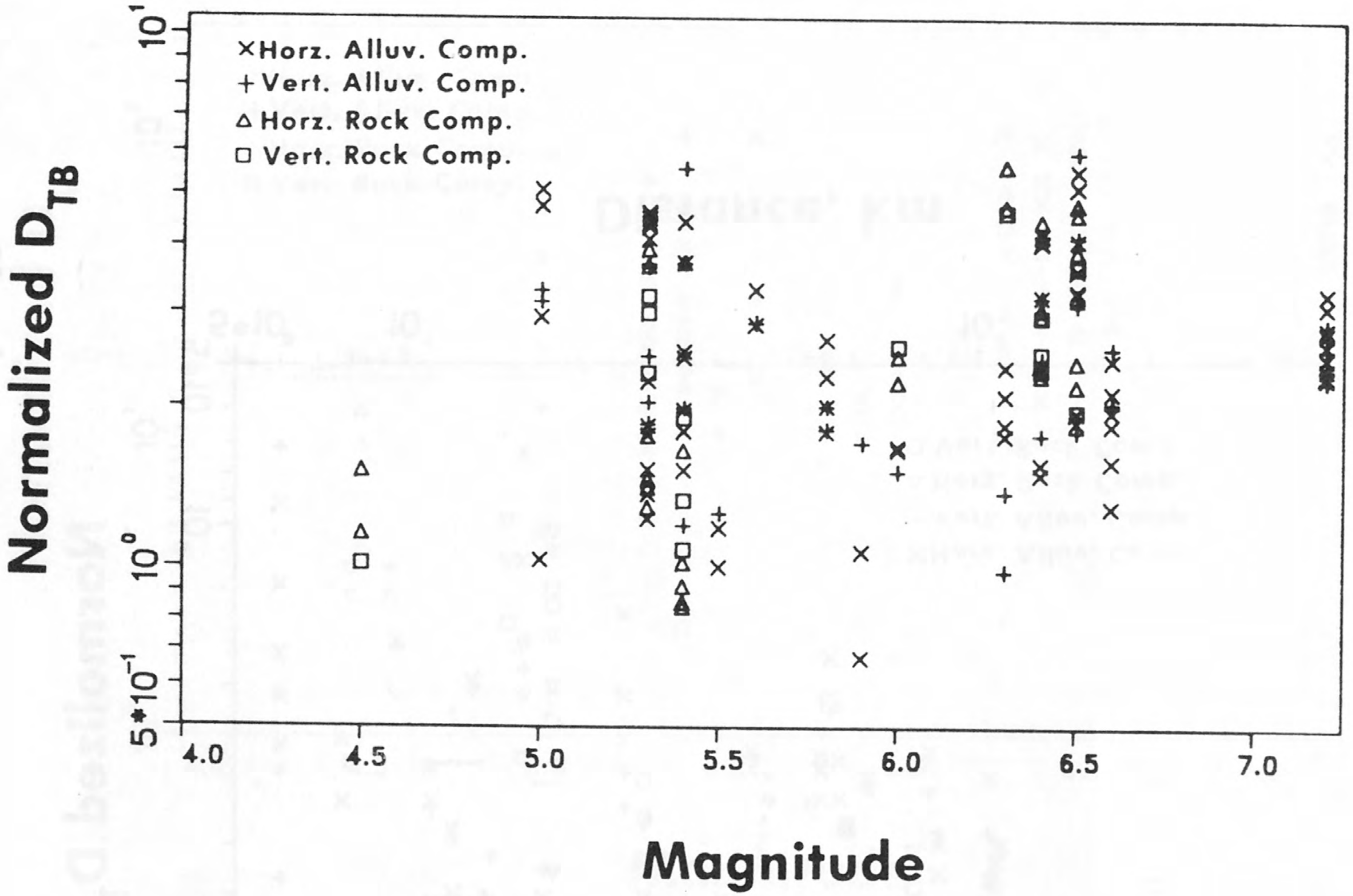

Figure 47.--D_{TB} normalized by R, S, and V versus M.

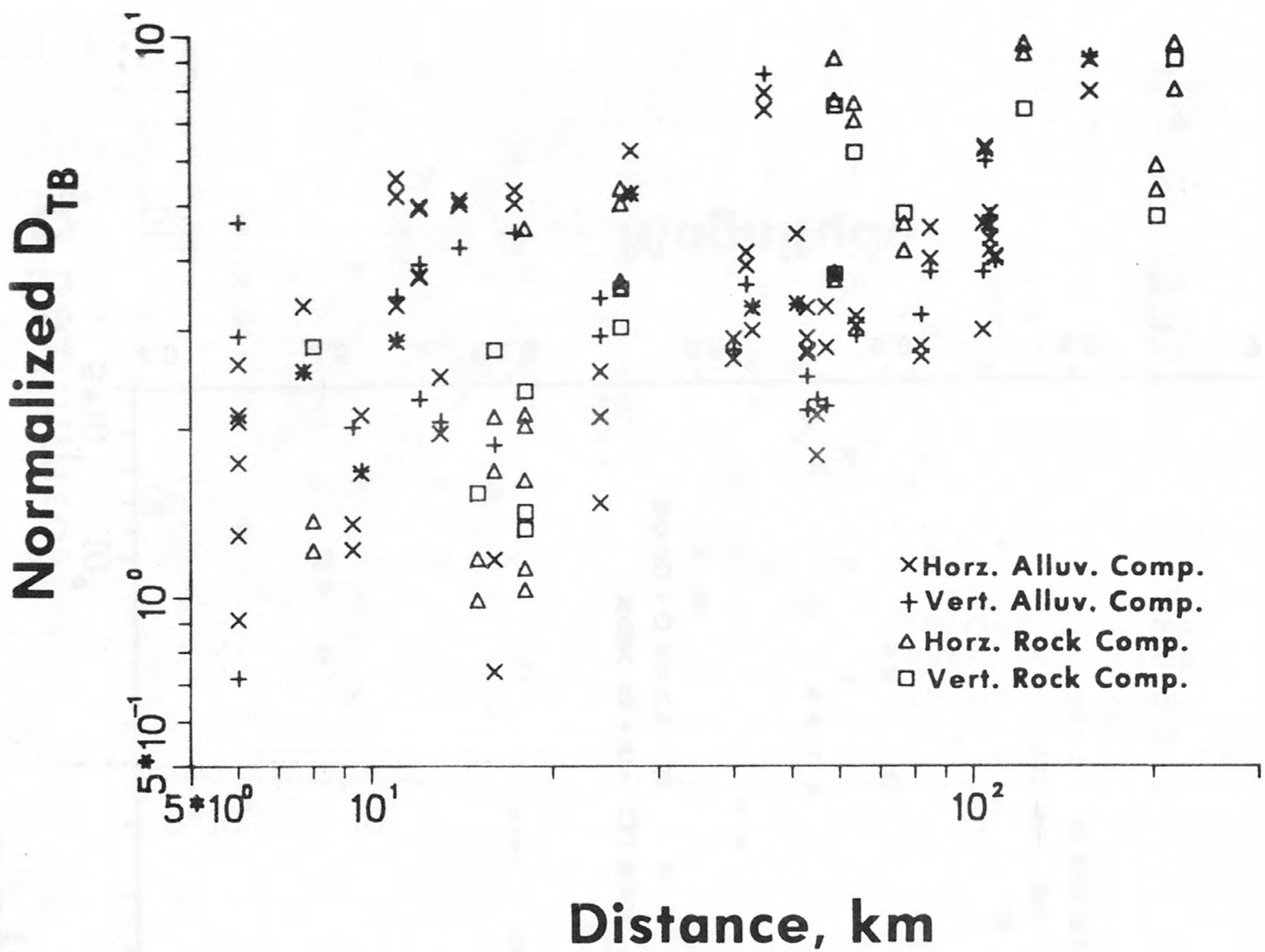

Figure 48.--D_{TB} normalized by M, S, and V versus R.

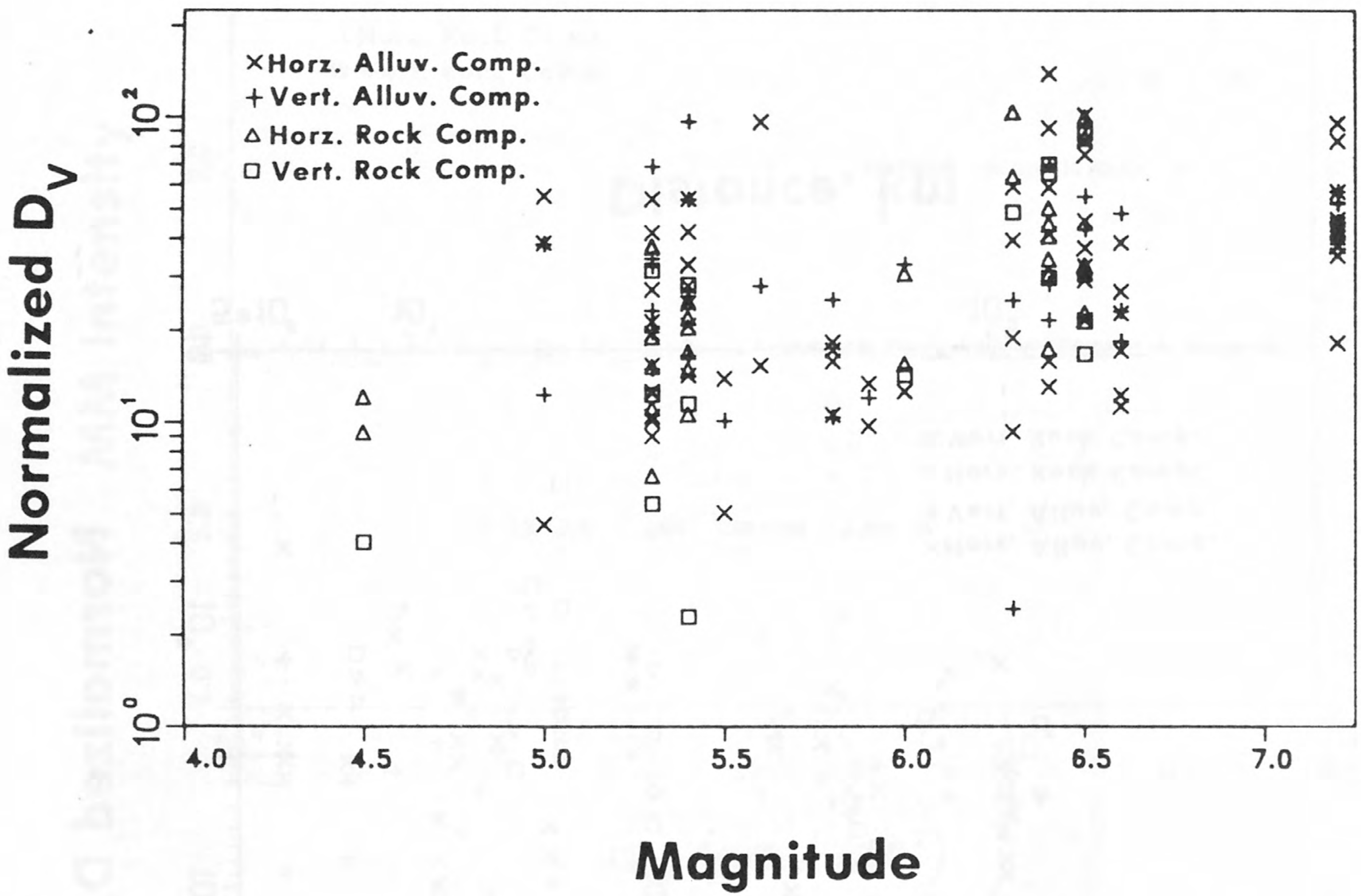

Figure 49.--D_V normalized by R, S, and V versus M.

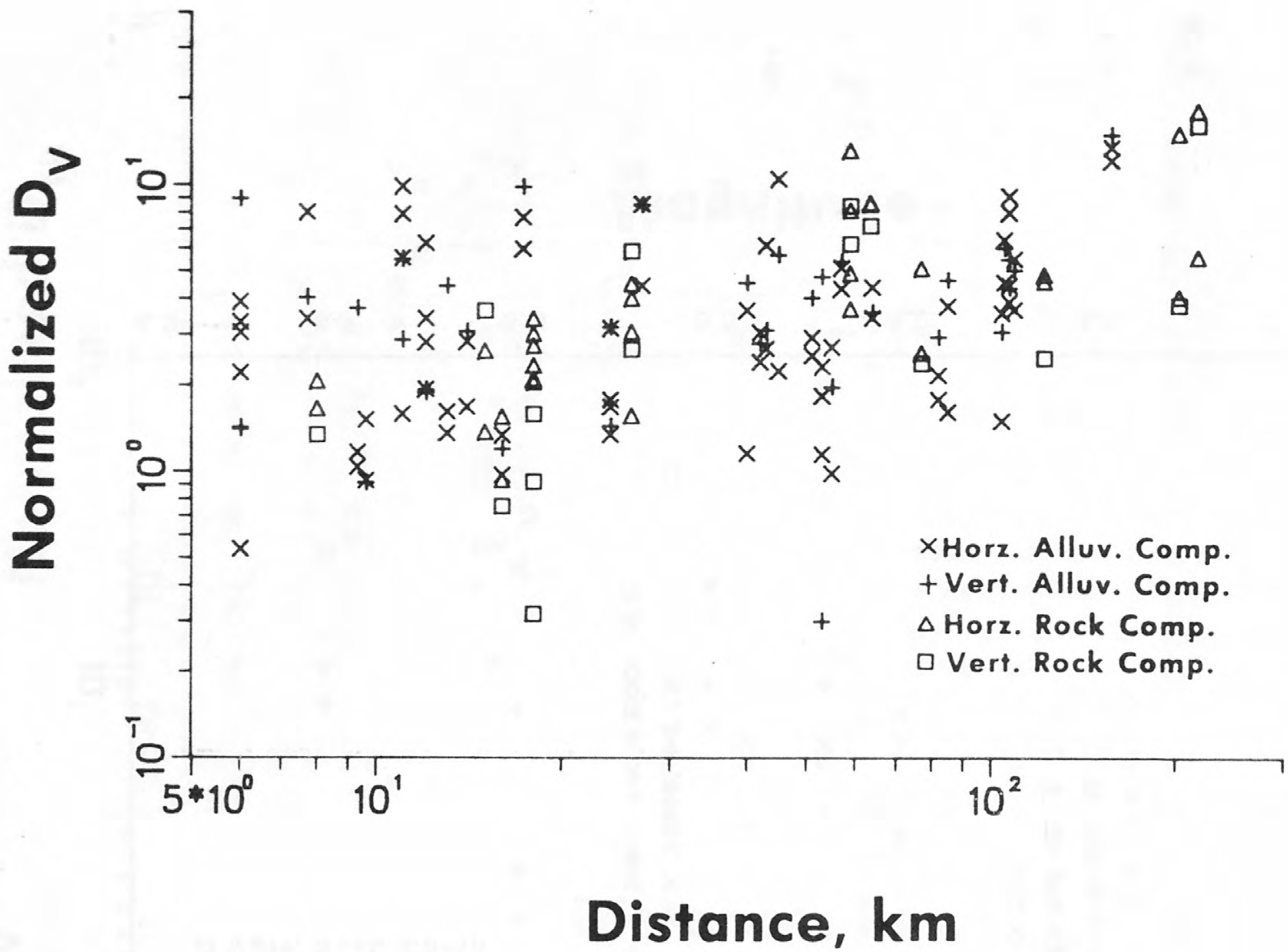

Figure 50.--D_V normalized by M, S, and V versus R.

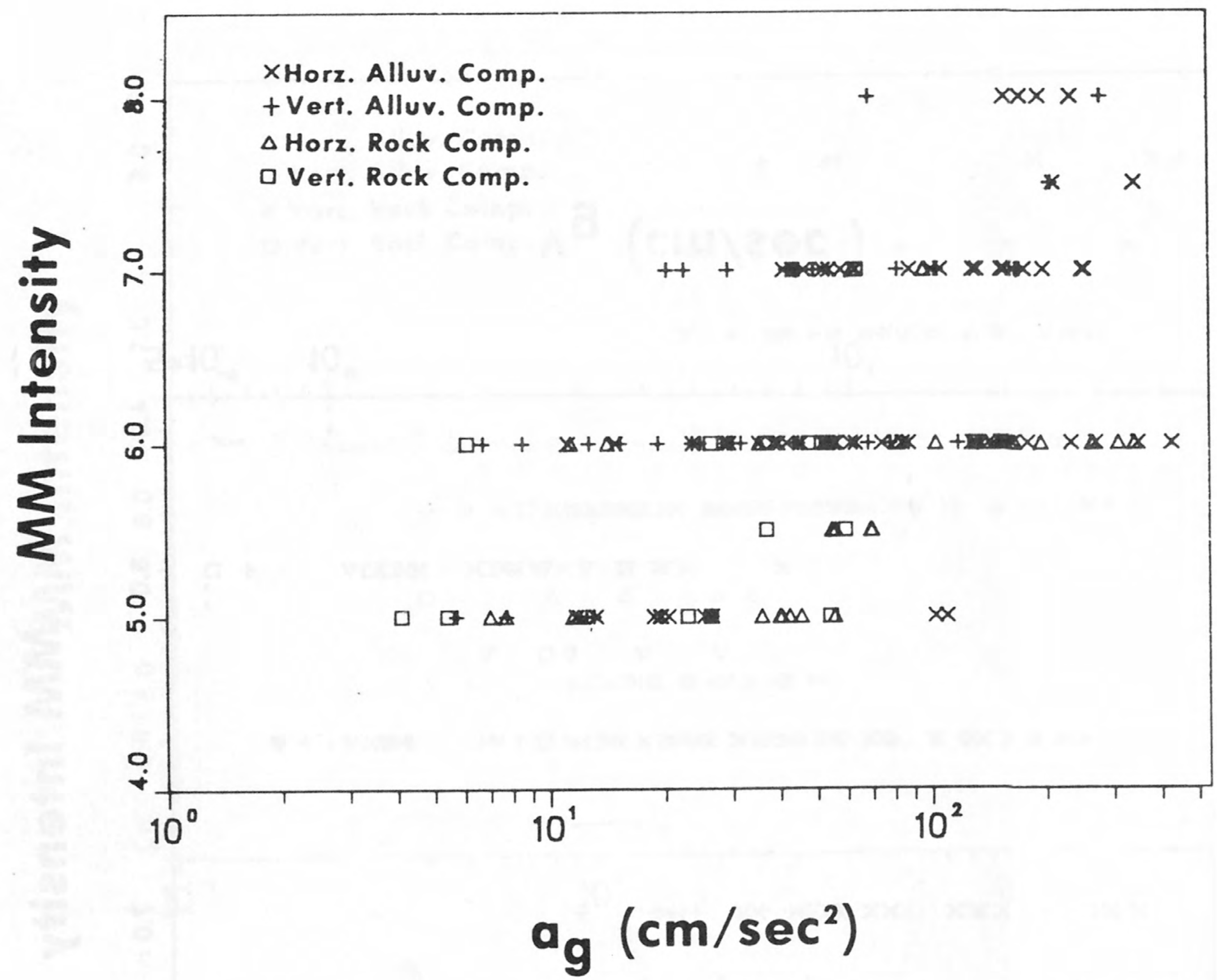

Figure 51.--MM intensity versus a_g.

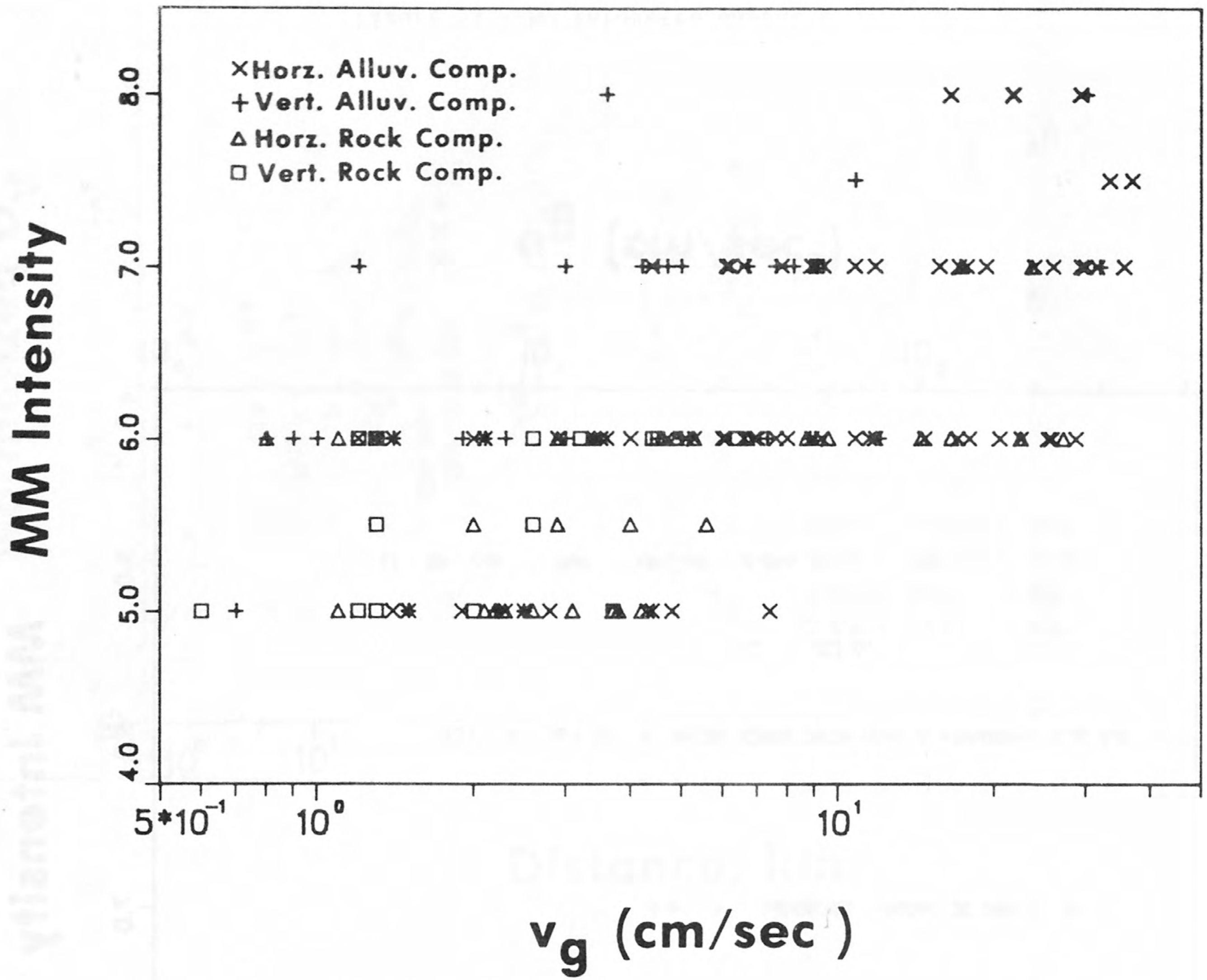

Figure 52.--MM intensity versus v_g.

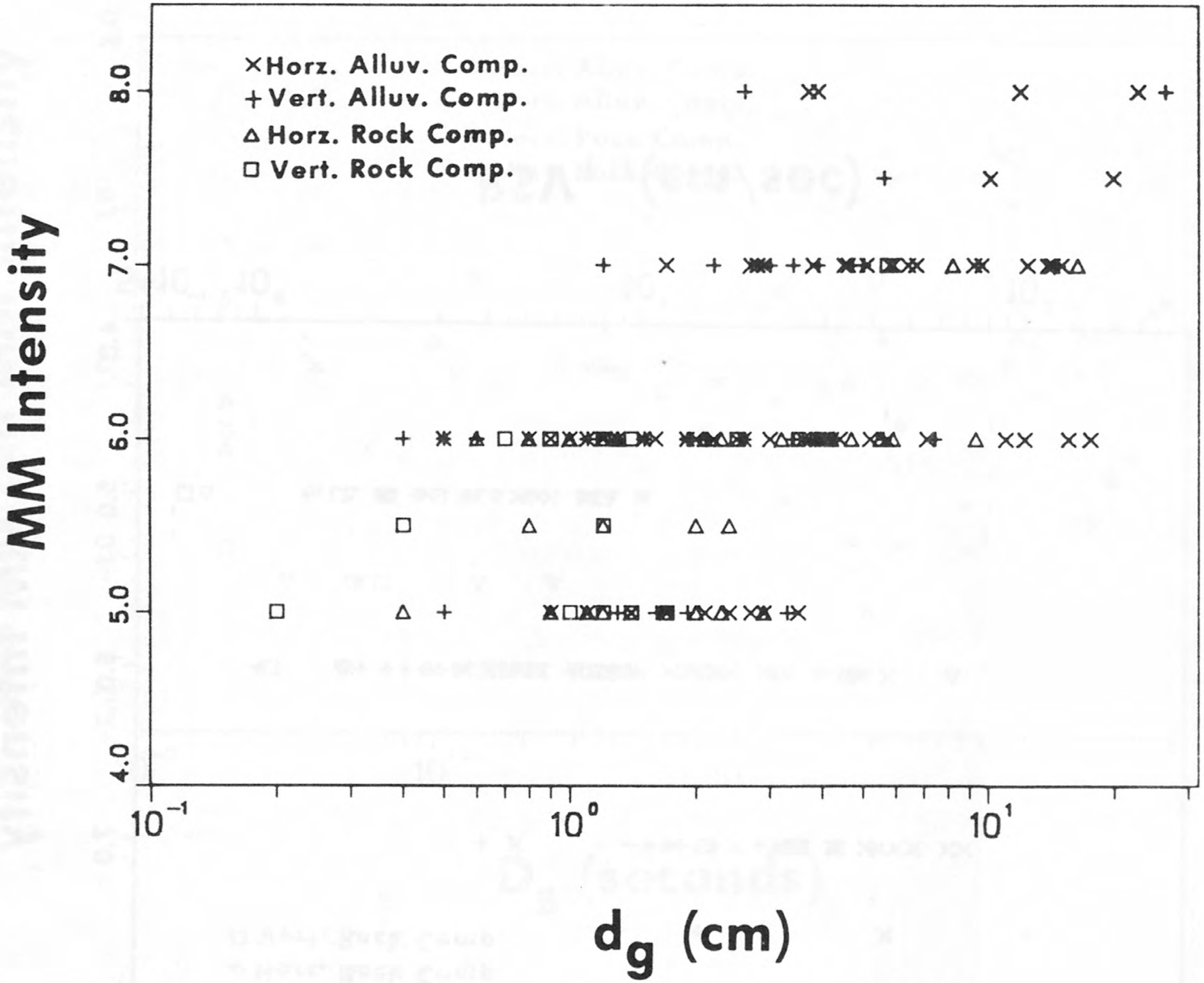

Figure 53.--MM intensity versus d_g.

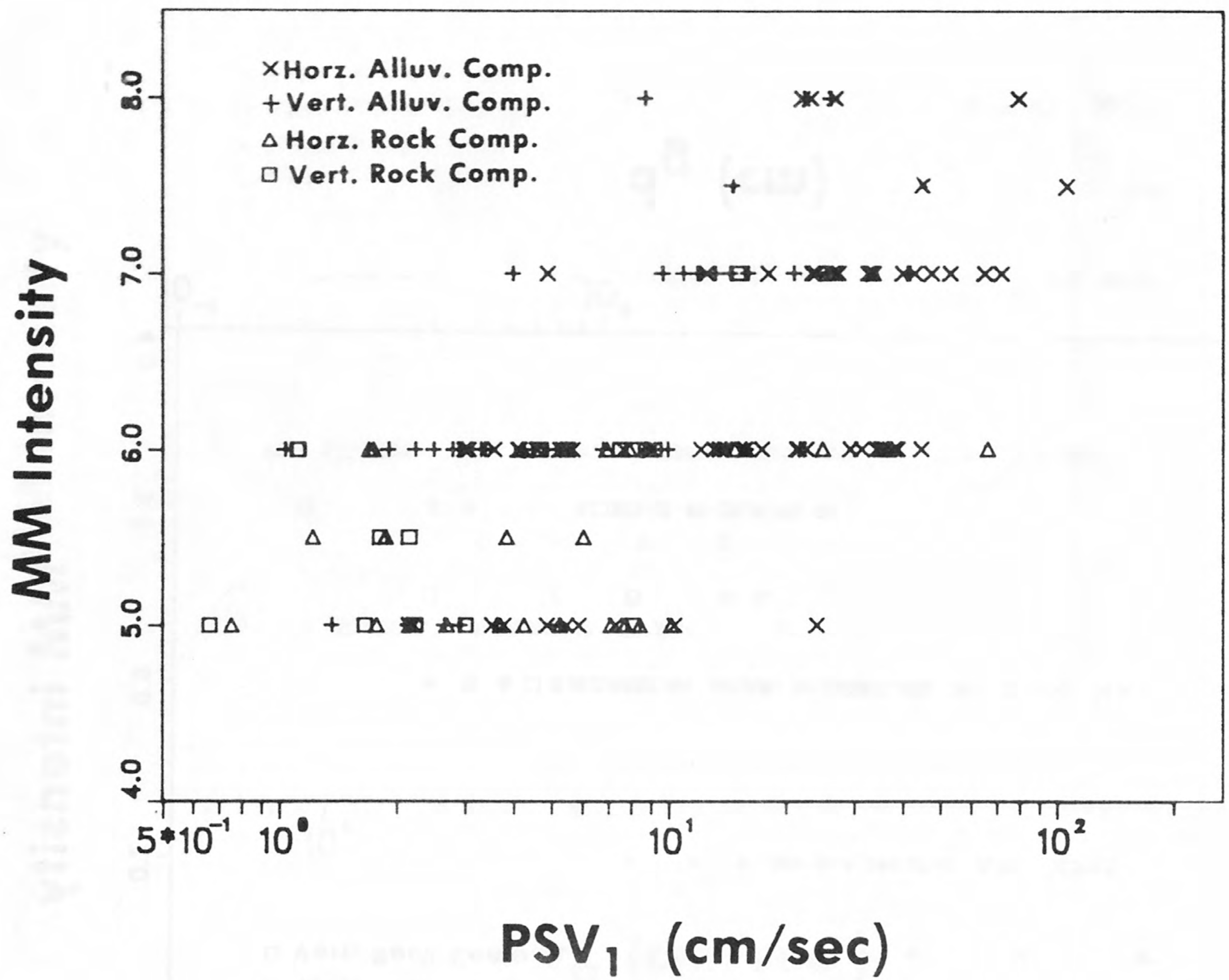

Figure 54.--MM intensity versus PSV_1.

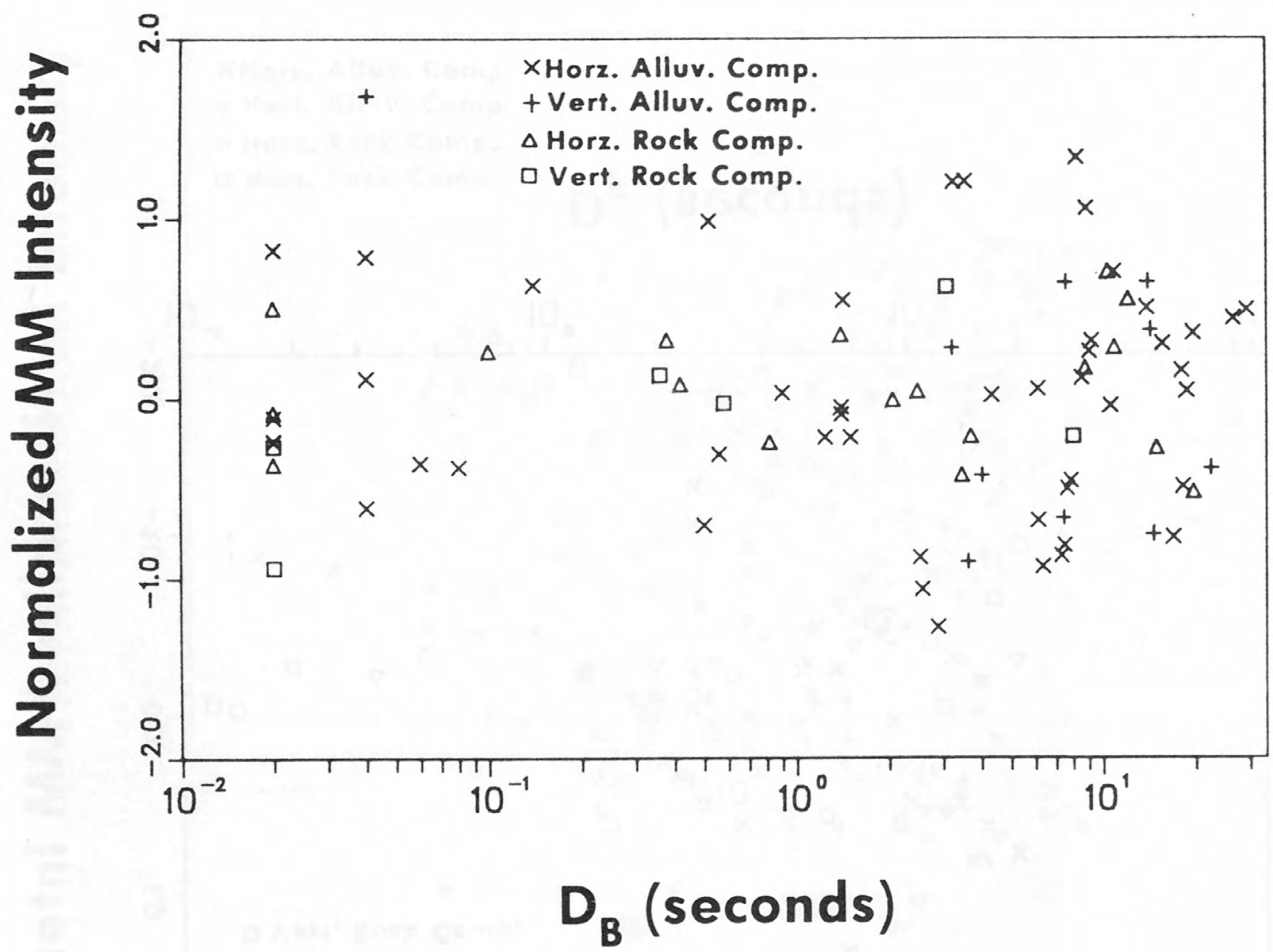

Figure 55.--MM intensity, normalized by $\ell n\ v_g$, S, and V, versus D_B.

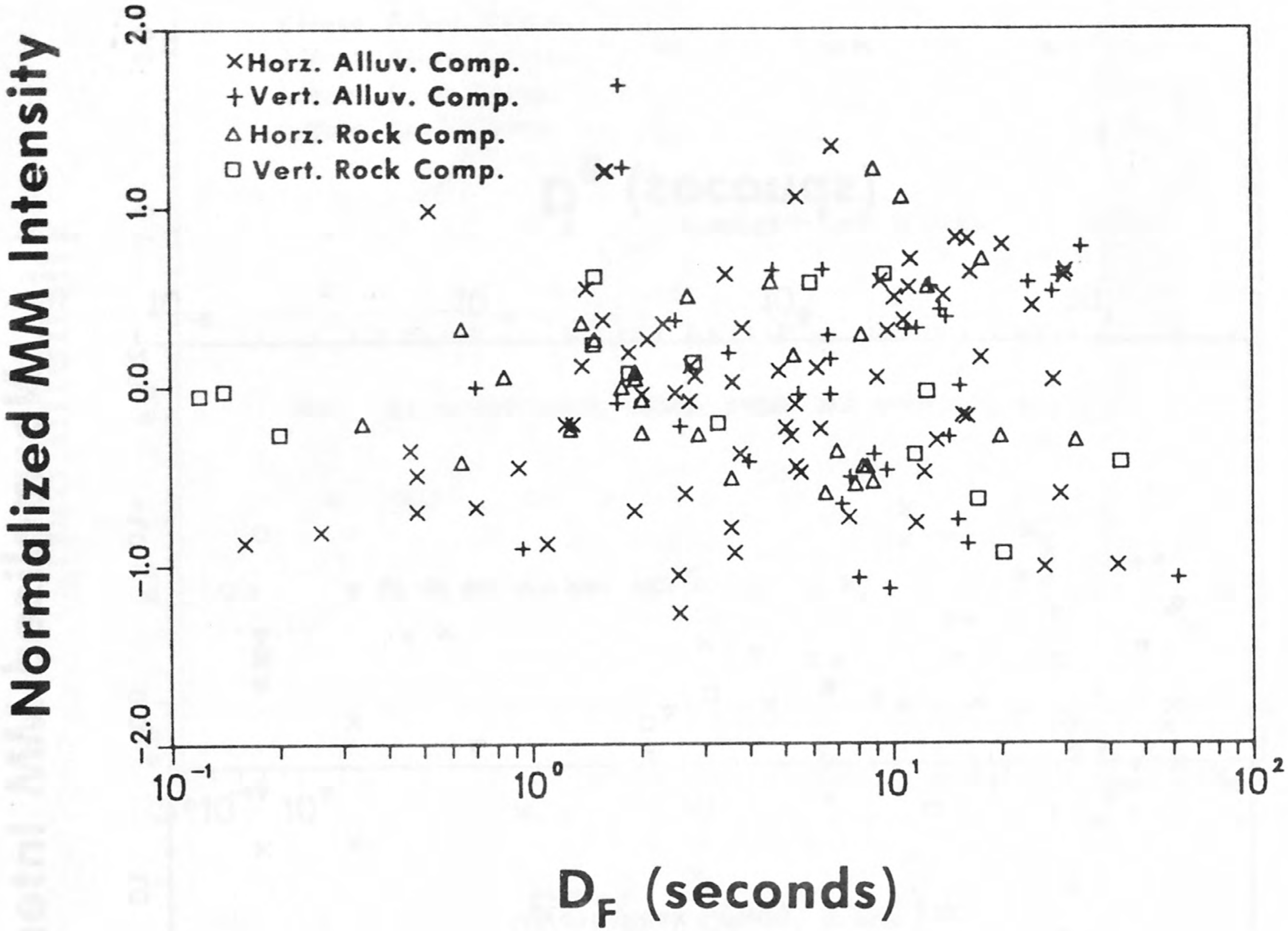

Figure 56.--MM intensity, normalized by $\ell n\ v_g$, S, and V, versus D_F.

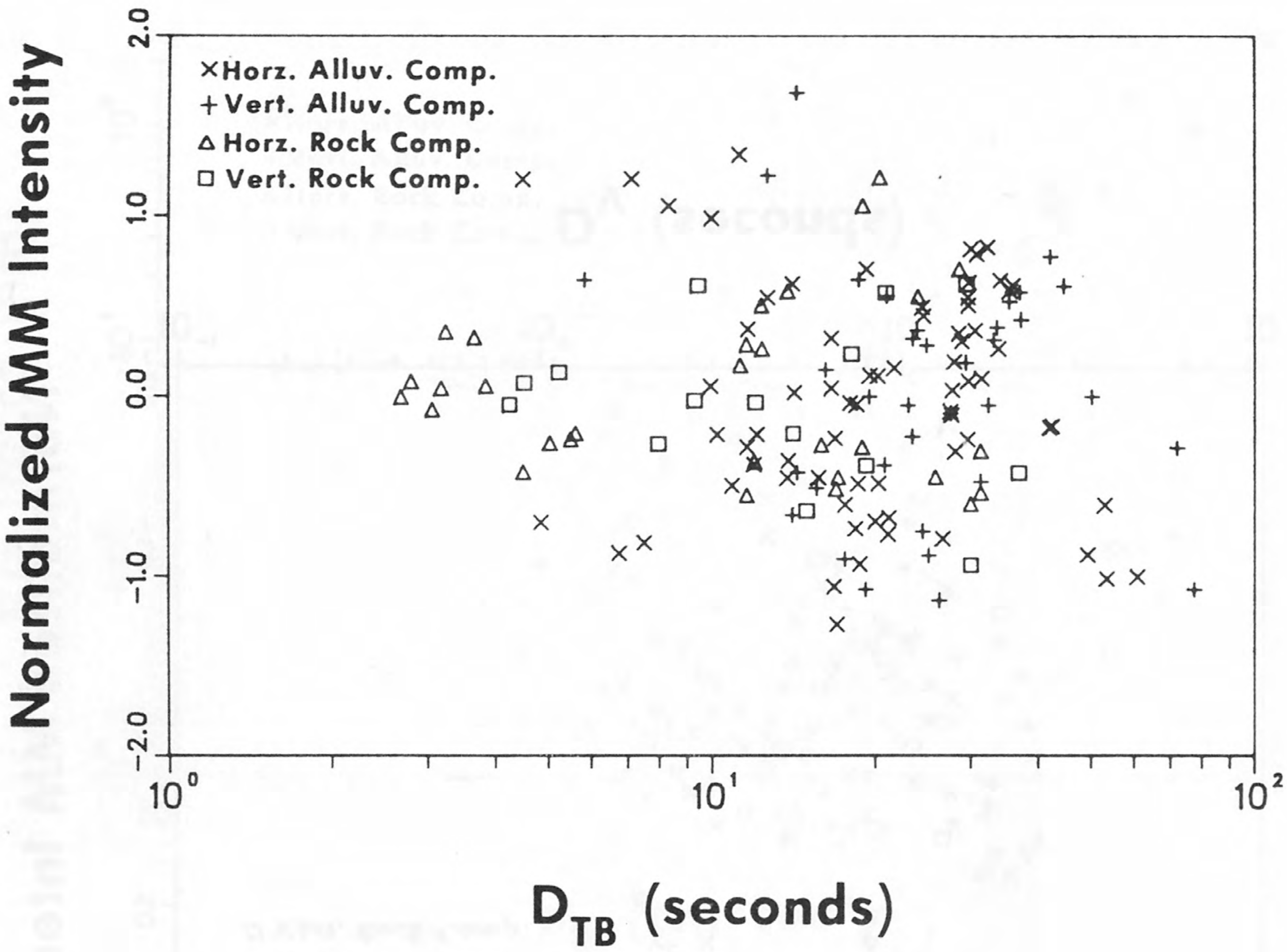

Figure 57.--MM intensity, normalized by $\ell n\ v_g$, S, and V, versus D_{TB}.

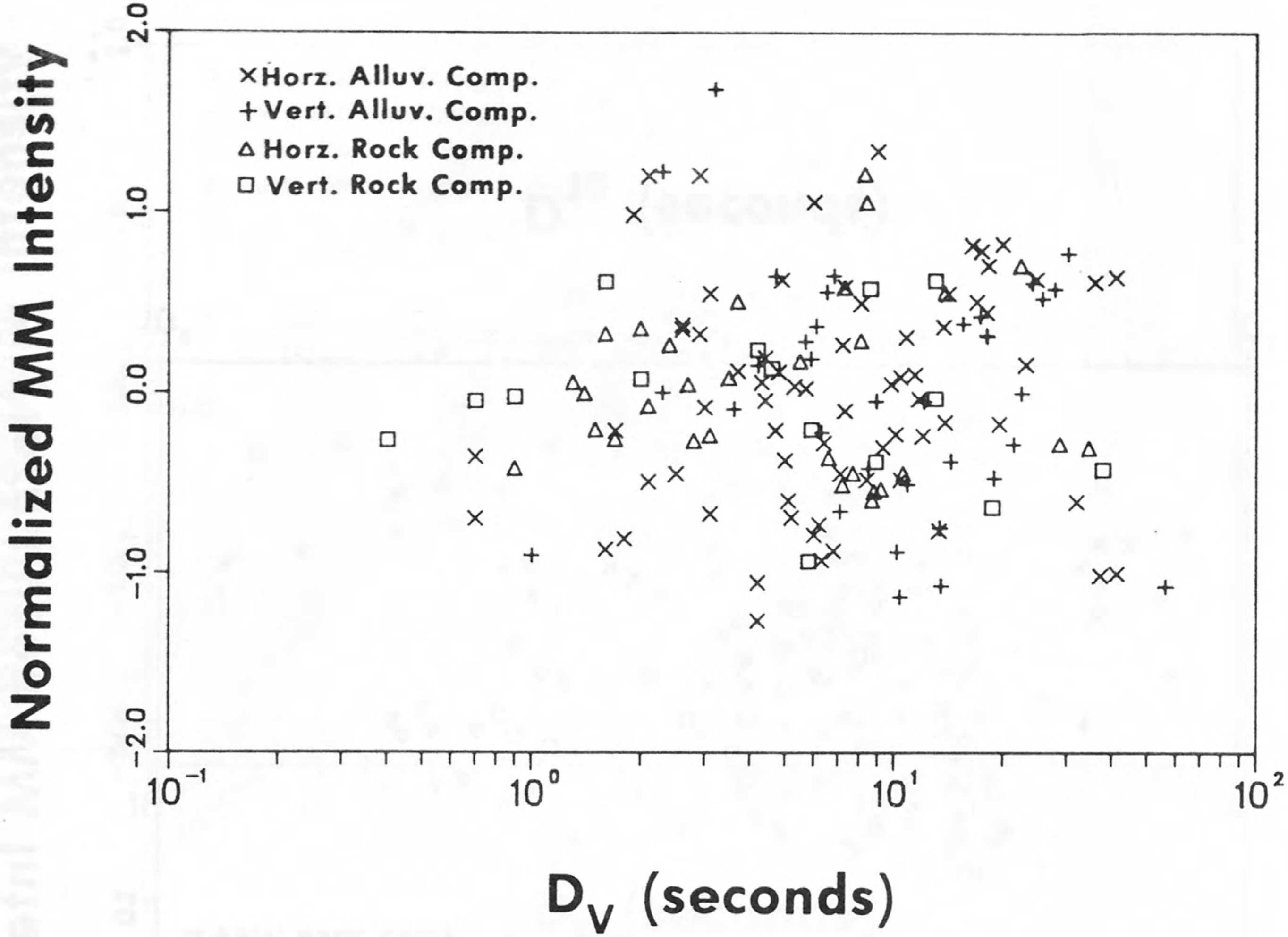

Figure 58.--MM intensity, normalized by $\ell n\ v_g$, S, and V, versus D_V.

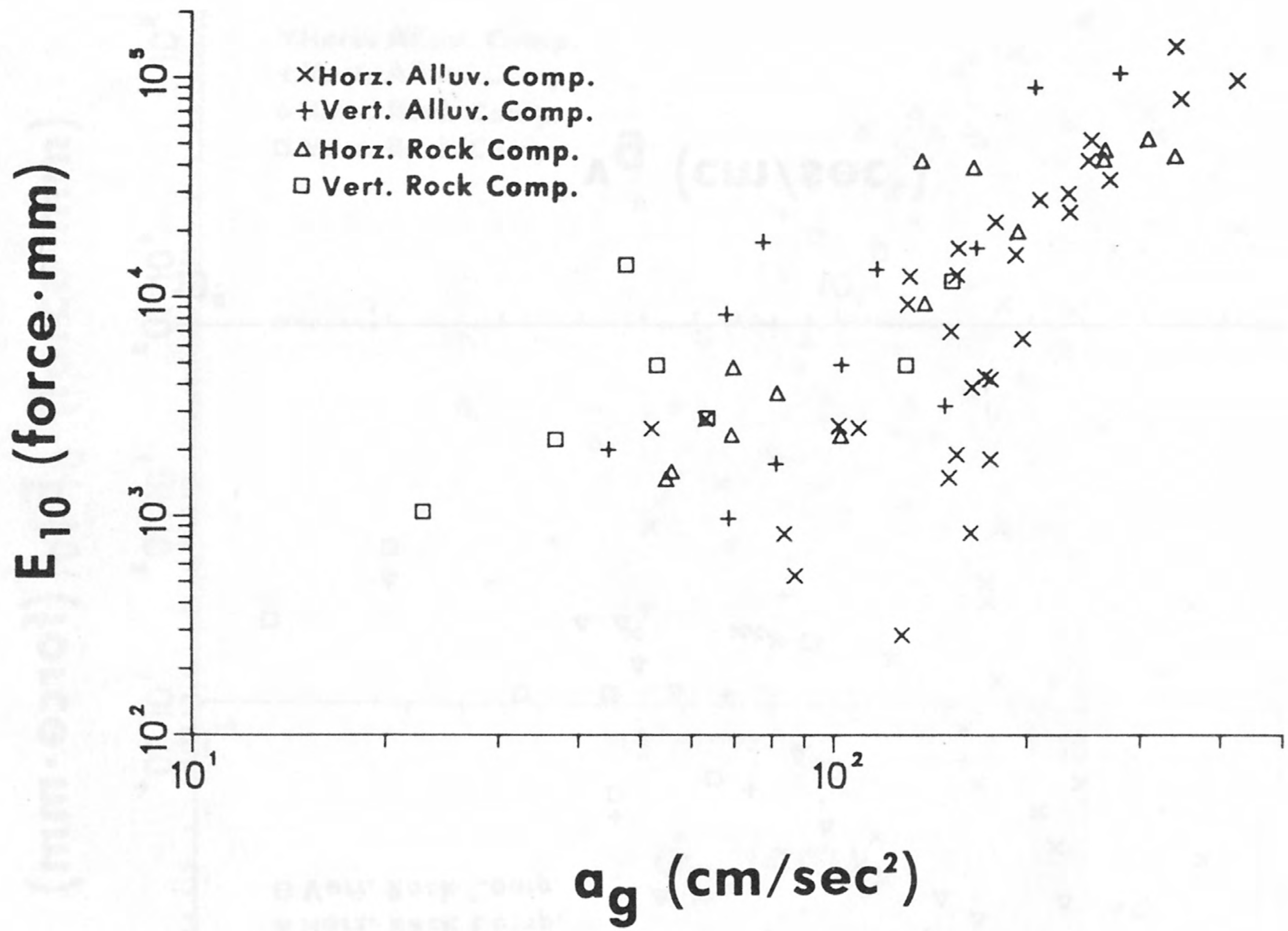

Figure 59.--E_{10} versus a_g.

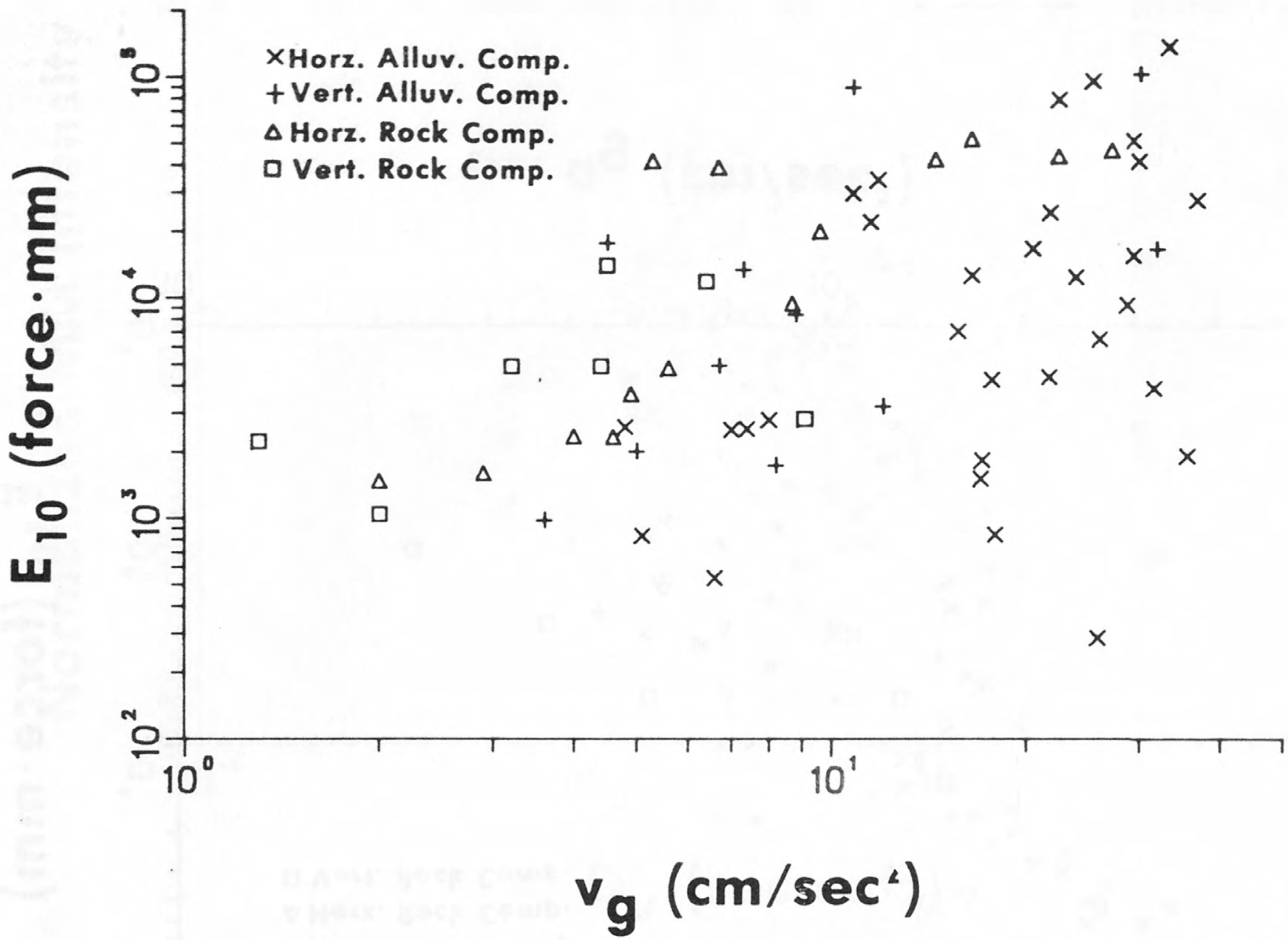

Figure 60.--E_{10} versus v_g.

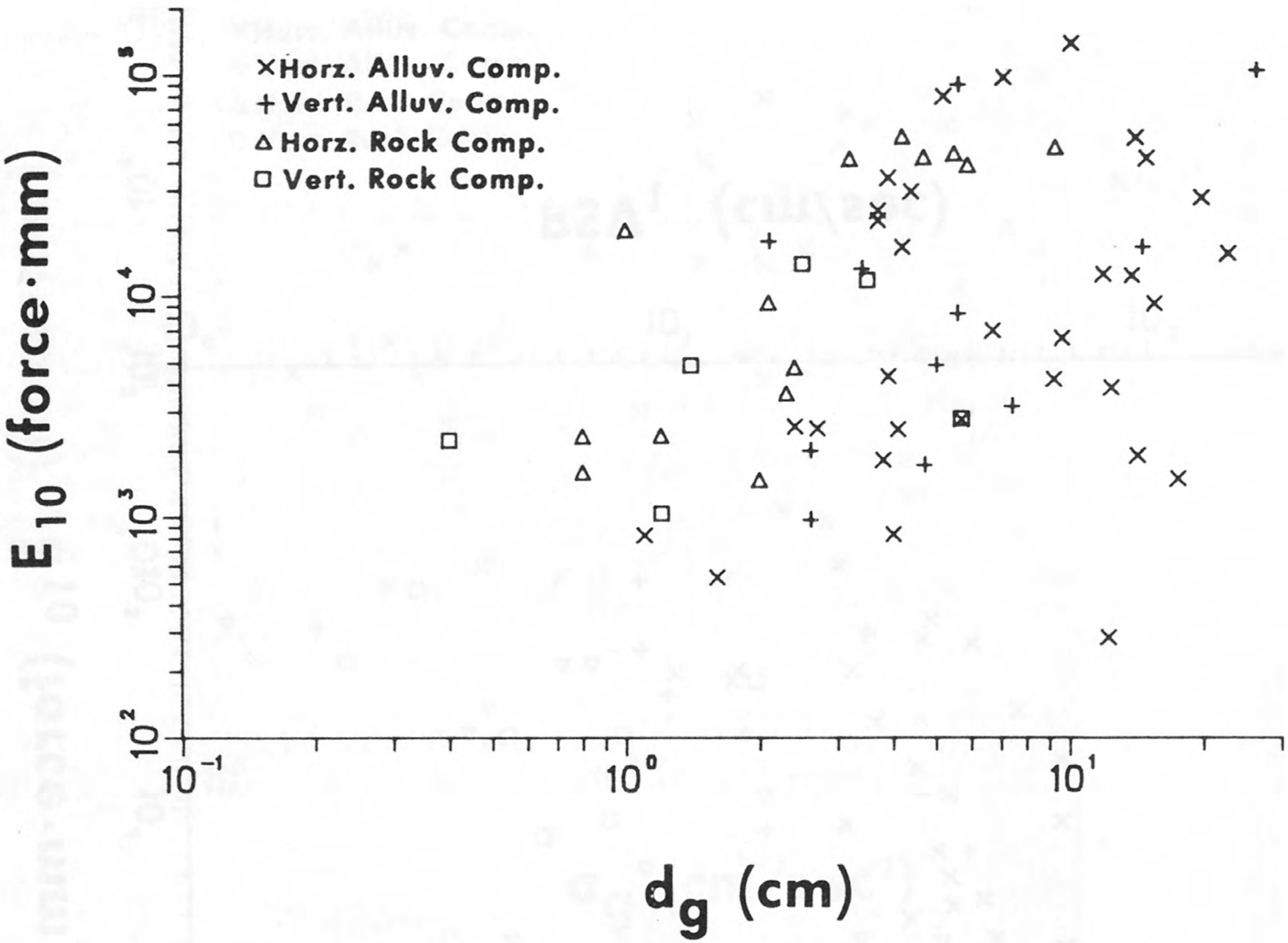

Figure 61.--E_{10} versus d_g.

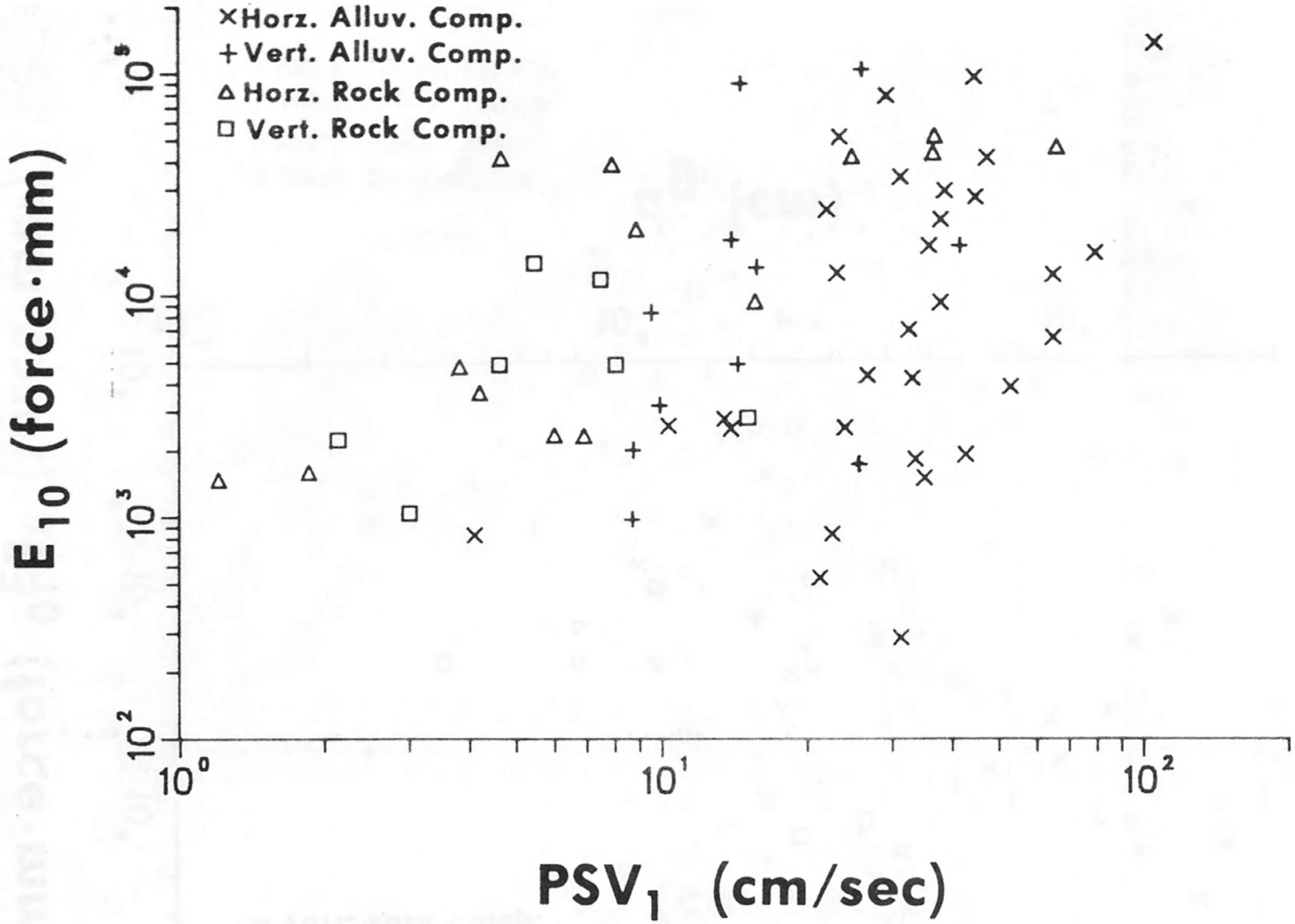

Figure 62.--E_{10} versus PSV_1.

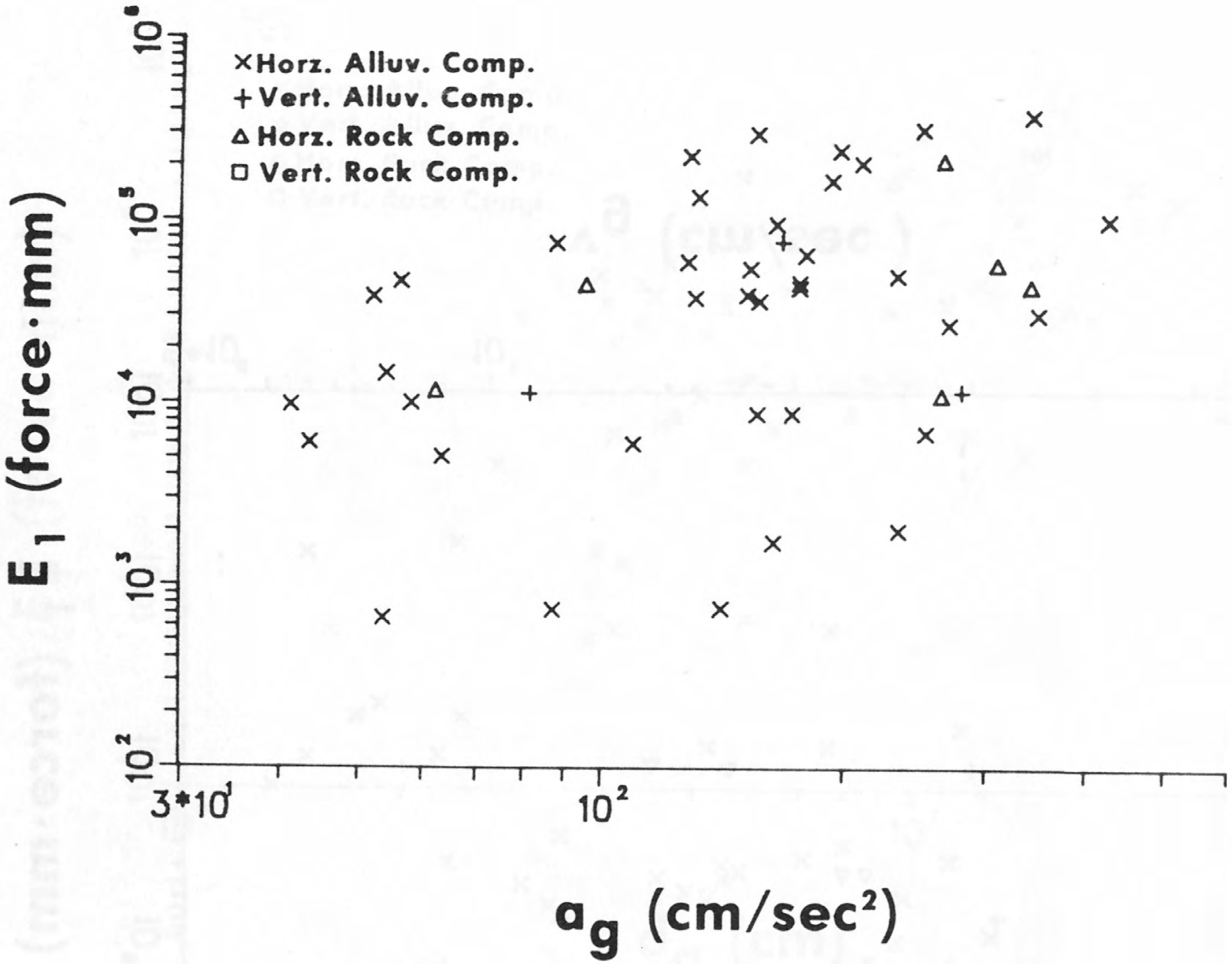

Figure 63.--E_1 versus a_g.

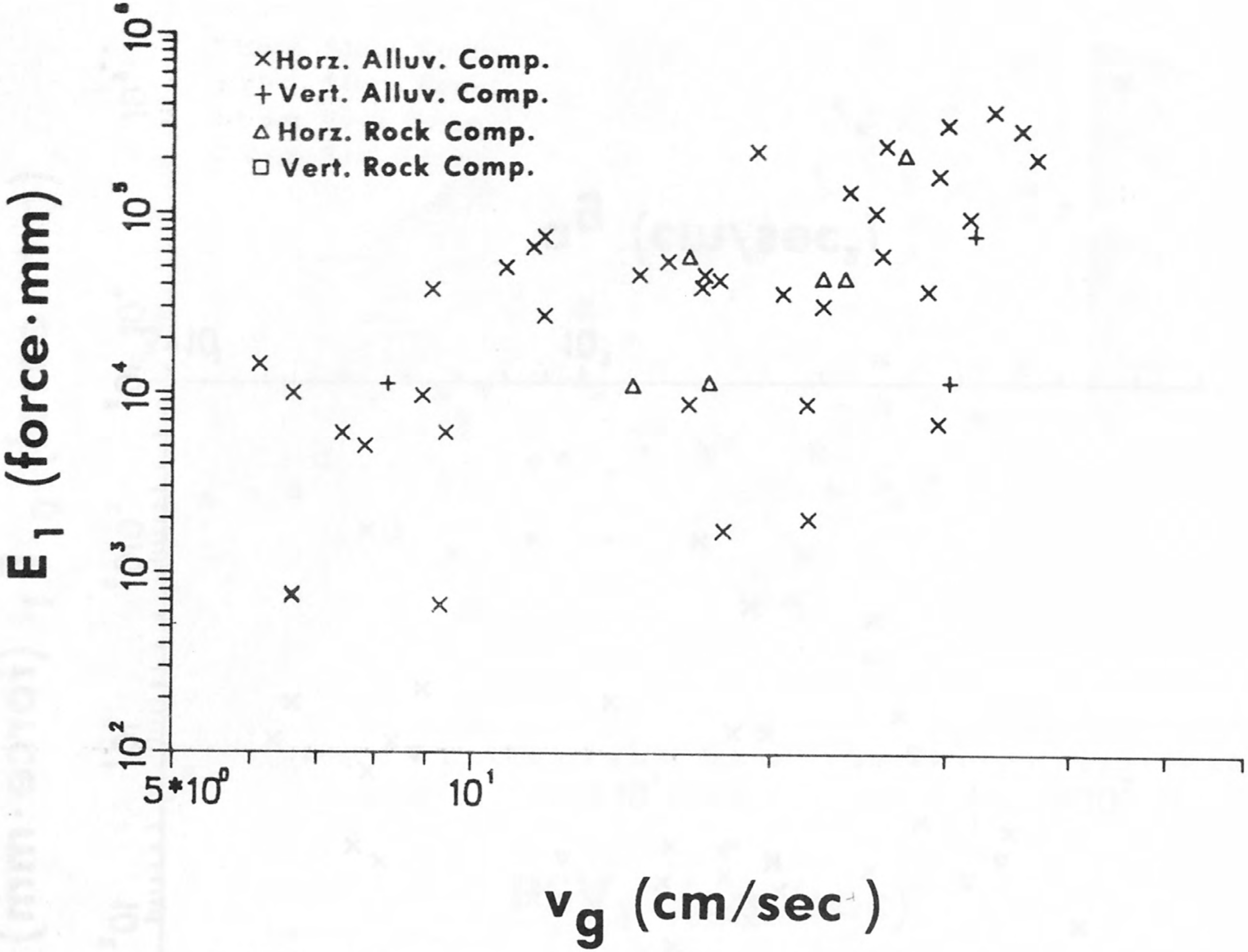

Figure 64.--E_1 versus v_g.

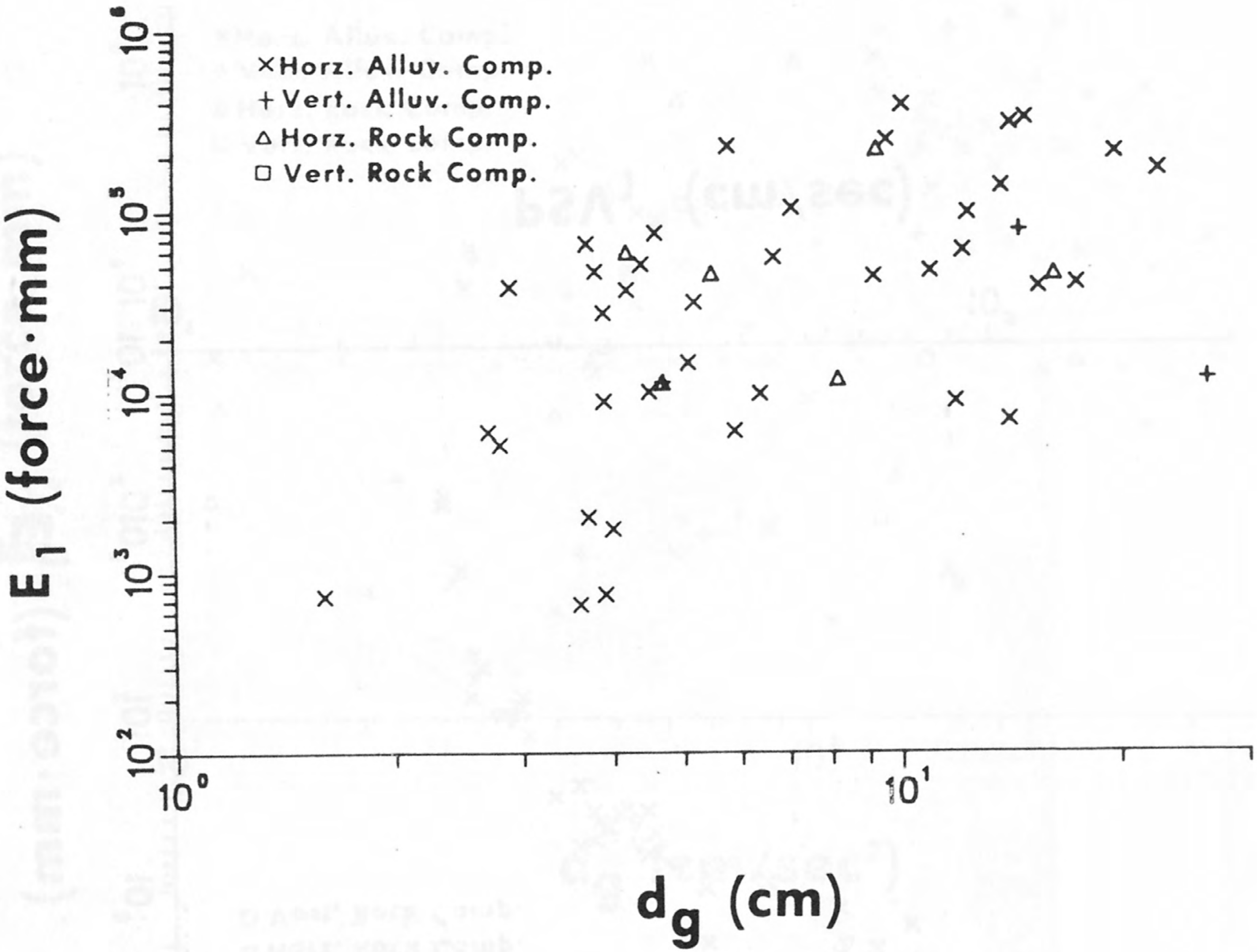

Figure 65.--E_1 versus d_g.

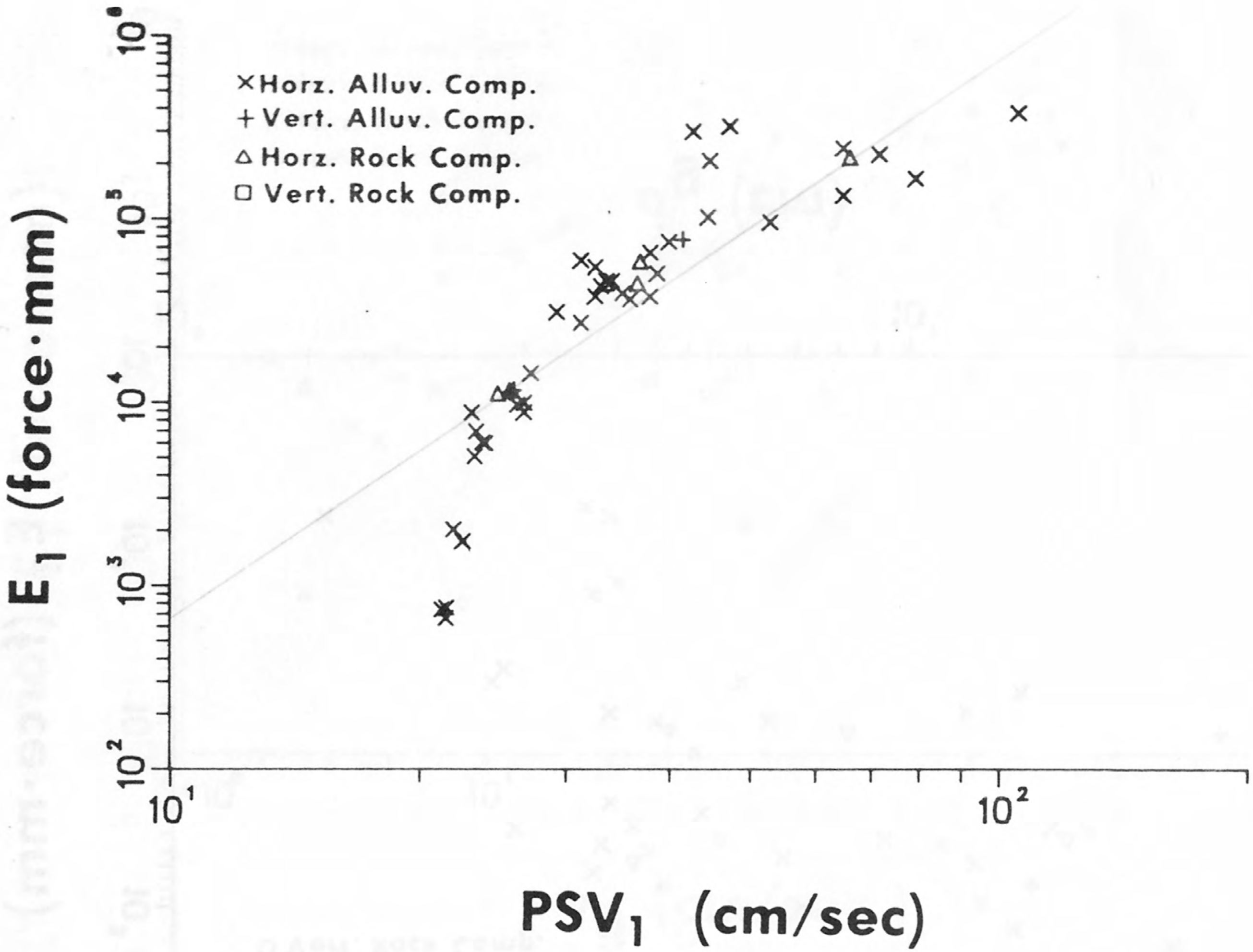

Figure 66.--E_1 versus PSV_1.

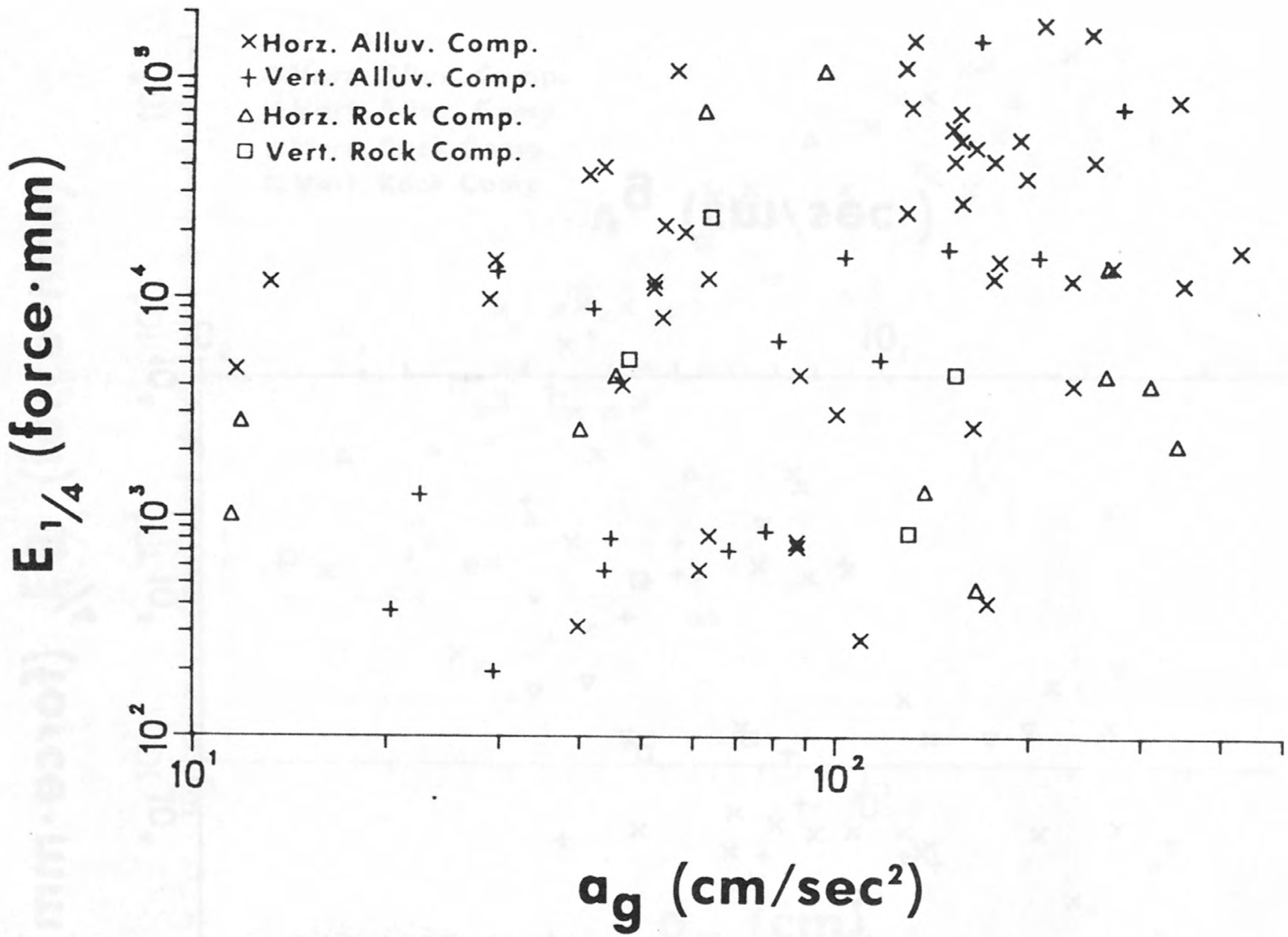

Figure 67.--$E_{\frac{1}{4}}$ versus a_g.

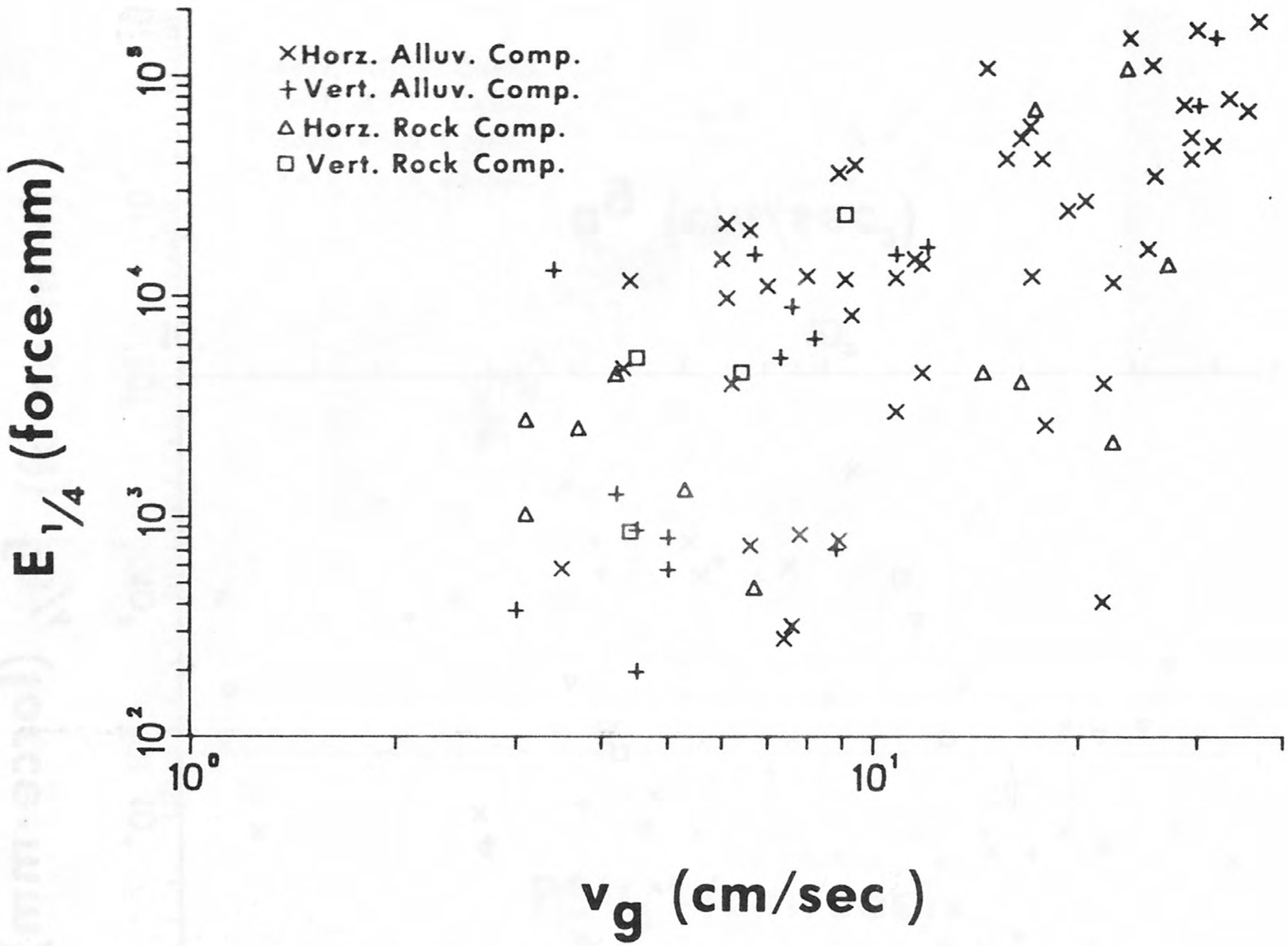

Figure 68.--$E_{\frac{1}{4}}$ versus v_g.

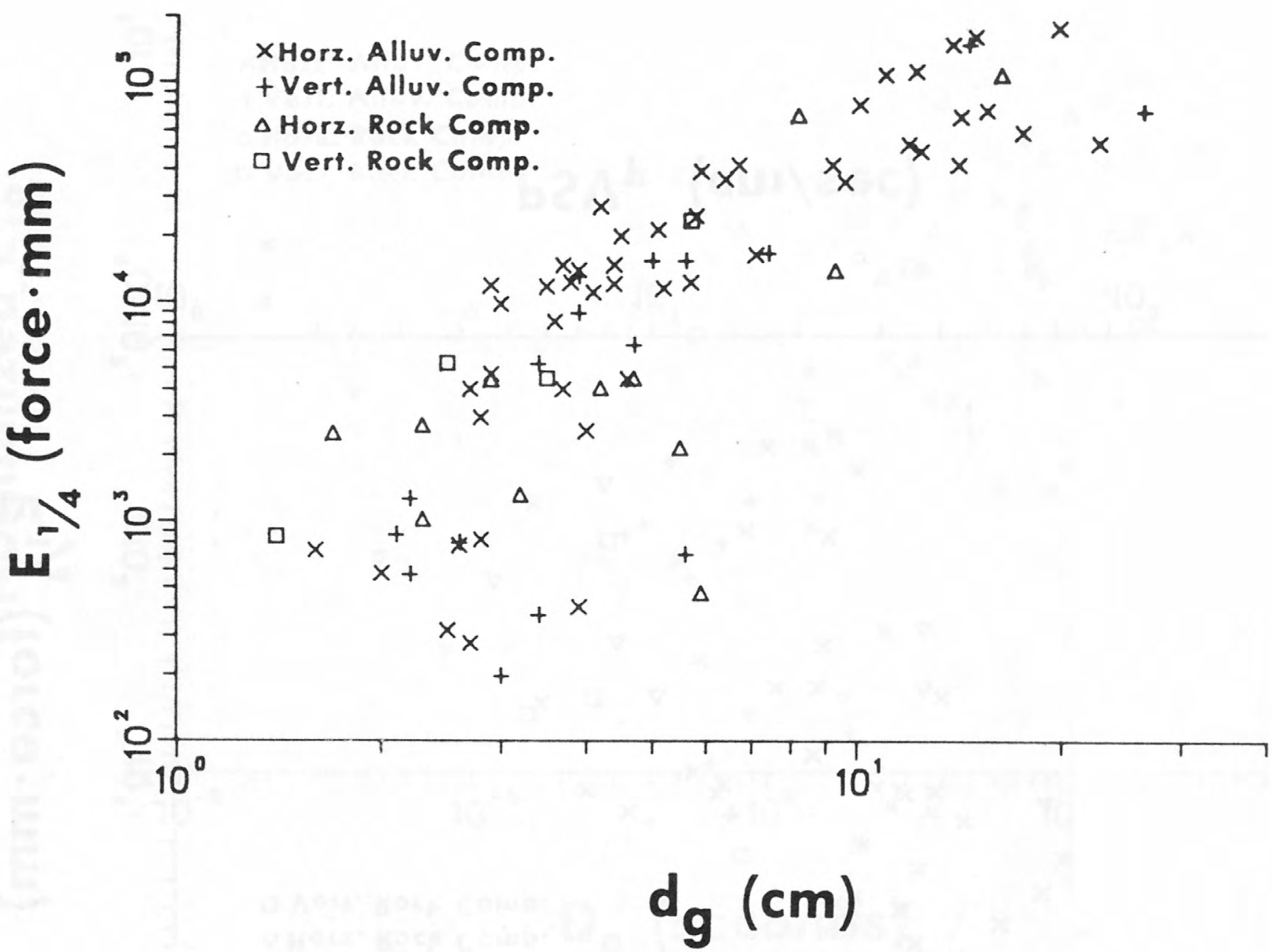

Figure 69.--$E_{1/4}$ versus d_g.

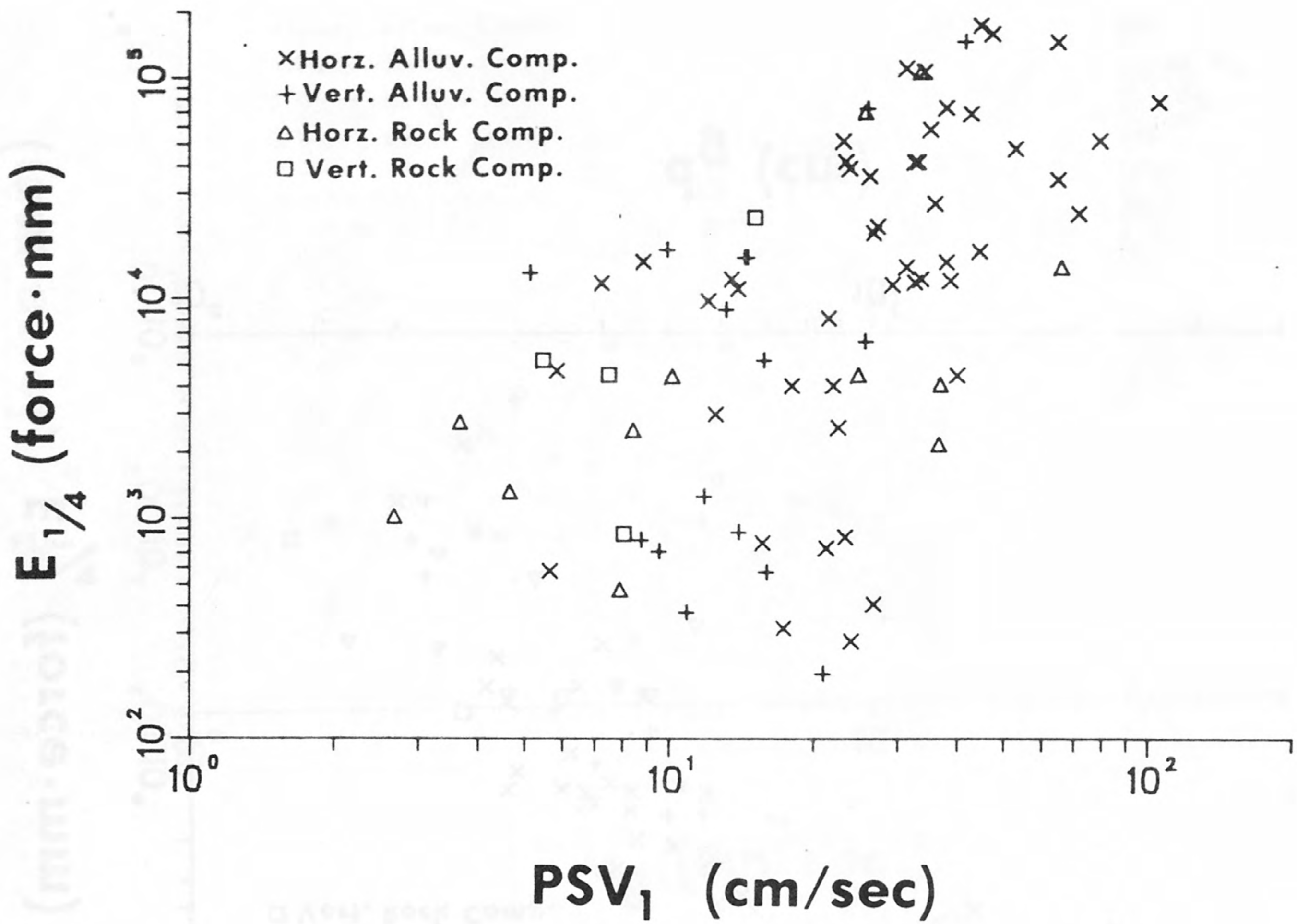

Figure 70.--$E_{\frac{1}{4}}$ versus PSV_1.

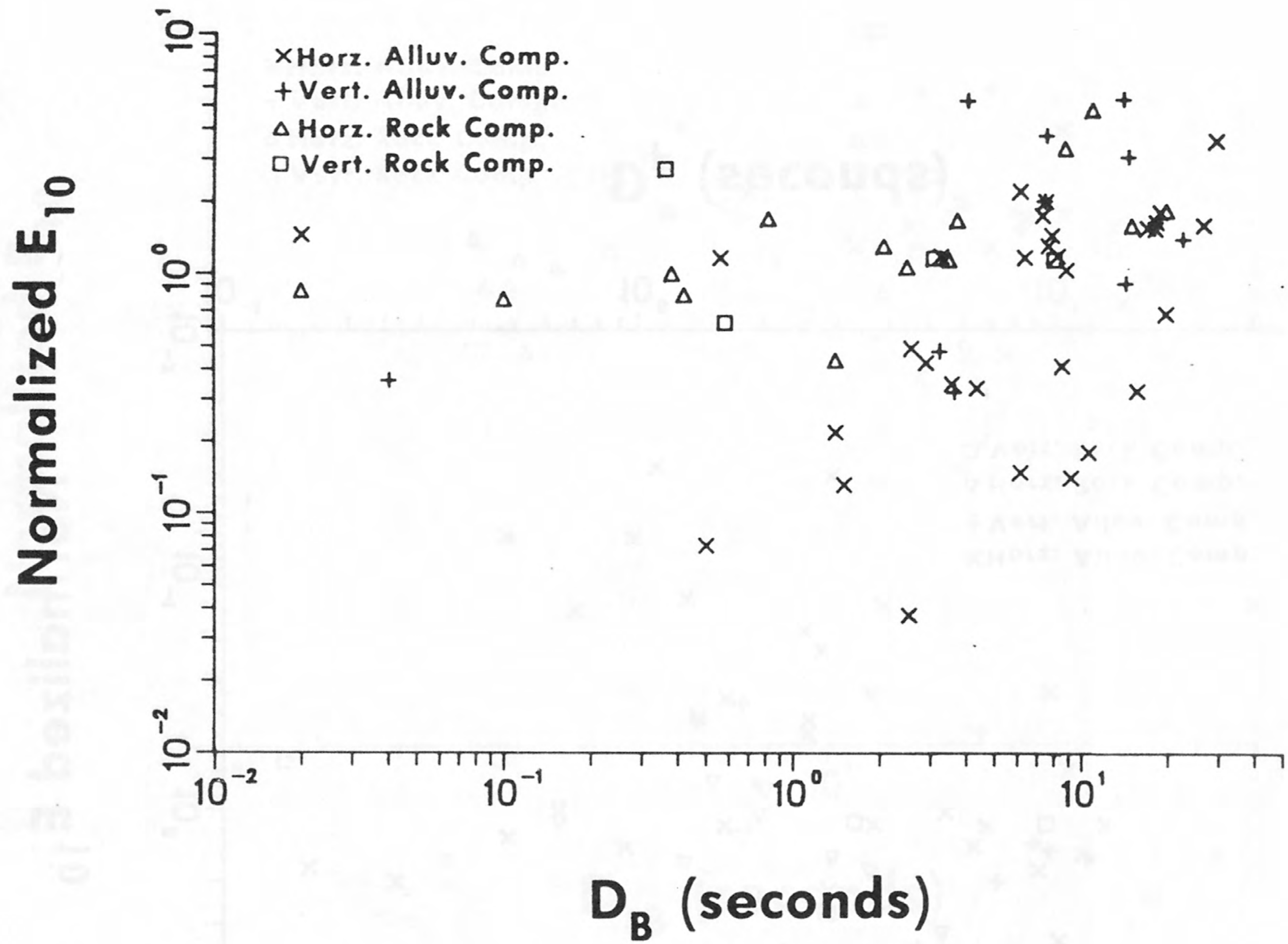

Figure 71.--E_{10} normalized by a_g versus D_B.

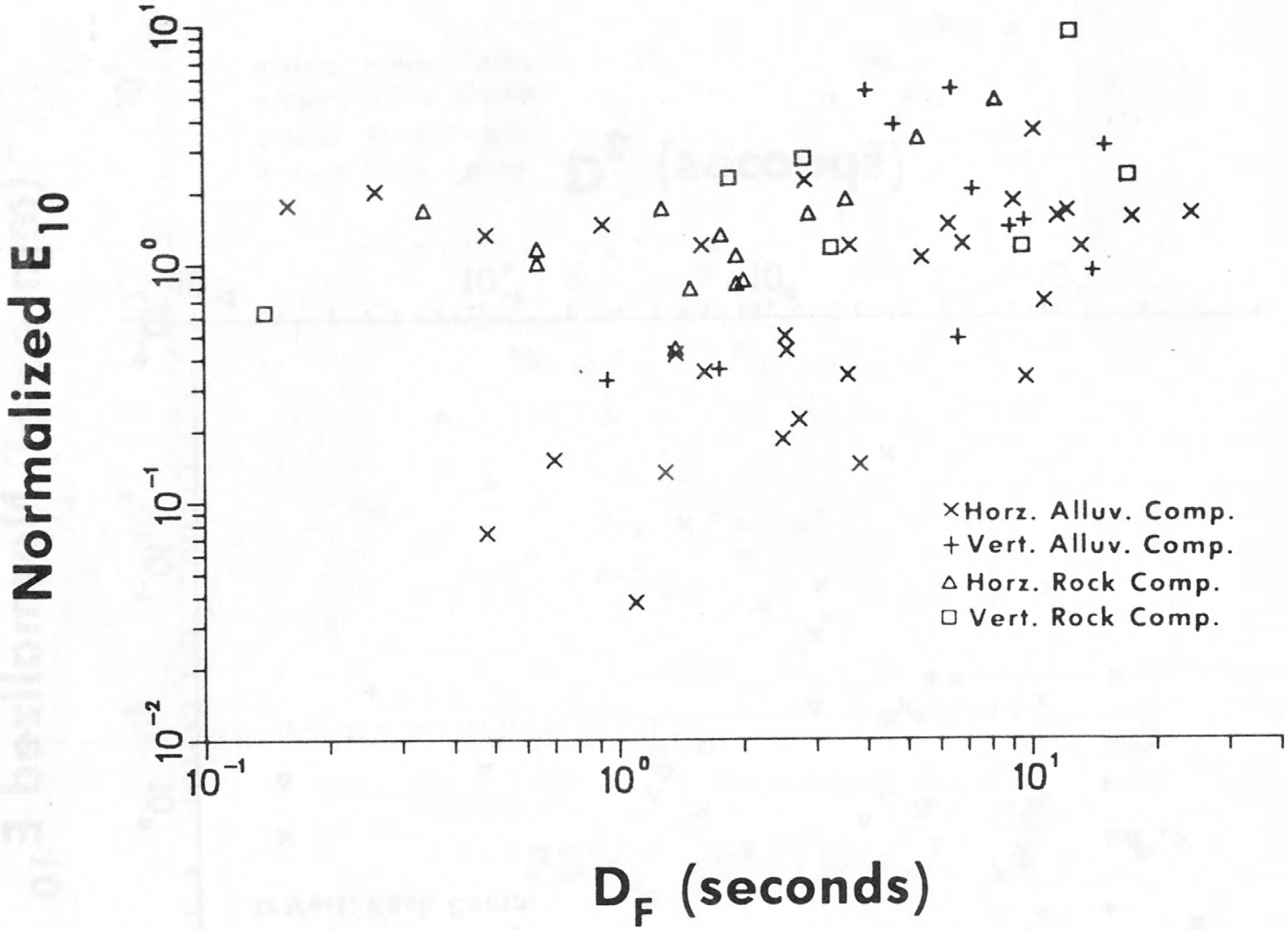

Figure 72.--E_{10} normalized by a_g versus D_F.

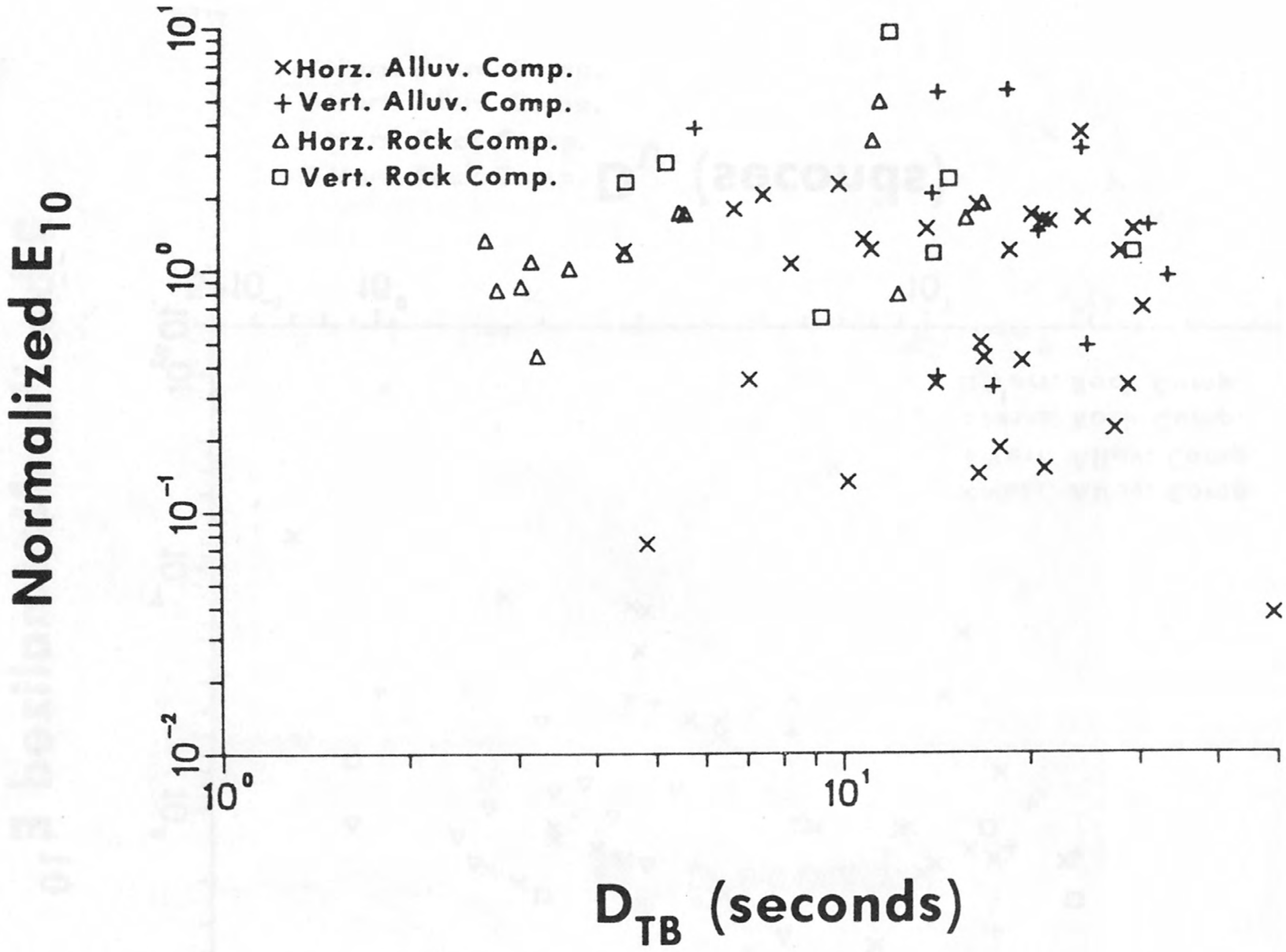

Figure 73.--E_{10} normalized by a_g versus D_{TB}.

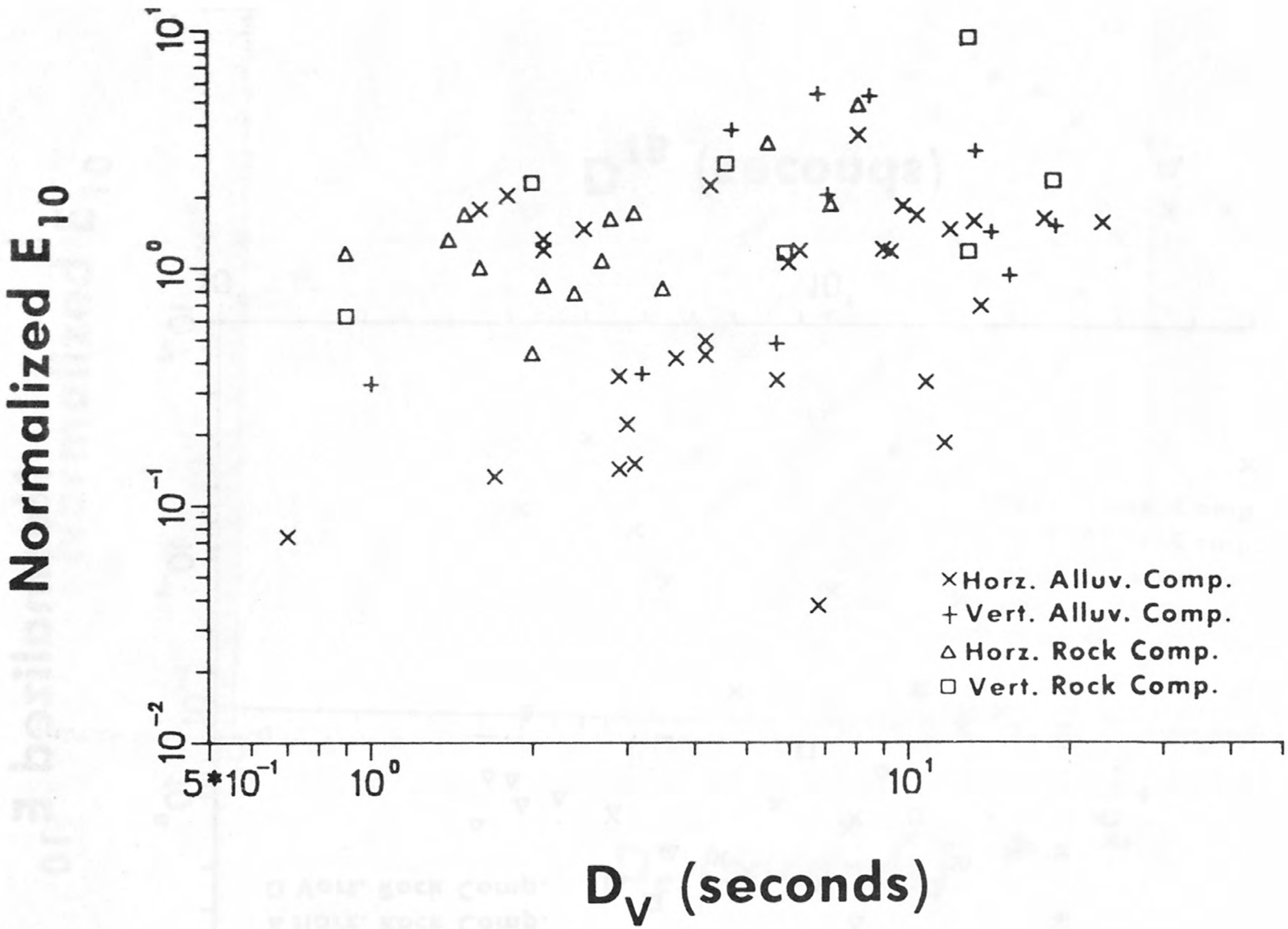

Figure 74.--E_{10} normalized by a_g versus D_V.

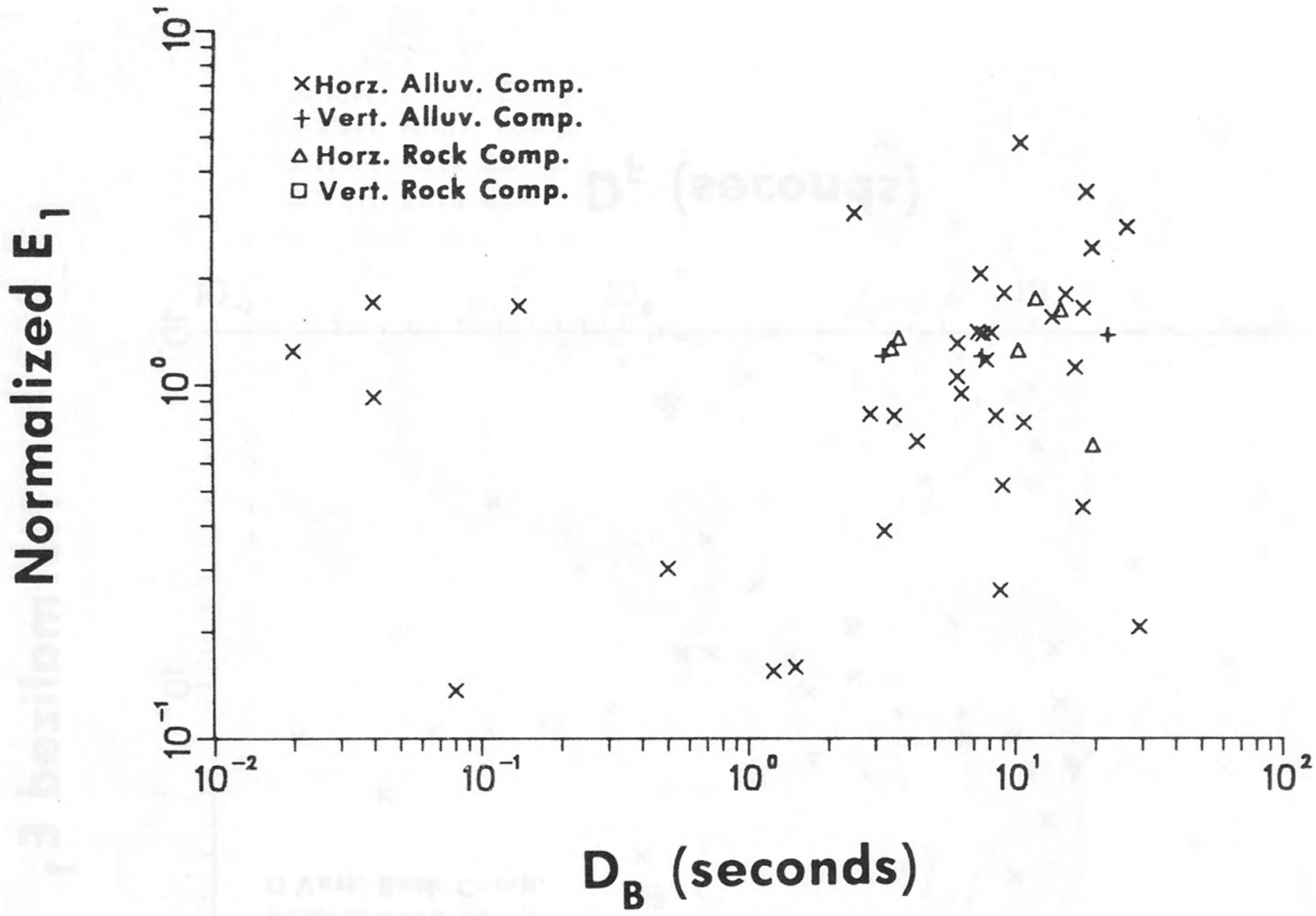

Figure 75.--E_1 normalized by PSV_1 versus D_B.

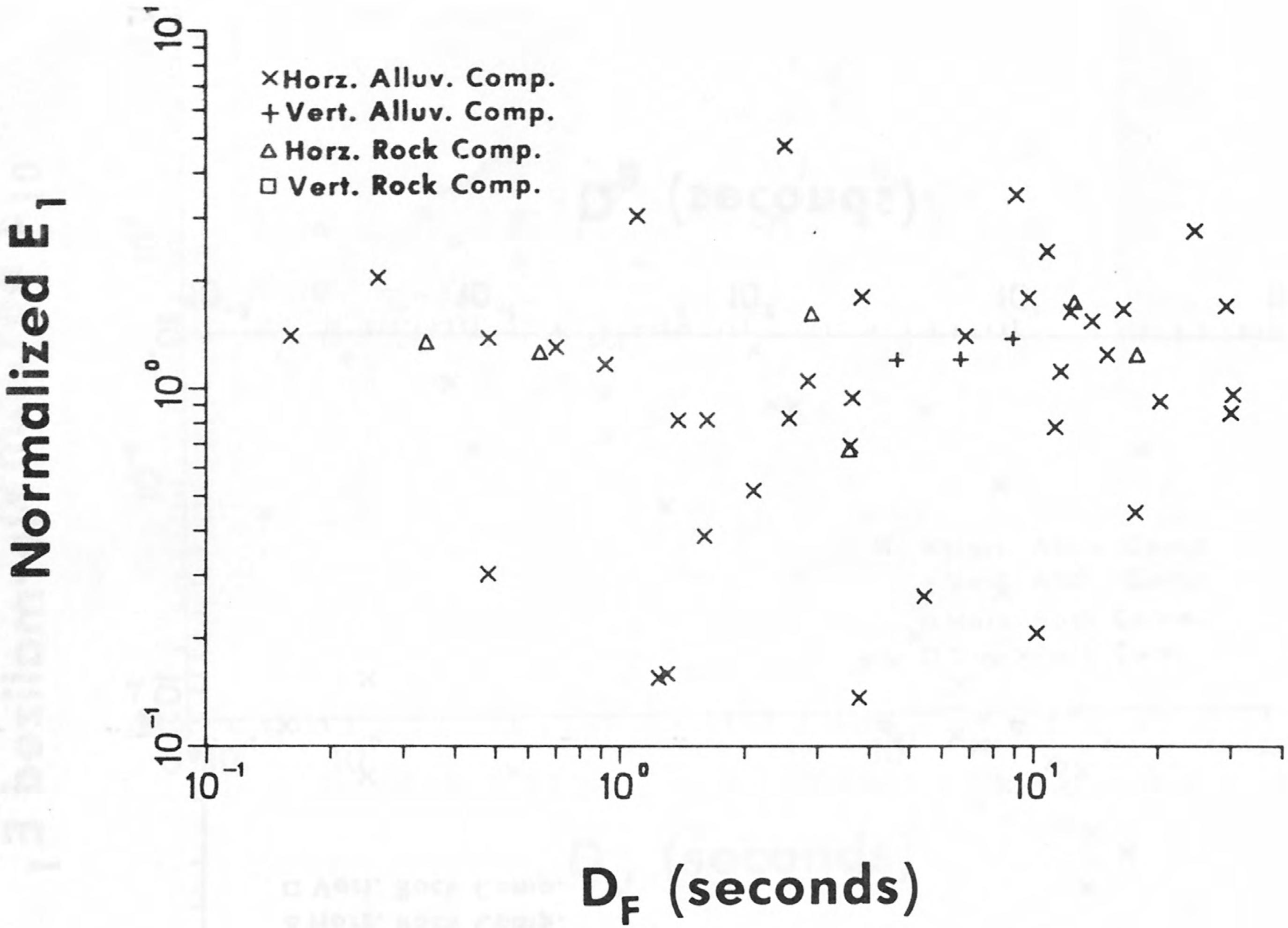

Figure 76.--E_1 normalized by PSV_1 versus D_F.

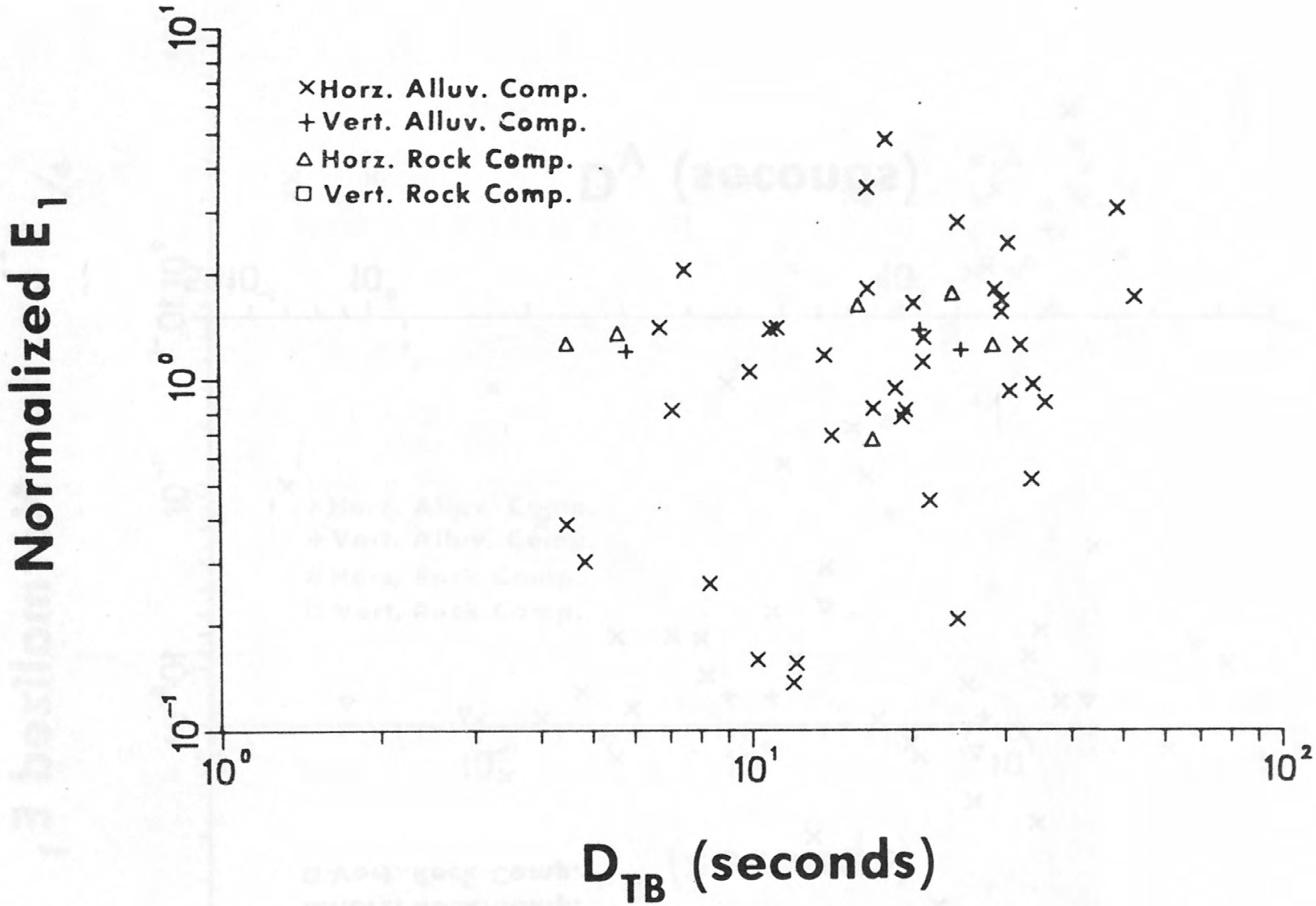

Figure 77.--E_1 normalized by PSV_1 versus D_{TB}.

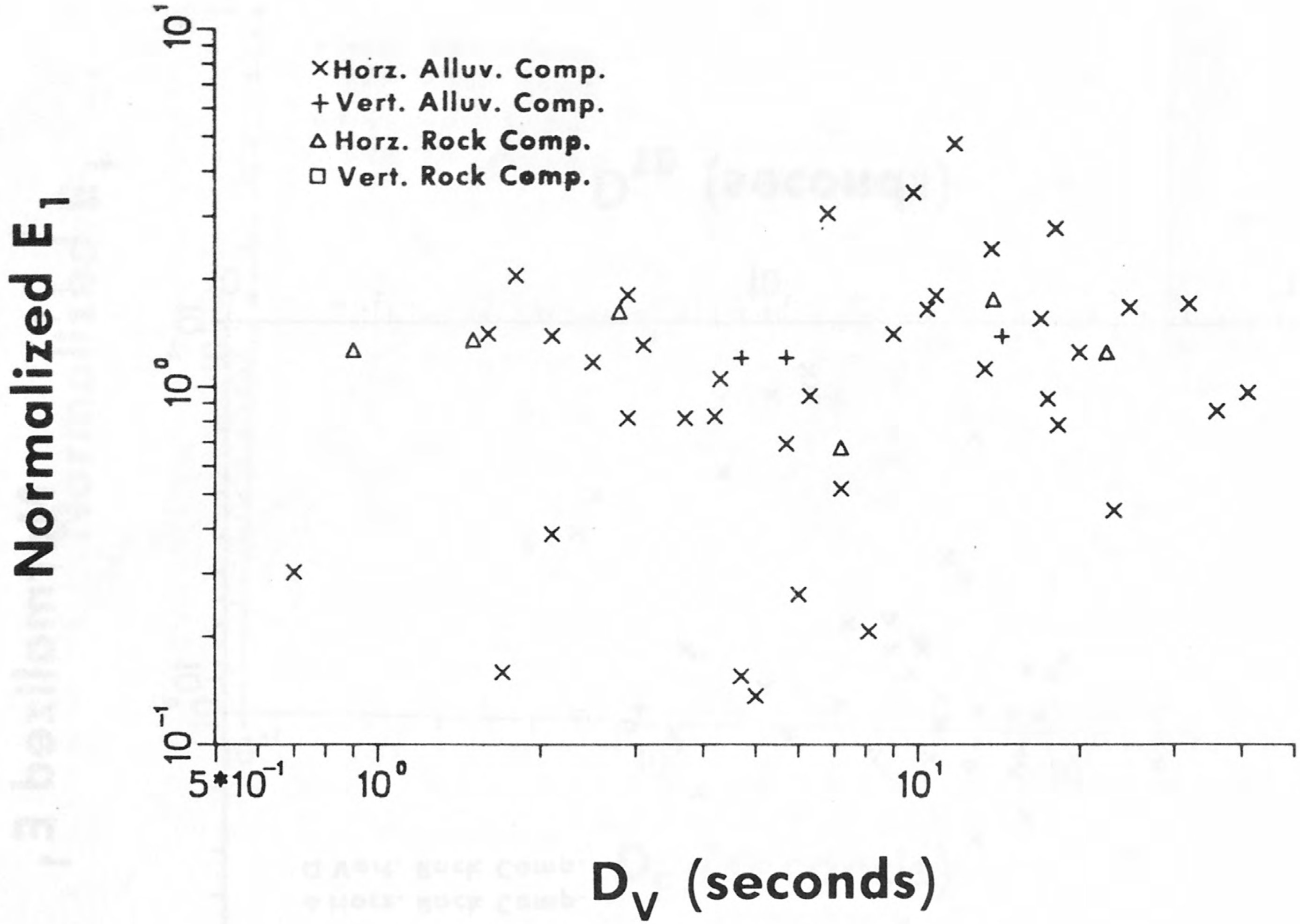

Figure 78.--E_1 normalized by PSV_1 versus D_V.

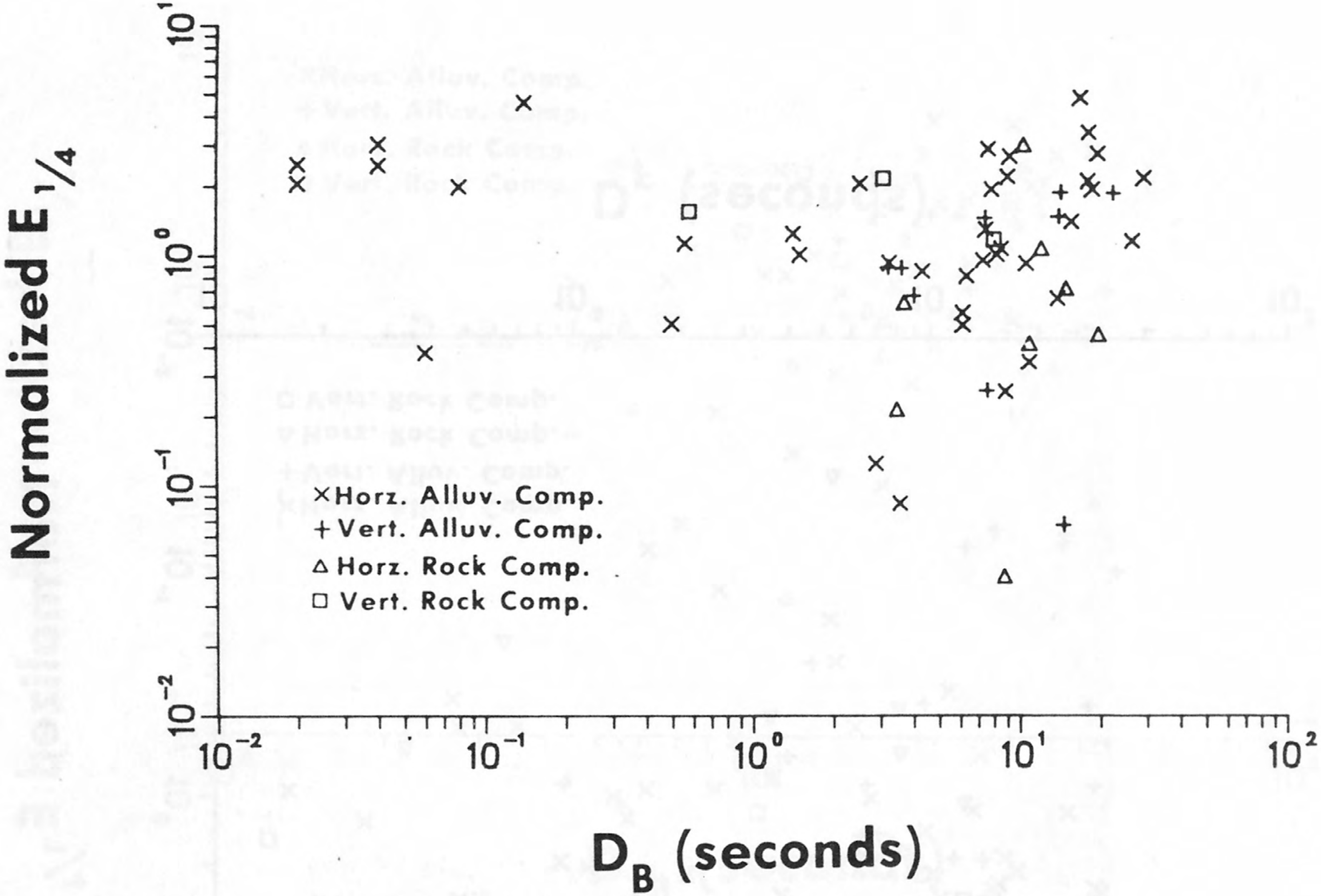

Figure 79.--$E_{\frac{1}{4}}$ normalized by d_g versus D_B.

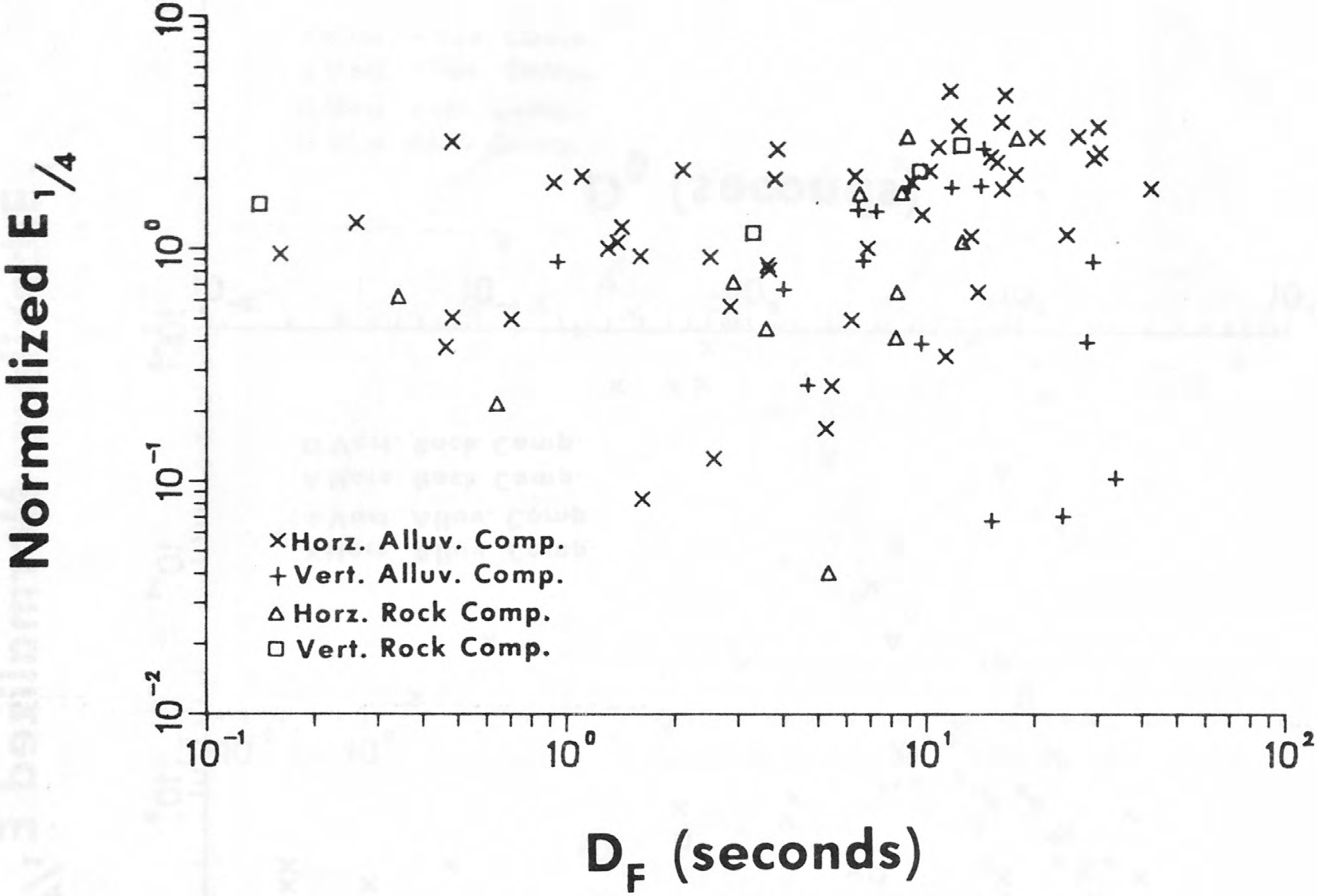

Figure 80.--$E_{\frac{1}{4}}$ normalized by d_g versus D_F.

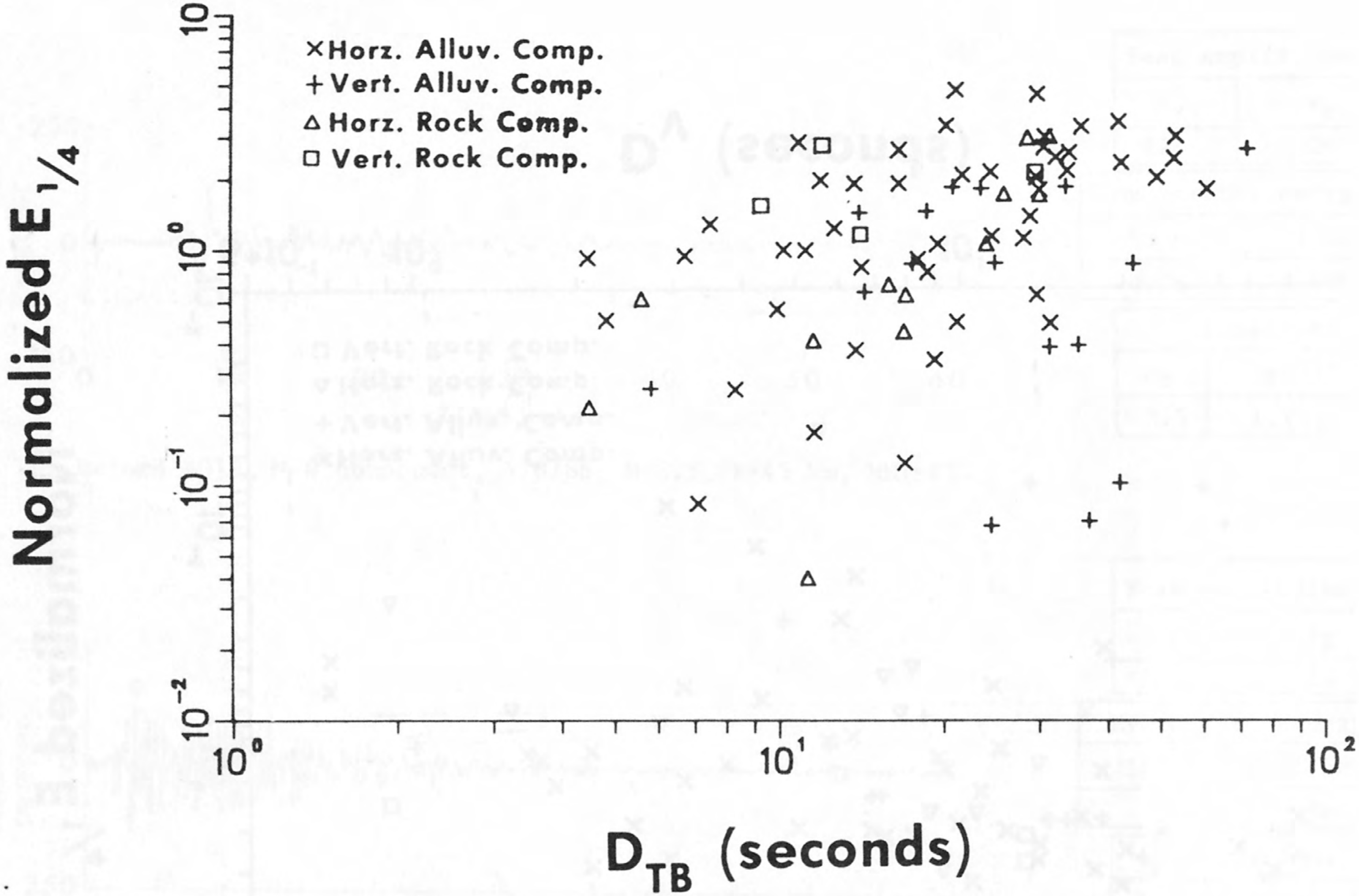

Figure 81.--$E_{1/4}$ normalized by d_g versus D_{TB}.

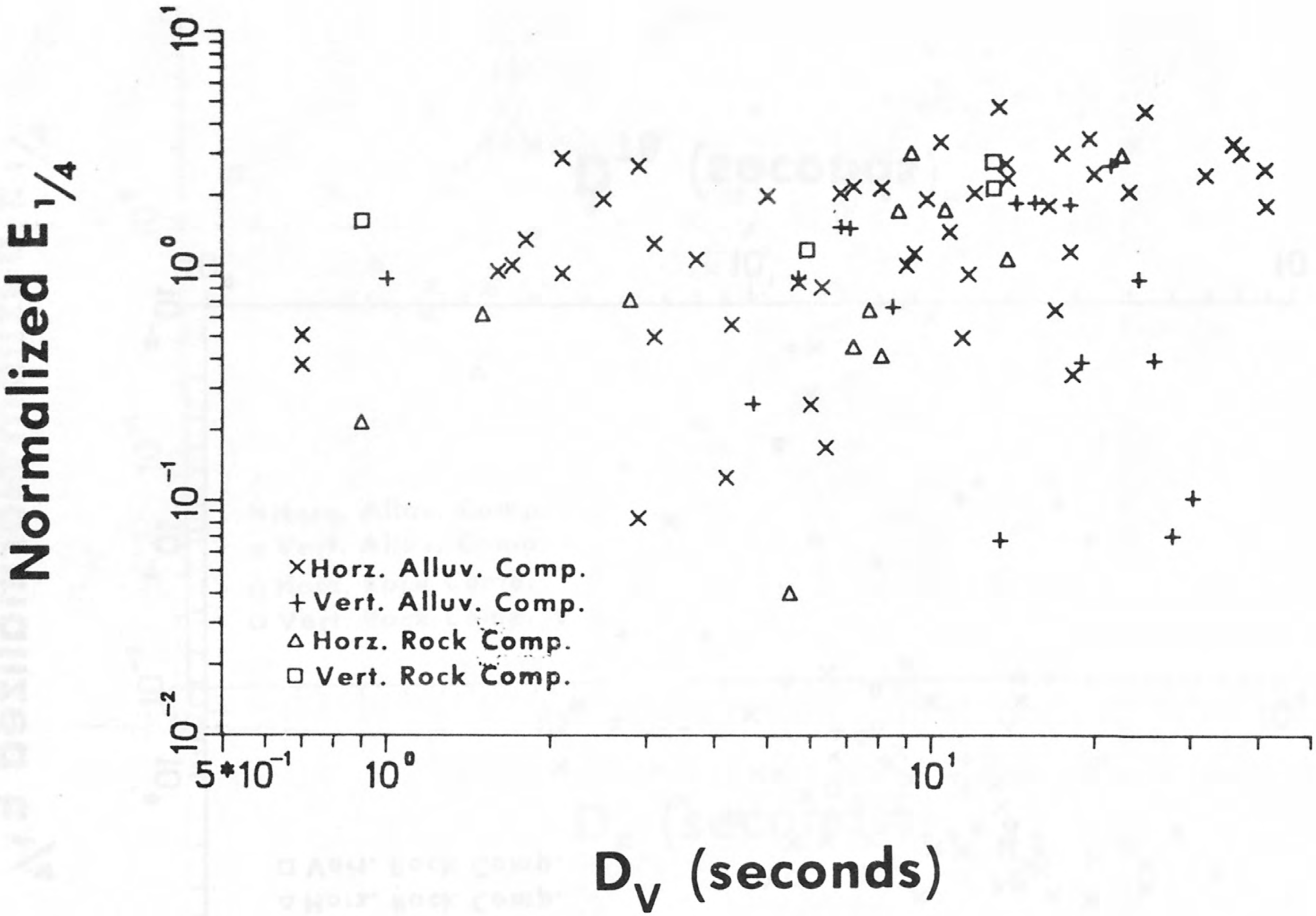

Figure 82.--$E_{1/4}$ normalized by d_g versus D_V.

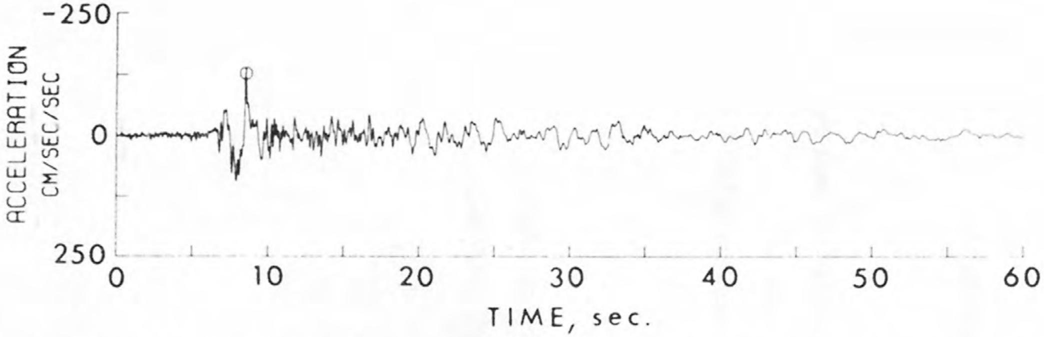

(a) Record A019, N-S component, 4/8/68, M=6.5, R=45 km, MMI=VI.

Peak amplitudes (cm & sec)		
a_g	v_g	d_g
128	26	12

Hysteretic energy (force x m)		
10 hz	1 hz	1/4 hz
0.28	60	110

Durations (sec)			
D_B	D_F	D_{TB}	D_V
2.5	1.1	49	7.1

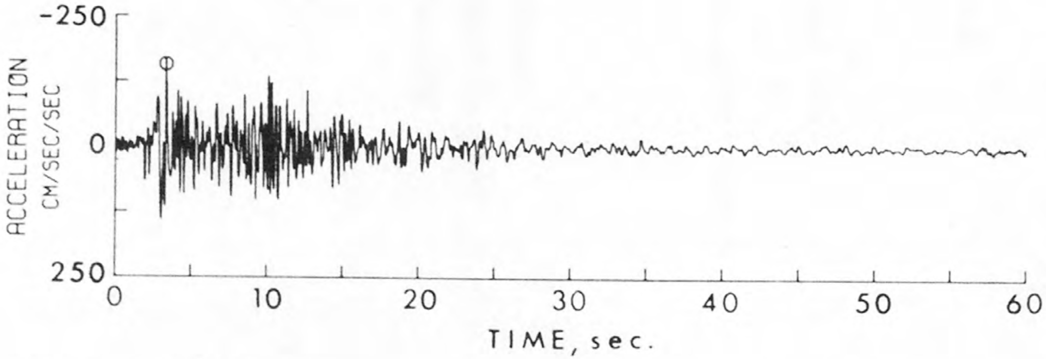

(b) Record B024, N-S component, 12/30/34, M=6.5, R=64 km, MMI=VI.

Peak amplitudes (cm & sec)		
a_g	v_g	d_g
157	21	4.2

Hysteretic energy (force x m)		
10 hz	1 hz	1/4 hz
17	36	27

Durations (sec)			
D_B	D_F	D_{TB}	D_V
17	12	21	13

Figure 83.--Two accelerograms recorded at El Centro.